Supporting information

Facile synthesis and separation of E/Z isomerization of aromatic-substituted tetraphenylethylene for investigating their fluorescent properties via single crystal analysis

Zhixiang Lu, Shaoxiong Yang, Xiaolan Liu, Yu Qin, Shuhan Lu,Yanxiong Liu, Ruidun Zhao, Liyan Zheng*and Hongbin Zhang *

Key Laboratory of Medicinal Chemistry for Natural Resource (Yunnan University), Ministry of Education, Functional Molecules Analysis and Biotransformation key laboratory of Universities in Yunnan Province, School of Chemical Science and Technology, Yunnan University, Kunming, Yunnan 650091, China.
E-mail: zhengliyan@ynu.edu.cn (L. Zheng), zhanghb@ynu.edu.cn (H. Zhang).

Table of Contents

Materials.

4-Hydroxybenzophenone, Titanium tetrachloride, Anhydrous tetrahydrofuran, 2-(Bromomethyl) pyridine hydrobromide, 3-(Bromomethyl) pyridine hydrobromide, 4-(Bromomethyl) pyridine hydrobromide, 4-Chloromethyl-2-methylthiazole hydrochloride, 4-(Chloromethyl)-3,5-dimethylisoxazole hydrochloride, Benzyl bromide, 1-(Bromomethyl)naphthalene, 2-(Chloromethyl)thiophene, Potassium tert-butanolate, Methanol-D_4 , Chloroform-*d*, 99.8 atom % D were purchased from Energy Chemical, all other reagents were of analytical grade and used as received. Ultrapure water was prepared using a Milli-Q water purification system.

Apparatus

Fluorescence spectra were recorded on a Hitachi High-Technologies Corporation Tokyo Japan 5J2-0004 model F-7000 FL spectrofluorometer. The NMR spectra were recorded using a AVANCEDRX600 NMR spectrometer (Bruker, Germany) operated at 600 MHz. Electrospray ionization mass spectra were obtained with a High Performance 1100 Liquid Chromatography-Mass Spectrometer (Agilent Technologies, USA). UV-Vis absorption was characterized using a UV/Vis/NIR spectrophotometer (Shimadzu, Japan). The Fourier transform infrared (FT-IR) spectra were obtained on a FT-IR spectrophotometer (Thermo Nicolet 365). Single crystal fluorescence pictures were obtained with a Fluorescent Inverted microscope (OLYMPUS U-HGLGPS). X-ray powder diffraction patterns were taken using a D/max-TTR III X-ray diffractometer (Rigaku, Japan) with a scan speed of 0.1 s per step and a step size of 0.01°. Fluorescence emission lifetimes were determined on an Edinburgh Analytical Instrument (FLS900 fluorescence spectrometer) with a light-emitting diode lamp and analyzed by the use of a program for exponential fits. Fluorescence quantum yields measurements were performed on an integrating sphere, with a 280 nm Edinburgh Instruments Ltd. light emitting diode as the excitation source (instrument model no. FLS920). The crystallographic data collection was performed without any inert gas protection at room temperature on a Bruker SMART APEX-II CCD area detector using graphite-monochromated Mo-Kα radiation ($\lambda = 0.71073$ Å). The data reduction and integration and global unit cell refinements were performed using the INTEGRATE program of the APEX2 software package. Semiempirical absorption corrections were applied using the SCALE program for the area detector. The structures were solved by direct methods and refined using the full-matrix leastsquares methods on F2 using SHELX. CCDC 1833475, 1833476, 1833477, 1833478, 1833479, 1833480, 1833481, 1833482, 1833483 and 1833484 contain the supplementary crystallographic data for TPE-2by-1-E, TPE-2by-1-Z, TPE-2by-2-E, TPE-2by-2-Z, TPE-2by-3-E, TPE-2by-3-Z, TPE-2TZ-E, TPE-2TZ-Z, TPE-2EZ-E and TPE-2EZ-Z.

Synthesis.

Synthesis of TPE-2OH. The synthesis of TPE-2OH was synthesized as the previous report. Zinc powder (1.0 g, 15.3 mmol) was added into a 100 mL double-neck flask. Under an N_2 atmosphere, 25 mL anhydrous THF was added, which was cooled to −5 °C, and then $TiCl_4$ (1.1 mL, 10 mmol) and pyridine (0.05 mL, 0.6 mmol) were added dropwise. The mixture was refluxed at 75 °C for 2 hours and 20 mL THF solution of 4-Hydroxybenzophenone (1.05 g, 5 mmol) was added. The solution was further refluxed at 75 °C for 12 hours. Upon completion of the reaction, the solution

was cooled to room temperature and poured into 40 mL 30% water solution of K_2CO_3, which was stirred strongly for 5 minutes and then filtered. The filtrate was extracted with ethyl acetate, washed with water successively, brine, and dried with Na_2SO_4. The crude products were obtained by rotary evaporation, and purified by column chromatography (silica gel, petroleum ether/ ethyl acetate=20:1) to result in a light green product TPE-2OH (Yield, 85%). The ^{1}H NMR and ^{13}C NMR spectrum of TPE-2OH (400 MHz, CD_3OH, 25 °C), δ (TMS, ppm) are showed as in Fig. S1 and S2, respectively. High resolution mass spectrometry of TPE-2OH is showed in Fig. S3, (m/z): calculated for $C_{26}H_{20}O_2$ $[M+Na]^+$ 387.1356, found 387.1356(high resolution). ^{1}H NMR (400 MHz, CD_3OH, 25 °C) 7.11-6.96(10 H, m), 6.82 -6.77(4 H, m), 6.76-6.47(4 H, m). ^{13}C NMR (400 MHz, CD_3OH, 25 °C) 157.09, 146.05, 145.94, 141.18, 136.89, 136.76, 133.79, 133.74, 132.64, 132.60, 128,69, 127.27, 115.62, 115.5.

Synthesis of TPE-2by-1. A solution of TPE-2OH (364 mg,1 mmol), 2-(Bromomethyl) pyridine hydrobromide (750 mg, 2.5 mmol) and potassium tert-butanolate (840 mg, 7.5 mmol) in methylbenzene (15 mL) was refluxed at 105 °C for 12 h. The solvent was removed in rotary evaporation, and the residue was dissolved in DCM and water. The organic layer was washed with brine and dried over Na_2SO_4. The crude products were obtained by rotary evaporation, and purified by column chromatography (silica gel, petroleum ether/ ethyl acetate=3:1) to result in two white solids (TPE-2by-1-E and TPE-2by-1-Z) (Yield, 40 %; 42 %). The ^{1}H NMR and ^{13}C NMR spectrum of TPE-2by-1-E (600 MHz, $CDCl_3$, 25 °C) δ (TMS, ppm) are showed as in Fig. S4 and S5, High resolution mass spectrometry of TPE-2by-1-E is showed in Fig. S6, (m/z): calculated for C_{38} H_{30} N_2 O_2 $[M+H]^+$ 547.2381, found 547.2385(high resolution). Crystal structure of TPE-2by-1-E is showed in Fig. S44 A. ^{1}H NMR (600 MHz, $CDCl_3$, 25 °C) 8.57(1 H, d, J=6 Hz),7.70(1 H, t, J=18 Hz), 7.49(1 H, d, J=6 Hz), 7.22(1 H, t, J=12 Hz), 7.10(3 H, m, J=12 Hz), 7.04(2 H, m, J=6 Hz), 6.93(2 H, d, J=12 Hz), 6.72(2 H, d, J=6 Hz), 5.11(2 H, s). ^{13}C NMR (600 MHz, $CDCl_3$, 25 °C) 157.30, 156.87, 149.16, 144.11, 139.77, 136.83, 136.71, 132.57, 131.34, 127.67, 126.23, 122.53, 121.28, 113.96, 70.55. The ^{1}H NMR and ^{13}C NMR spectrum of TPE-2by-1-Z (600 MHz, $CDCl_3$, 25 °C) δ (TMS, ppm) are showed as in Fig. S6 and S7, High resolution mass spectrometry of TPE-2by-1-Z is showed in Fig. S8, (m/z): calculated for C_{38} H_{30} N_2 O_2 $[M+H]^+$ 547.2381, found 547.2382(high resolution). Crystal structure of TPE-2by-1-Z is showed in Fig. S44 B. ^{1}H NMR (600 MHz, $CDCl_3$, 25 °C) 8.57(1 H, d, J=6 Hz),7.71(1 H, t, J=18 Hz), 7.51(1 H, d, J=12 Hz), 7.21(1 H, t, J=12 Hz), 7.08(3 H, m, J=12 Hz), 7.06(2 H, m, J=6 Hz), 6.94(2 H, d, J=6 Hz), 6.74(2 H, d, J=12 Hz), 5.13(2 H, s). ^{13}C NMR (600 MHz, $CDCl_3$, 25 °C) 157.31, 156.88, 149.16, 144.04, 139.78, 136.88, 136.74, 132.55, 131.36, 127.57, 126.22, 122.56, 121.31, 114.05, 70.55.

Synthesis of TPE-2by-2. The method of synthesizing TPE-2by-2 is the same as that of TPE-2by-1. (TPE-2by-2-E and TPE-2by-2-Z) (Yield, 38%; 40 %). The ^{1}H NMR and ^{13}C NMR spectrum of TPE-2by-2-E (600 MHz, $CDCl_3$, 25 °C) δ (TMS, ppm) are showed as in Fig. S10 and S11, High resolution mass spectrometry of TPE-2by-2-E is showed in Fig. S12, (m/z): calculated for C_{38} H_{30} N_2 O_2 $[M+H]^+$ 547.2381, found 547.2381(high resolution). Crystal structure of TPE-2by-2-E is showed in Fig. S44 C. ^{1}H NMR (600 MHz, $CDCl_3$, 25 °C) 8.64(1 H, d), 8.57 (1 H, dd, J=6 Hz), 7.74(1 H, d, J=12 Hz), 7.32(1 H, m, J=6 Hz), 7.13(3 H, m, J=18 Hz), 7.05(2 H, m, J=6 Hz), 6.94(2 H, d, J=12 Hz), 6.71(2 H, d, J=12 Hz), 4.99(2 H, s). ^{13}C NMR (600 MHz, $CDCl_3$, 25 °C) 157.01, 149.57, 149.20, 144.22, 139.95, 137.19, 135.40, 132.78, 132.68, 131.50, 127.88, 126.46, 123.58,

114.11, 67.61. The ^{1}H NMR and ^{13}C NMR spectrum of TPE-2by-2-Z (600 MHz, $CDCl_3$, 25 °C) δ (TMS, ppm) are showed as in Fig. S13 and S14, High resolution mass spectrometry of TPE-2by-2-Z is showed in Fig. S15, (m/z): calculated for $C_{38}H_{30}N_2O_2$ $[M+H]^+$ 547.2381, found 547.2385(high resolution). Crystal structure of TPE-2by-2-Z is showed in Fig. S44 D. ^{1}H NMR (600 MHz, CDCl3, 25 °C) 8.64(1 H, d),8.57 (1 H, dd, J=6 Hz), 7.74(1 H, d, J=12 Hz), 7.31(1 H, m, J=12 Hz), 7.10(3 H, m, J=18 Hz), 7.05(2 H, m, J=12 Hz), 6.96(2 H, d, J=12 Hz), 6.71(2 H, d, J=12 Hz), 4.99(2 H, s). ^{13}C NMR (600 MHz, $CDCl_3$, 25 °C) 156.96, 149.40, 149.03, 144.09, 139.74, 137.01, 135.28, 132.68, 132.54, 131.33, 127.71, 126.20, 123.45, 113.98, 67.46.

Synthesis of TPE-2by-3. The method of synthesizing TPE-2by-3 is the same as that of TPE-2by-1. (TPE-2by-3-E and TPE-2by-3-Z) (Yield, 36%; 40 %). The ^{1}H NMR and ^{13}C NMR spectrum of TPE-2by-3-E (600 MHz, $CDCl_3$, 25 °C) δ (TMS, ppm) are showed as in Fig. S16 and S17. High resolution mass spectrometry of TPE-2by-3-E is showed in Fig. S18, (m/z): calculated for $C_{38}H_{30}N_2O_2$ $[M+H]^+$ 547.2381, found 547.2383(high resolution). Crystal structure of TPE-2by-4-E is showed in Fig. 1 A. ^{1}H NMR (600 MHz, $CDCl_3$, 25 °C) 8.51(2 H, dd, J=6 Hz), 7.23 (2 H, d, J=6 Hz), 7.03(3 H, m, J=18 Hz), 6.96(2 H, m, J=12 Hz), 6.85(2 H, d, J=6 Hz), 6.61(2 H, d, J=6 Hz), 4.93(2 H, s). ^{13}C NMR (600 MHz, $CDCl_3$, 25 °C) 156.96, 149.40, 149.03, 144.09, 139.74, 137.01, 135.28, 132.68, 132.54, 131.33, 127.71, 126.20, 123.45, 113.98, 67.46. The ^{1}H NMR and ^{13}C NMR spectrum of TPE-2by-3-Z (600 MHz, CDCl3, 25 °C) δ (TMS, ppm) are showed as in Fig. S19 and S20. High resolution mass spectrometry of TPE-2by-3-Z is showed in Fig. S21, (m/z): calculated for $C_{38}H_{30}N_2O_2$ $[M+H]^+$ 547.2381, found 547.2378(high resolution). Crystal structure of TPE-2by-3-Z is showed in Fig. 1 B. ^{1}H NMR (600 MHz, $CDCl_3$, 25 °C) 8.51(2 H, dd, J=6 Hz),7.23 (2 H, d, J=6 Hz), 6.99(3 H, m, J=18 Hz), 6.91(2 H, m, J=12 Hz), 6.85(2 H, d, J=6 Hz), 6.61(2 H, d, J=12 Hz), 4.92(2 H, s). ^{13}C NMR (600 MHz, $CDCl_3$, 25 °C) 156.66, 146.18, 143.91, 139.80, 137.19, 133.64, 131.34, 127.63, 126.35, 121.53, 114.04, 68.08.

Synthesis of TPE-2TZ. The method of synthesizing TPE-2TZ is the same as that of TPE-2by-1. (TPE-2TZ -E and TPE-2TZ -Z) (Yield, 40%; 42 %). The ^{1}H NMR and ^{13}C NMR spectrum of TPE-2TZ -E (600 MHz, $CDCl_3$, 25 °C) δ (TMS, ppm) are showed as in Fig. S22 and S23. High resolution mass spectrometry of TPE-2TZ -E is showed in Fig. S24, (m/z): calculated for $C_{36}H_{30}N_2O_2S_2$ $[M+H]^+$ 587.1821, found 587.1820 (high resolution). Crystal structure of TPE-2by-4-E is showed in Fig. S44 E. 1H NMR (600 MHz, $CDCl_3$, 25 °C) 7.11(1 H, s),7.09 (3 H, m, J=6 Hz), 7.04 (2 H, m, J=6 Hz), 6.91(2 H, d, J=12 Hz), 6.70(2 H, d, J=6 Hz), 5.05(2 H, s), 2.72(3 H, s). ^{13}C NMR (600 MHz, $CDCl_3$, 25 °C) 166.59, 157.07, 152.10, 144.28, 139.92, 136.96, 132.66, 131.51, 127.82, 126.37, 115.90, 114.06, 66.17, 19.28. The ^{1}H NMR and ^{13}C NMR spectrum of TPE-2TZ-Z (600 MHz, $CDCl_3$, 25 °C) δ (TMS, ppm) are showed as in Fig. S25 and S26, High resolution mass spectrometry of TPE-2by-3-Z is showed in Fig. S27, (m/z): calculated for $C_{36}H_{30}N_2O_2S_2$ [M+H]+ 587.1821, found 587.1822 (high resolution). Crystal structure of TPE-2by-3-Z is showed in Fig. S44 F. ^{1}H NMR (600 MHz, $CDCl_3$, 25 °C) 7.11(1 H, s),7.09 (3 H, m, J=12 Hz), 7.04 (2 H, m, J=6 Hz), 6.92(2 H, d, J=12 Hz), 6.70(2 H, d, J=6 Hz), 5.05(2 H, s), 2.71(3 H, s). ^{13}C NMR (600 MHz, $CDCl_3$, 25 °C) 166.45, 156.94, 151.96, 144.14, 139.78, 136.82, 132.53, 131.37, 127.68, 126.23, 115.77, 113.92, 66.04, 19.16.

Synthesis of TPE-2EZ. The method of synthesizing TPE-2EZ is the same as that of TPE-2by-1.

(TPE-2EZ -E and TPE-2EZ -Z) (Yield, 43%; 44 %). The ^{1}H NMR and ^{13}C NMR spectrum of TPE-2EZ -E (600 MHz, $CDCl_3$, 25 °C) δ (TMS, ppm) are showed as in Fig. S28 and S29. High resolution mass spectrometry of TPE-2EZ -E is showed in Fig. S30, (m/z): calculated for C_{38} H_{35} N_2 O_4 $[M+H]^+$ 583.2591, found 583.2591 (high resolution). Crystal structure of TPE-2EZ -E is showed in Fig. S44 G. ^{1}H NMR (600 MHz, $CDCl_3$, 25 °C) 7.13 (3 H, m, J=18 Hz), 7.05 (2 H, d, J=12 Hz), 6.93(2 H, d, J=6 Hz), 6.66(2 H, d, J=6 Hz), 4.71(2 H, s), 2.36(3 H, s), 2.26(3 H, s). ^{13}C NMR (600 MHz, $CDCl_3$, 25 °C) 167.42, 159.72, 156.76, 144.08, 139.76, 137.13, 132.60, 131.35, 127.76, 126.35, 114.15, 110.28, 59.47, 11.14, 10.15. The ^{1}H NMR and ^{13}C NMR spectrum of TPE-2TZ-Z (600 MHz, $CDCl_3$, 25 °C) δ (TMS, ppm) are showed as in Fig. S31 and S32， High resolution mass spectrometry of TPE-2EZ -Z is showed in Fig. S33, (m/z): calculated for C_{38} H_{35} N_2 O_4 $[M+H]^+$ 583.2591, found583.2590 (high resolution). Crystal structure of TPE-2TZ-Z is showed in Fig. S44 H. ^{1}H NMR (600 MHz, $CDCl_3$, 25 °C) 7.08 (3 H, m, J=6 Hz), 7.02 (2 H, d, J=12 Hz), 6.96(2 H, d, J=6 Hz), 6.69(2 H, d, J=12 Hz), 4.75(2 H, s), 2.37(3 H, s), 2.27(3 H, s). ^{13}C NMR (600 MHz, $CDCl_3$, 25 °C) 167.44, 159.73, 156.72, 143.94, 139.81, 137.25, 132.60, 131.34, 127.64, 126.35, 114.35, 110.29, 59.54, 11.16, 10.18.

Synthesis of TPE-2B. The method of synthesizing TPE-2B is the same as that of TPE-2by-1. (TPE-2B is a mixture of cis and trans isomers) (Yield, 92 %). The ^{1}H NMR and ^{13}C NMR spectrum of TPE-2B (600 MHz, $CDCl_3$, 25 °C) δ (TMS, ppm) are showed as in Fig. S34 and S35. High resolution mass spectrometry of TPE-2B is showed in Fig. S36, (m/z): calculated for C_{40} H_{33} O_2 $[M+H]^+$ 545.2475, found 545.2467 (high resolution). ^{1}H NMR (600 MHz, $CDCl_3$, 25 °C) 7.31 (5 H, m, J=30 Hz), 7.22 (5 H, m, J=18 Hz), 7.02(2 H, m, J=24 Hz), 6.86(2 H, m, J=24 Hz), 4.90(1 H, s), 4.87(1 H, s). ^{13}C NMR (600 MHz, $CDCl_3$, 25 °C) 157.25, 144.17, 139.71, 136.94, 136.69, 132.56, 131.42, 128.55, 127.96, 127.57, 126.21, 114.02, 113.91, 69.90.

Synthesis of TPE-2T. The method of synthesizing TPE-2T is the same as that of TPE-2by-1. (TPE-2T is a mixture of cis and trans isomers) (Yield, 95 %). The ^{1}H NMR and ^{13}C NMR spectrum of TPE-2B (600 MHz, $CDCl_3$, 25 °C) δ (TMS, ppm) are showed as in Fig. S37 and S38. High resolution mass spectrometry of TPE-2T is showed in Fig. S39, (m/z): calculated for C_{36} H_{29} O_2 S_2 $[M+H]^+$ 557.1603, found 557.1603 (high resolution). ^{1}H NMR (600 MHz, $CDCl_3$, 25 °C) 7.32 (2 H, m, J=24 Hz), 7.10 (6 H, m, J=18 Hz), 6.96(2 H, m, J=30 Hz), 6.72(2 H, m, J=24 Hz), 5.00(1 H, s), 4.96(1 H, s). ^{13}C NMR (600 MHz, $CDCl_3$, 25 °C) 157.11, 144.14, 139.75, 137.94, 136.77, 132.57, 131.43, 127.60, 127.13, 126.24, 123.17, 114.00, 113.91,65.43.

Synthesis of TPE-2N. The method of synthesizing TPE-2N is the same as that of TPE-2by-1. (TPE-2N is a mixture of cis and trans isomers) (Yield, 97 %). The ^{1}H NMR and ^{13}C NMR spectrum of TPE-2N (600 MHz, $CDCl_3$, 25 °C) δ (TMS, ppm) are showed as in Fig. S40 and S41. High resolution mass spectrometry of TPE-2N is showed in Fig. S41, (m/z): calculated for C_{48} H_{36} O_2C_{48} $[M+Na]^+$ 667.2608, found 667.2608 (high resolution). ^{1}H NMR (600 MHz, $CDCl_3$, 25 °C) 7.76 (4 H, m, J=24 Hz), 7.40 (4 H, m, J=24Hz), 6.95(4 H, m, J=24 Hz), 6.86(2 H, m, J=24 Hz), 6.66(2 H, m, J=18 Hz) 5.05(2 H, s). ^{13}C NMR (600 MHz, $CDCl_3$, 25 °C) 157.27, 144.17, 139.74, 136.71, 134.51, 132.97, 132.97, 132.60, 131.44, 128.34, 127.96, 127.75, 127.59,126.44,126.24, 126.08, 125.43, 114.14, 70.01.

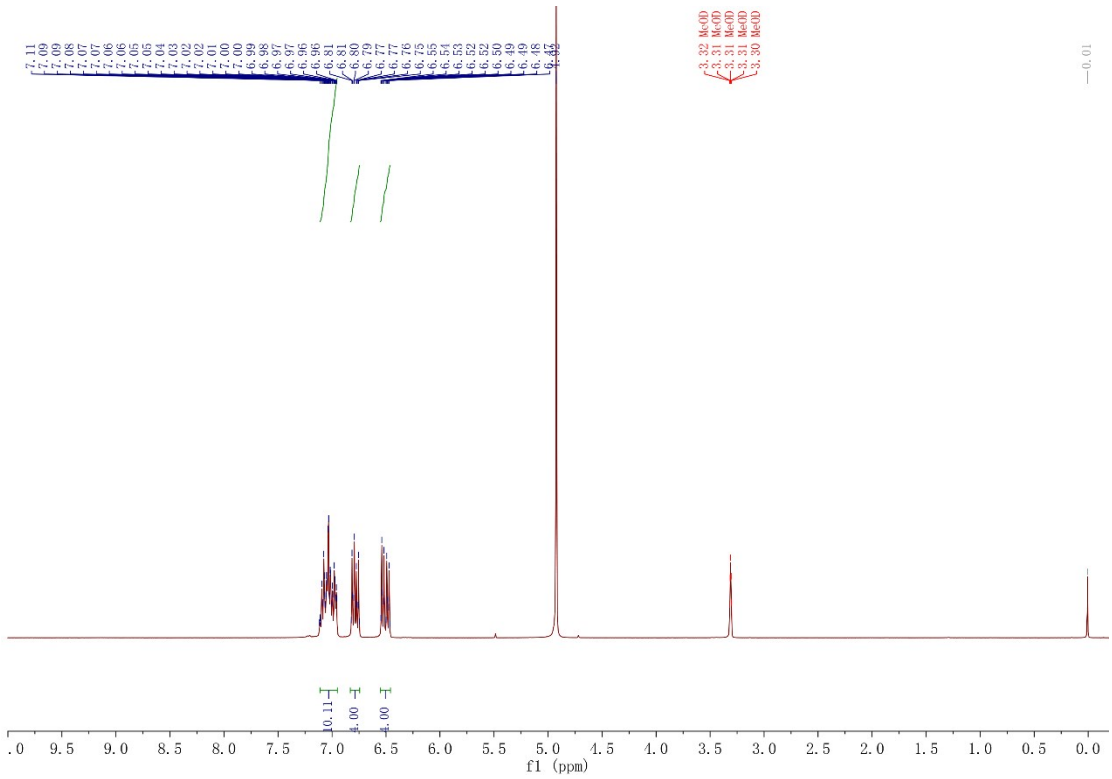

Fig. S1 ^{1}H NMR spectrum of compound TPE-2OH in CD_3OH.

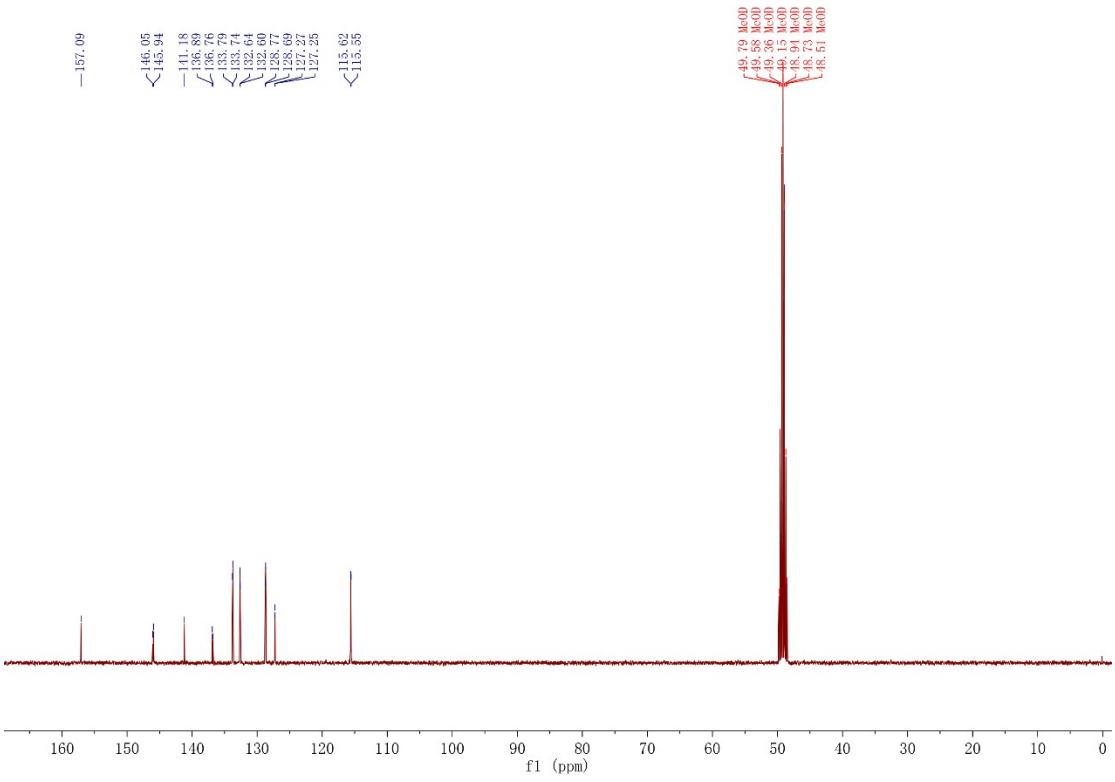

Fig. S2 ^{13}C NMR spectrum of compound TPE-2OH in CD_3OH.

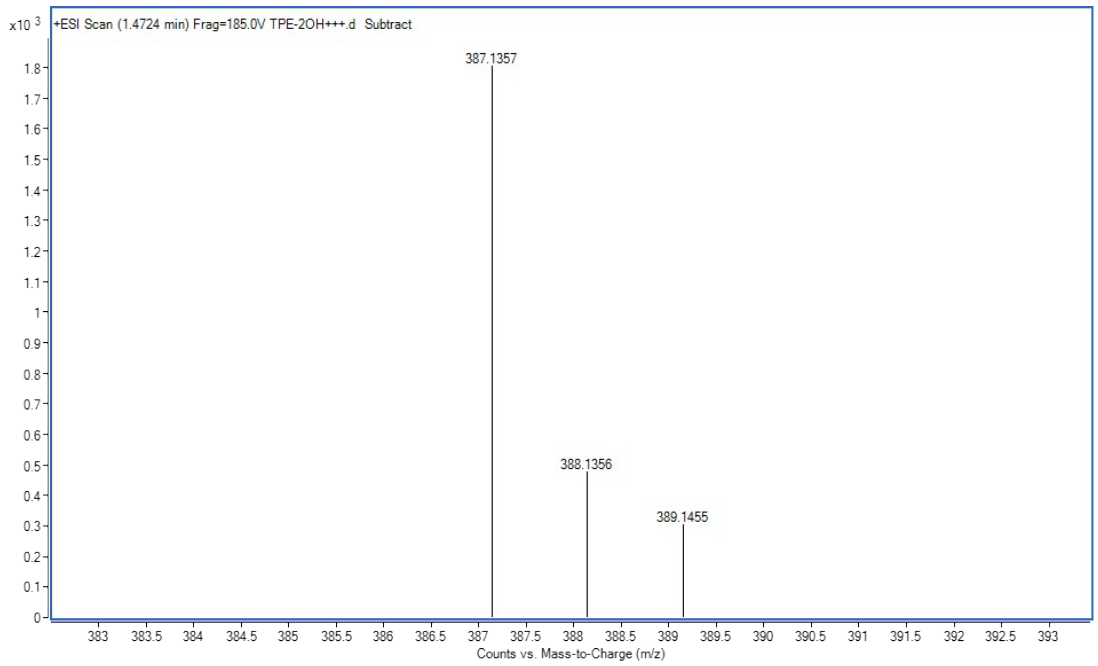

Fig. S3 High-resolution mass spectrum of TPE-2OH.

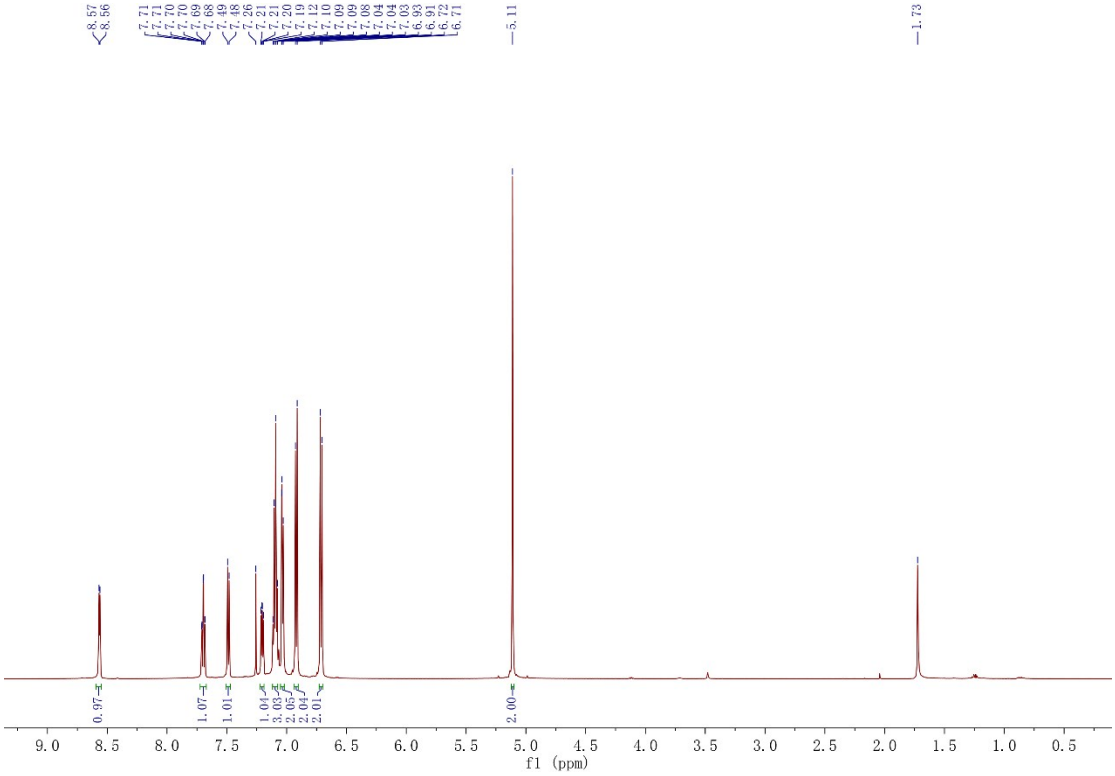

Fig. S4 ^{1}H NMR spectrum of compound TPE-2by-1-E in $CDCl_3$.

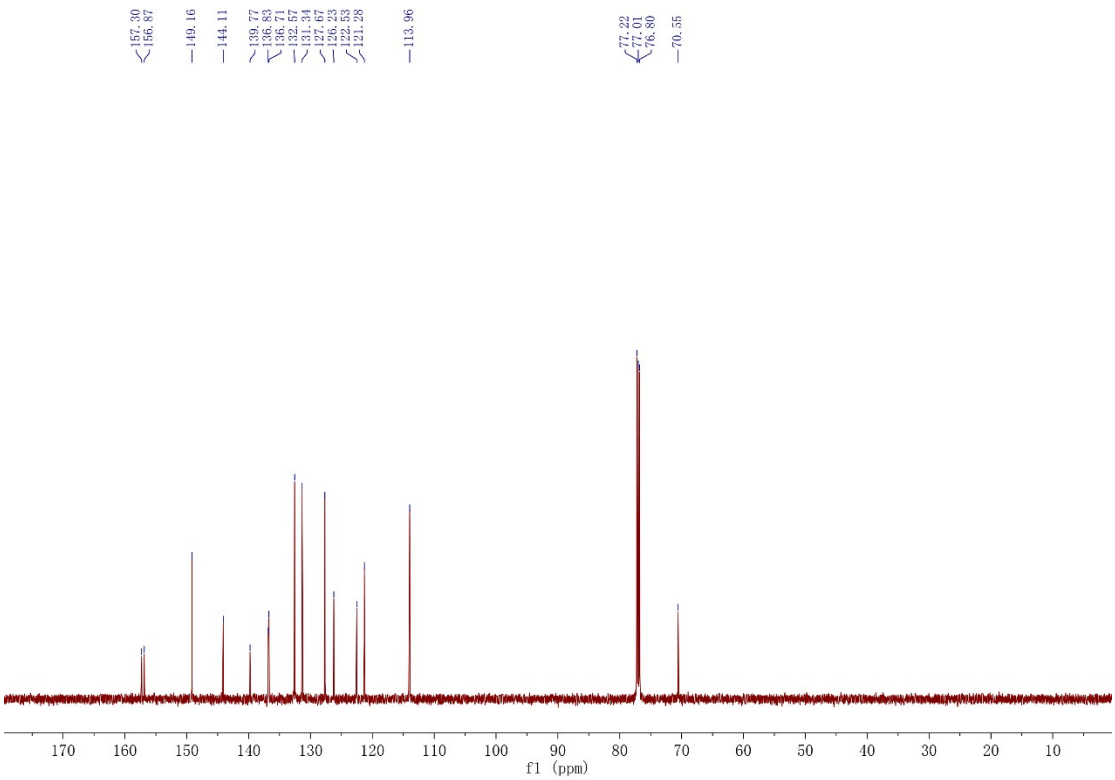

Fig. S5 ^{13}C NMR spectrum of compound TPE-2by-1-E in $CDCl_3$.

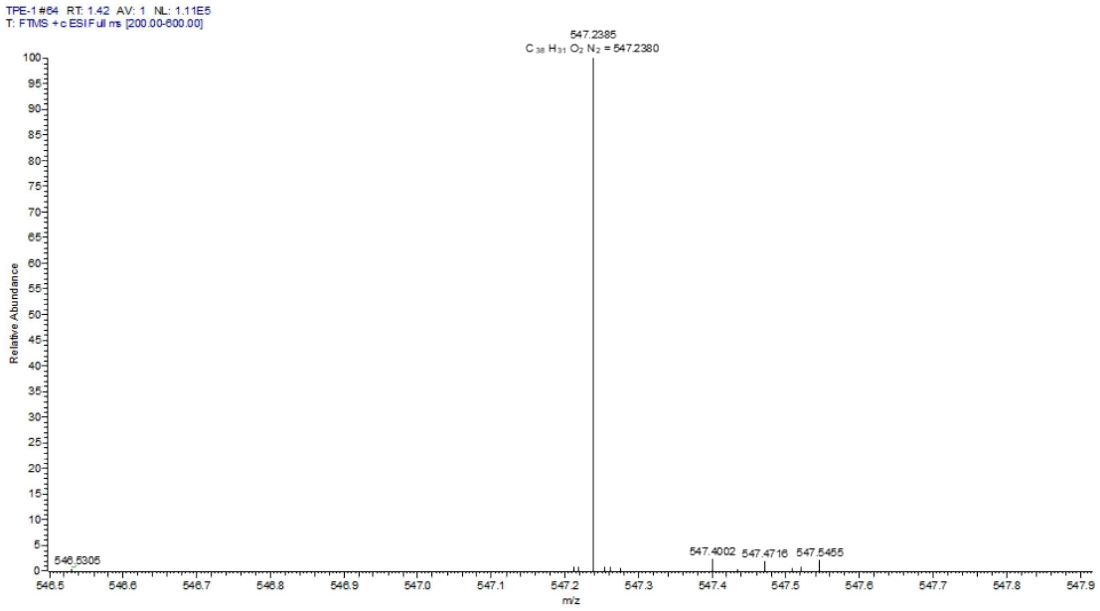

Fig. S6 High-resolution mass spectrum of compound TPE-2by-1-E.

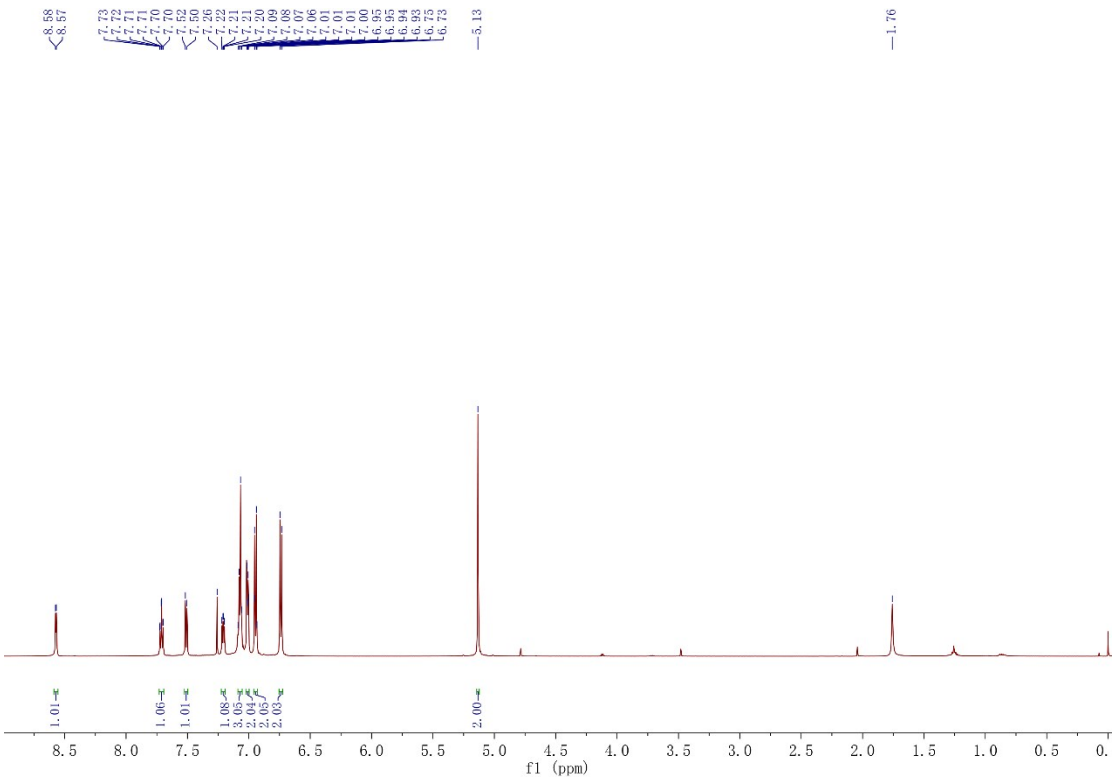

Fig. S7 ^{1}H NMR spectrum of compound TPE-2by-1-Z in $CDCl_3$.

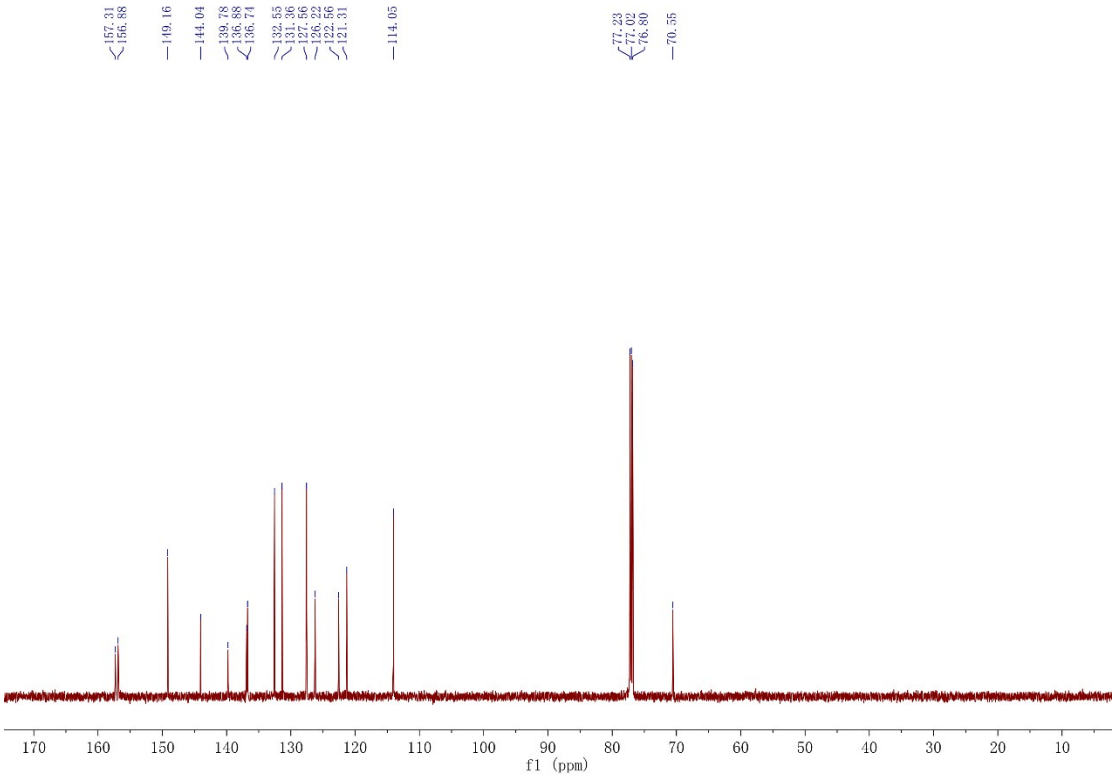

Fig. S8 ^{13}C NMR spectrum of compound TPE-2by-1-Z in $CDCl_3$.

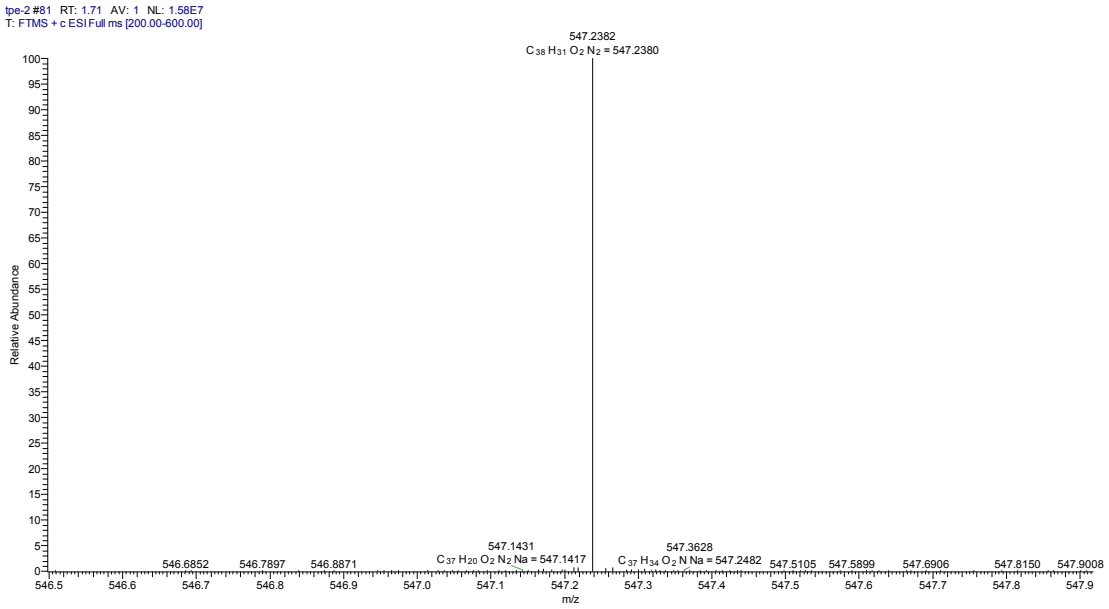

Fig. S9 High-resolution mass spectrum of compound TPE-2by-1-Z.

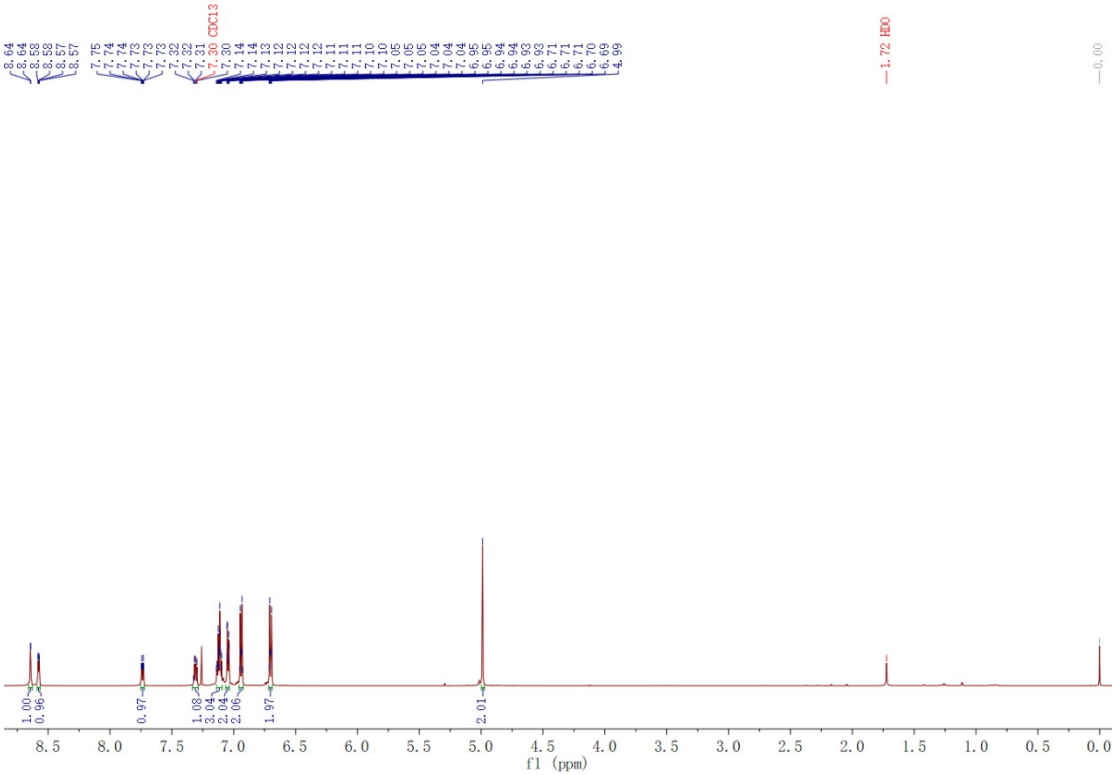

Fig. S10 ^{1}H NMR spectrum of compound TPE-2by-2-E in $CDCl_3$.

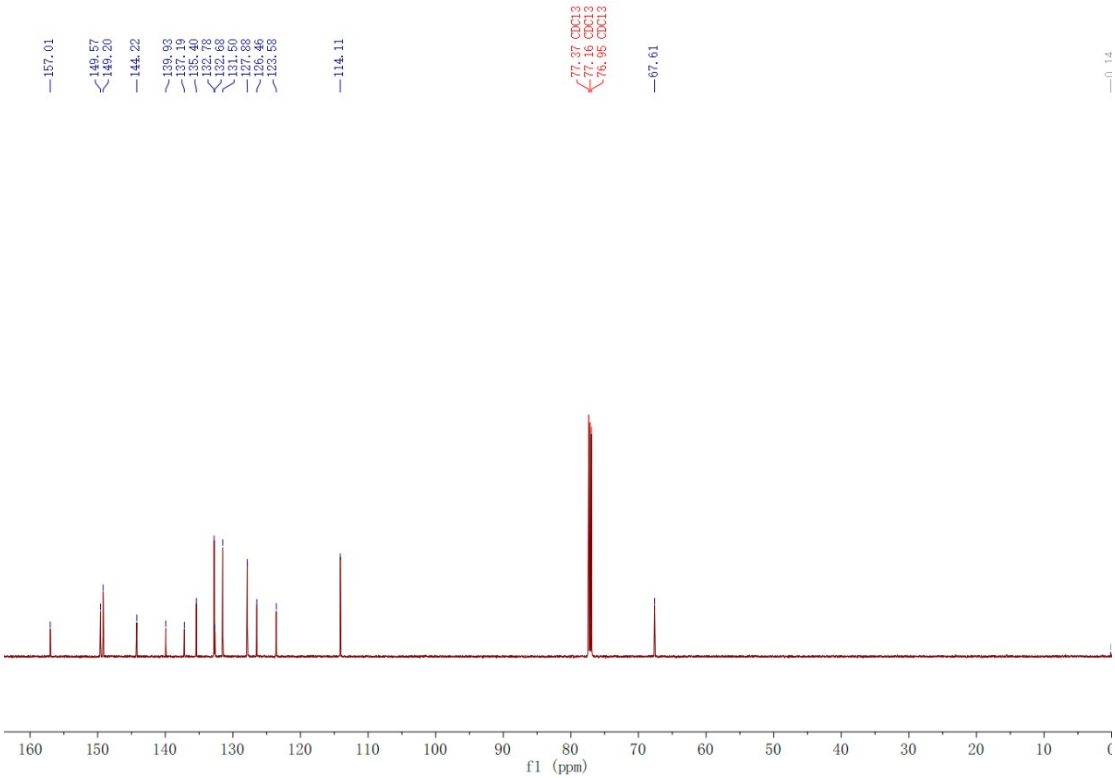

Fig. S11 ^{13}C NMR spectrum of compound TPE-2by-2-E in $CDCl_3$.

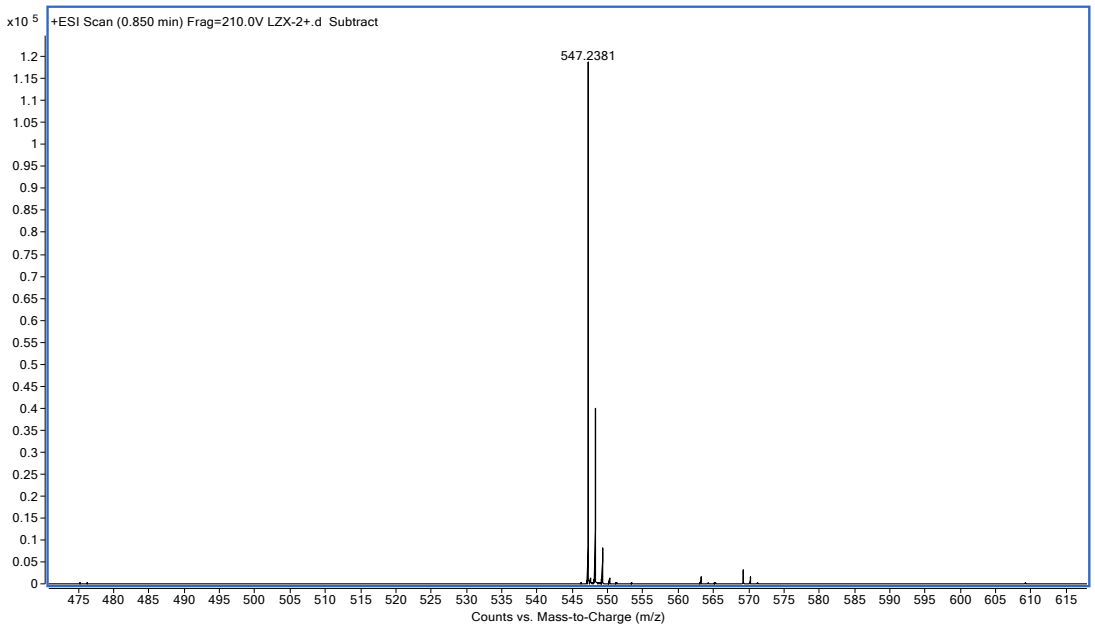

Fig. S12 High-resolution mass spectrum of compound TPE-2by-2-E.

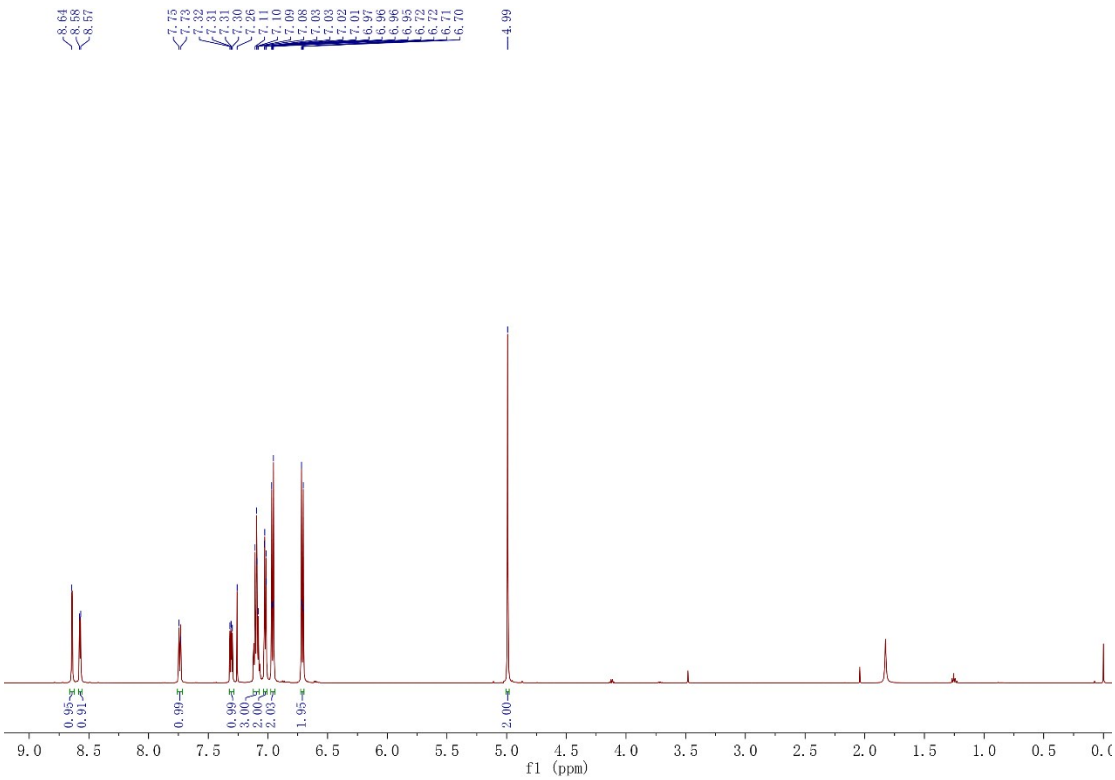

Fig. S13 ^{1}H NMR spectrum of compound TPE-2by-2-Z in $CDCl_3$.

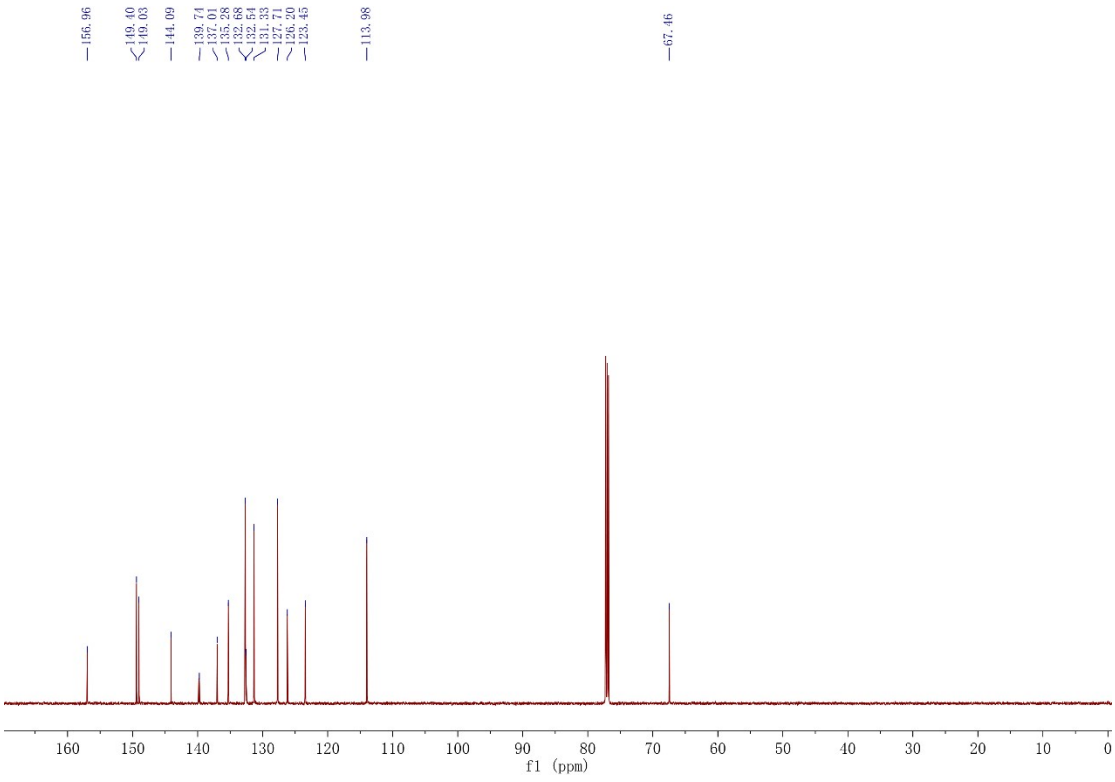

Fig. S14 ^{13}C NMR spectrum of compound TPE-2by-2-Z in $CDCl_3$.

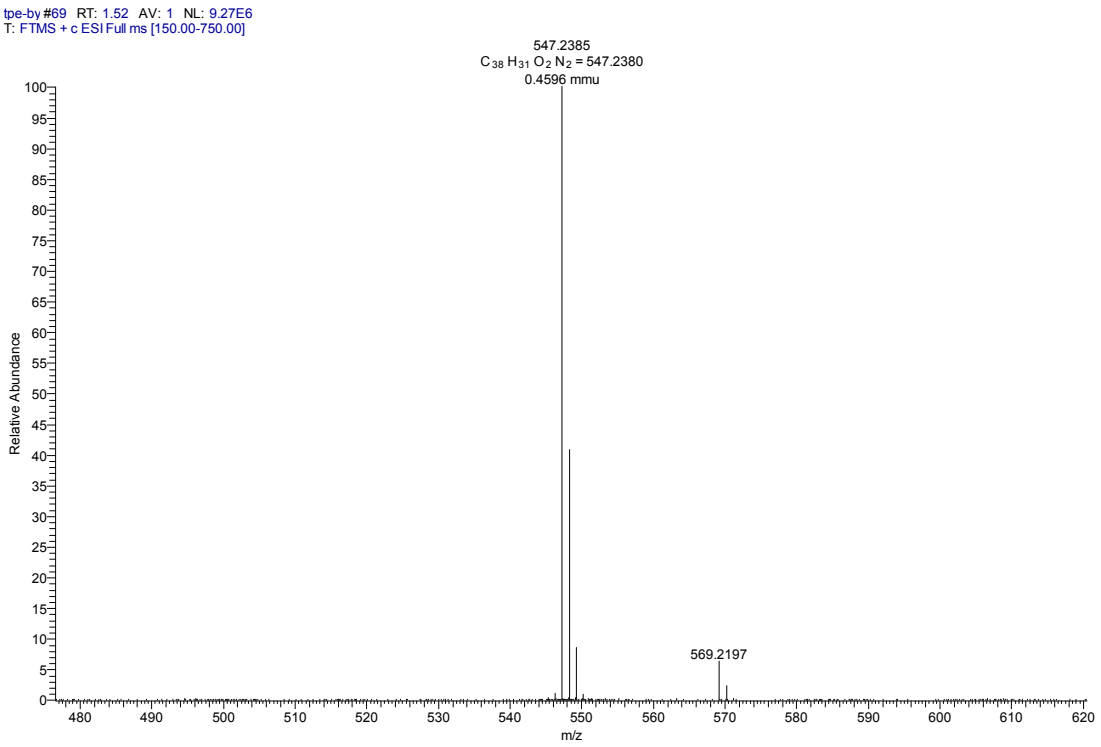

Fig. S15 High-resolution mass spectrum of compound TPE-2by-2-Z.

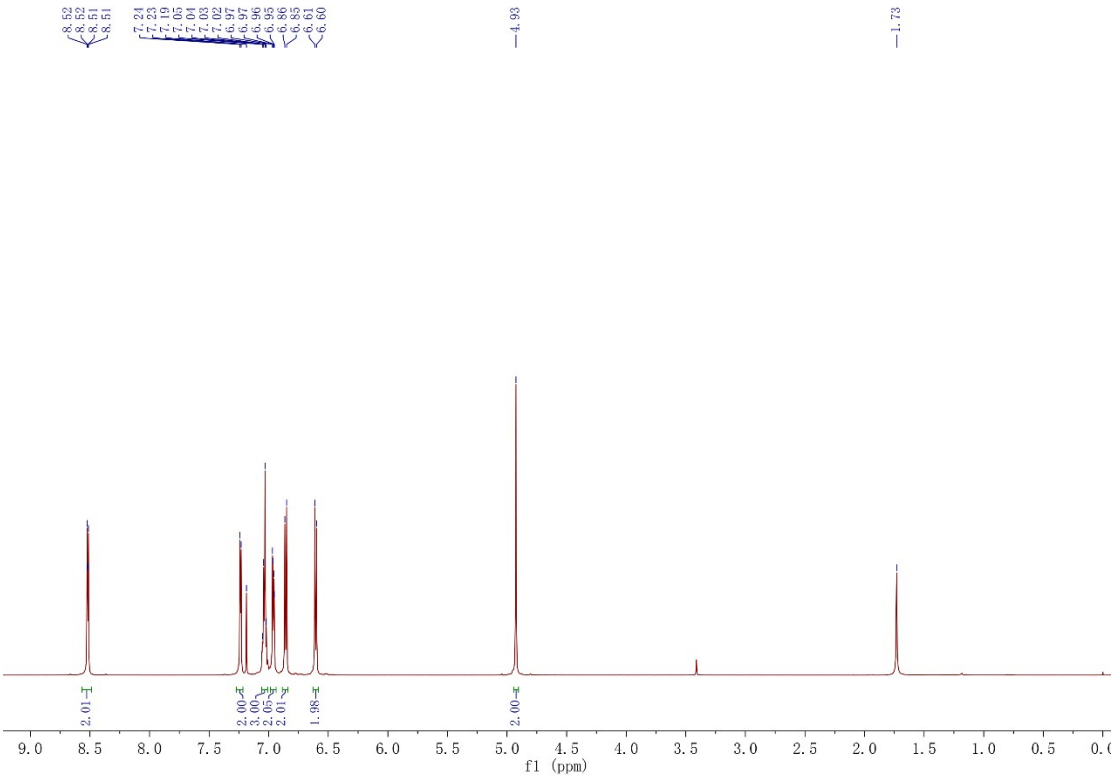

Fig. S16 ^{1}H NMR spectrum of compound TPE-2by-3-E in $CDCl_3$.

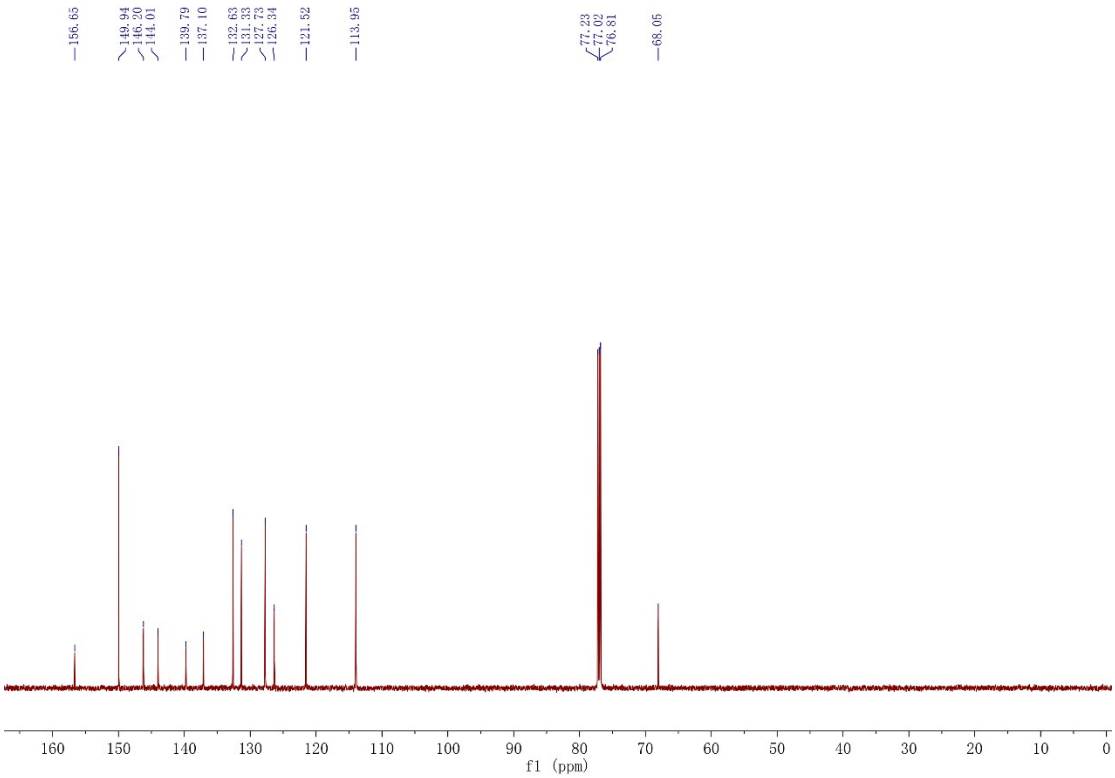

Fig. S17 ^{13}C NMR spectrum of compound TPE-2by-3-E in $CDCl_3$.

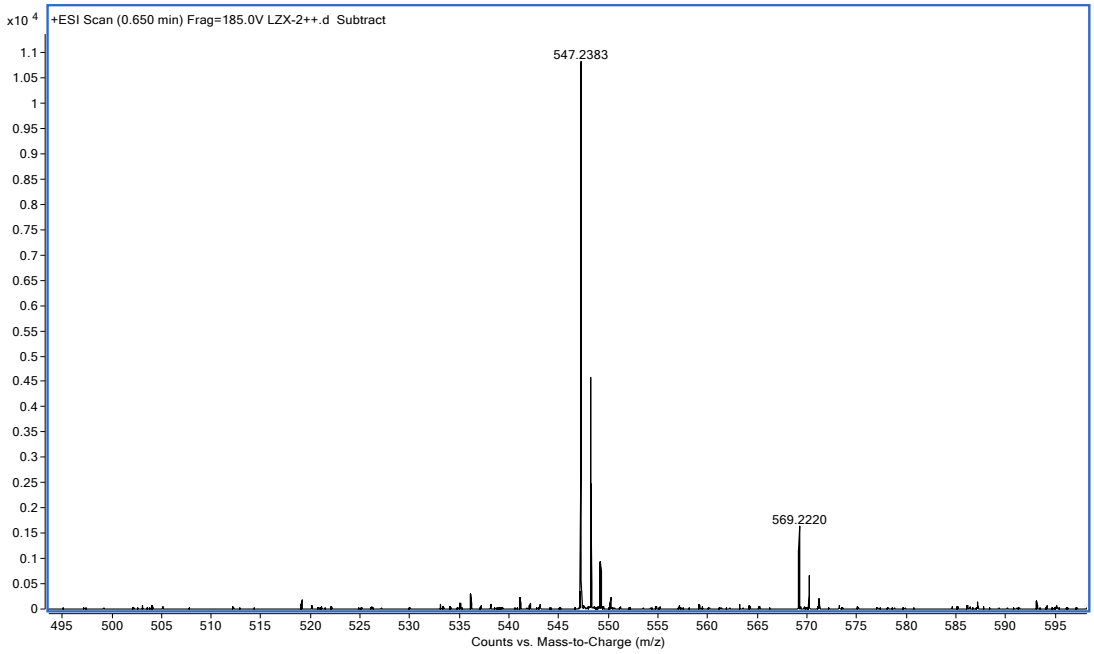

Fig. S18 High-resolution mass spectrum of compound TPE-2by-3-E.

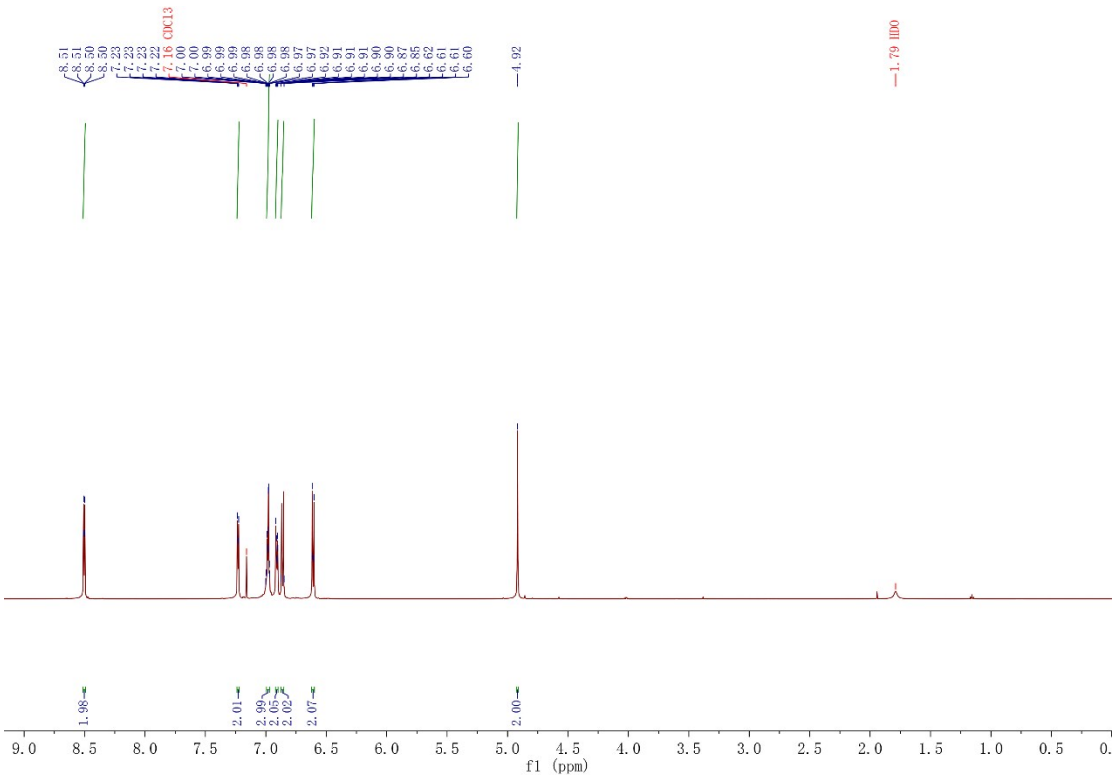

Fig. S19 ^{1}H NMR spectrum of compound TPE-2by-3-Z in $CDCl_3$.

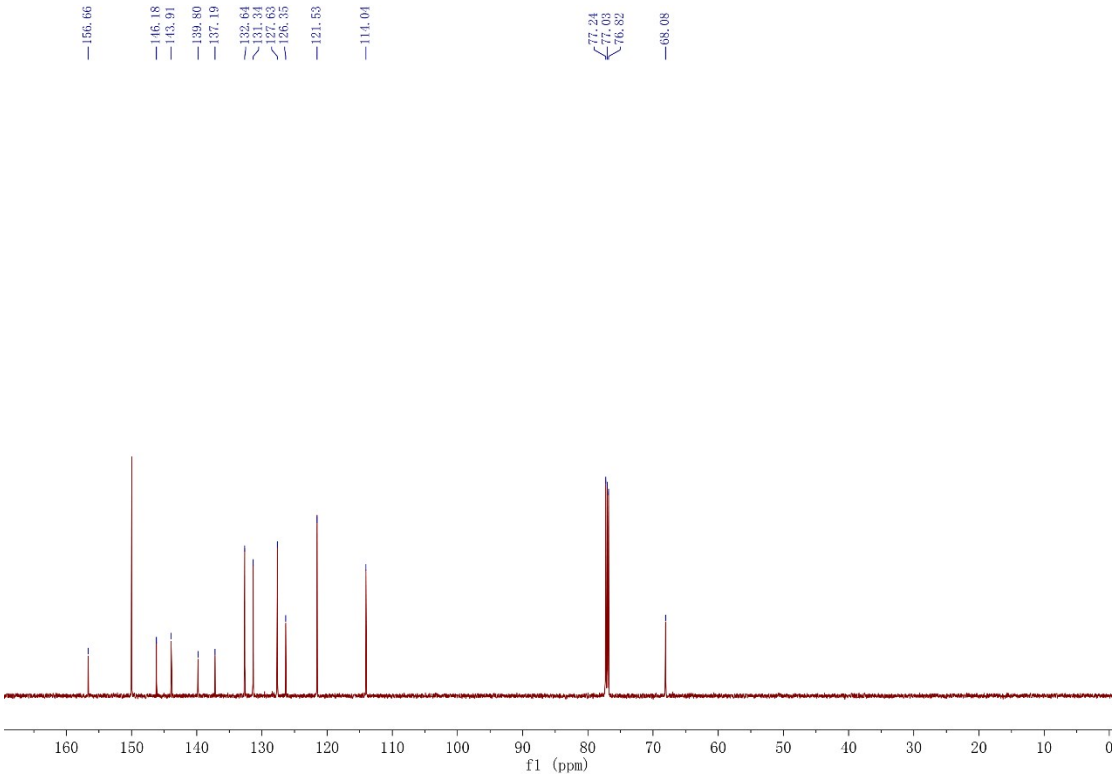

Fig. S20 ^{13}C NMR spectrum of compound TPE-2by-3-Z in $CDCl_3$.

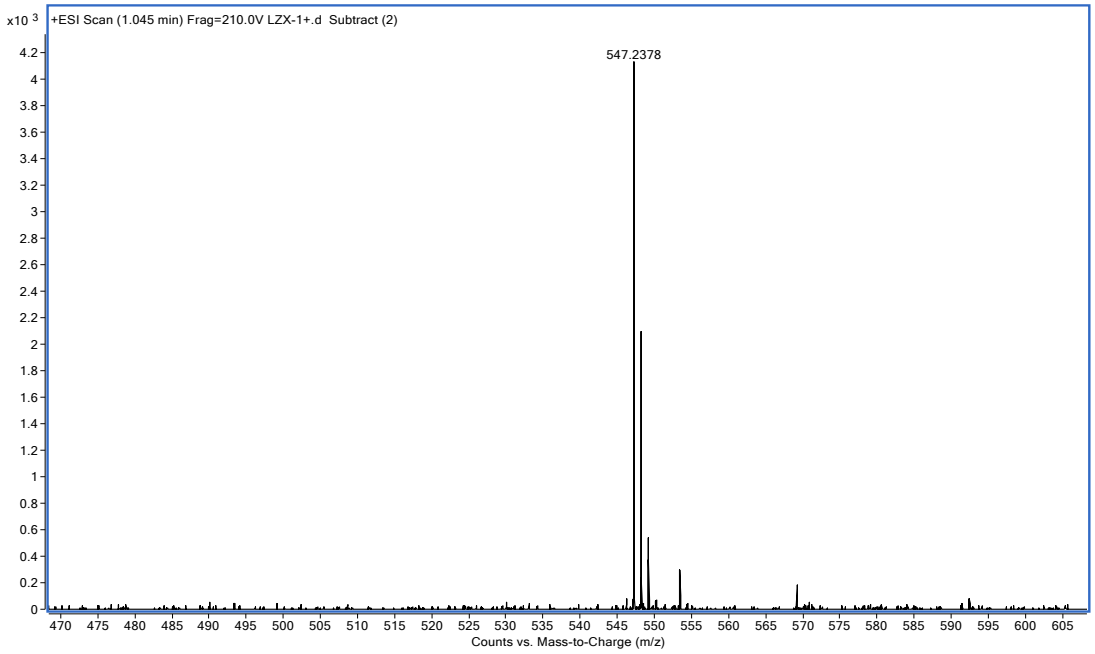

Fig. S21 High-resolution mass spectrum of compound TPE-2by-3-Z.

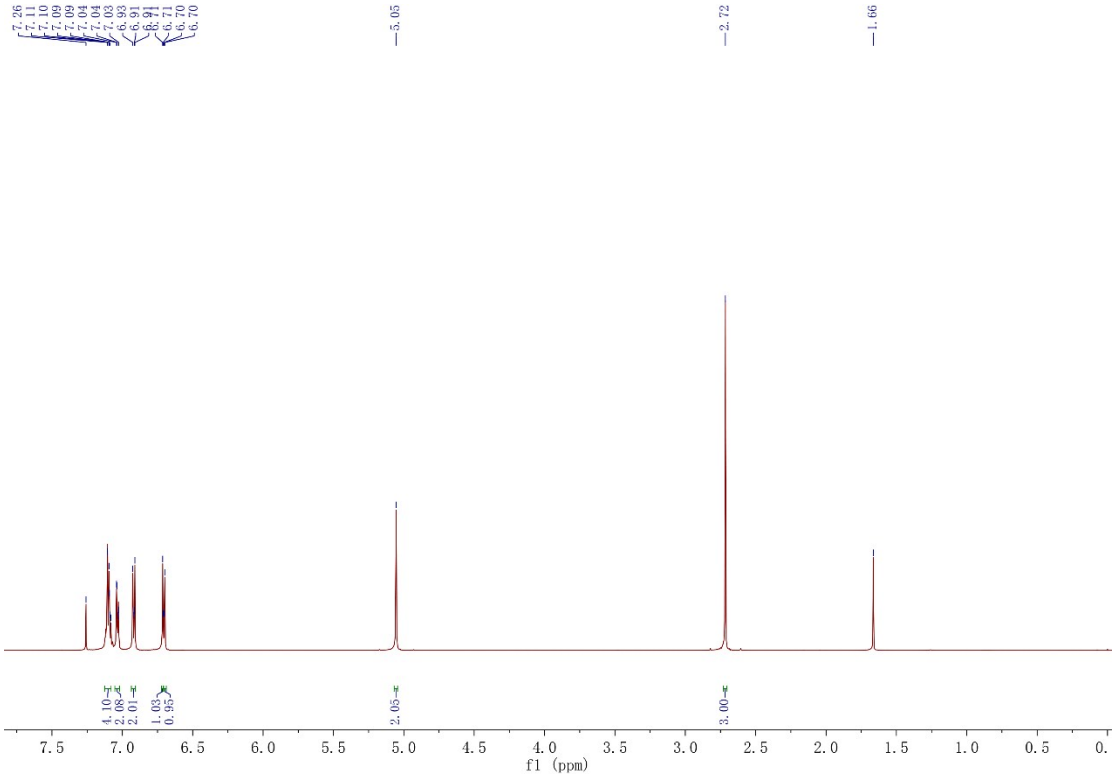

Fig. S22 ^{1}H NMR spectrum of compound TPE-2TZ-E in $CDCl_3$.

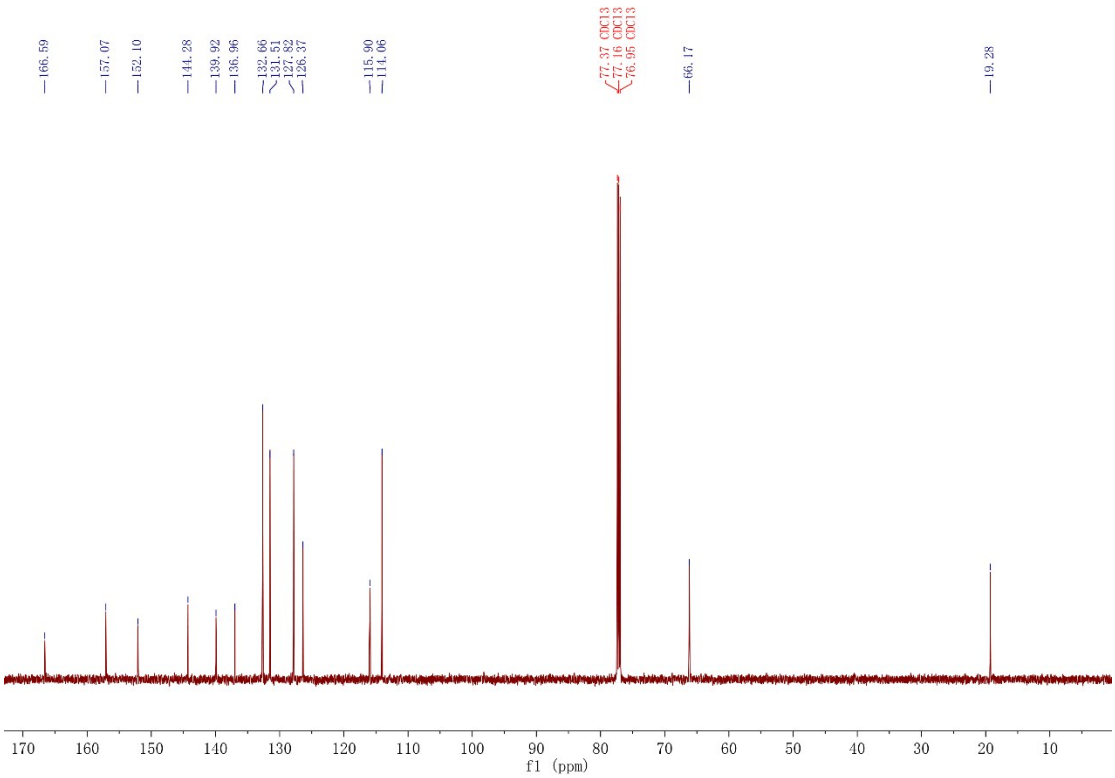

Fig. S23 ^{13}C NMR spectrum of compound TPE-2TZ-E in $CDCl_3$.

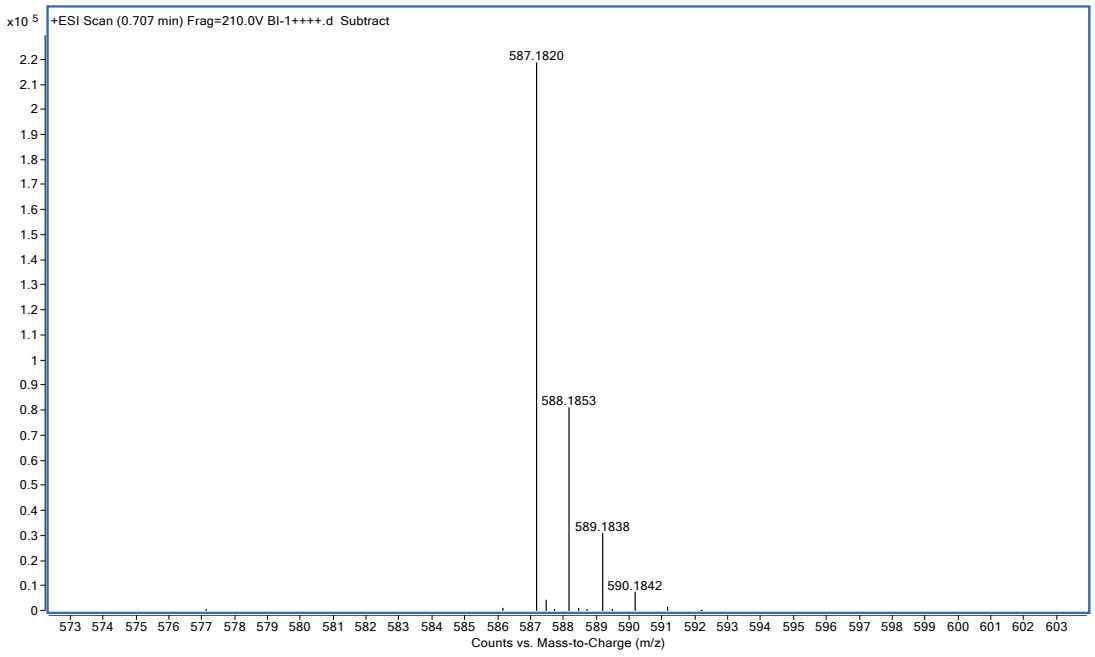

Fig. S24 High-resolution mass spectrum of compound TPE-2TZ-E.

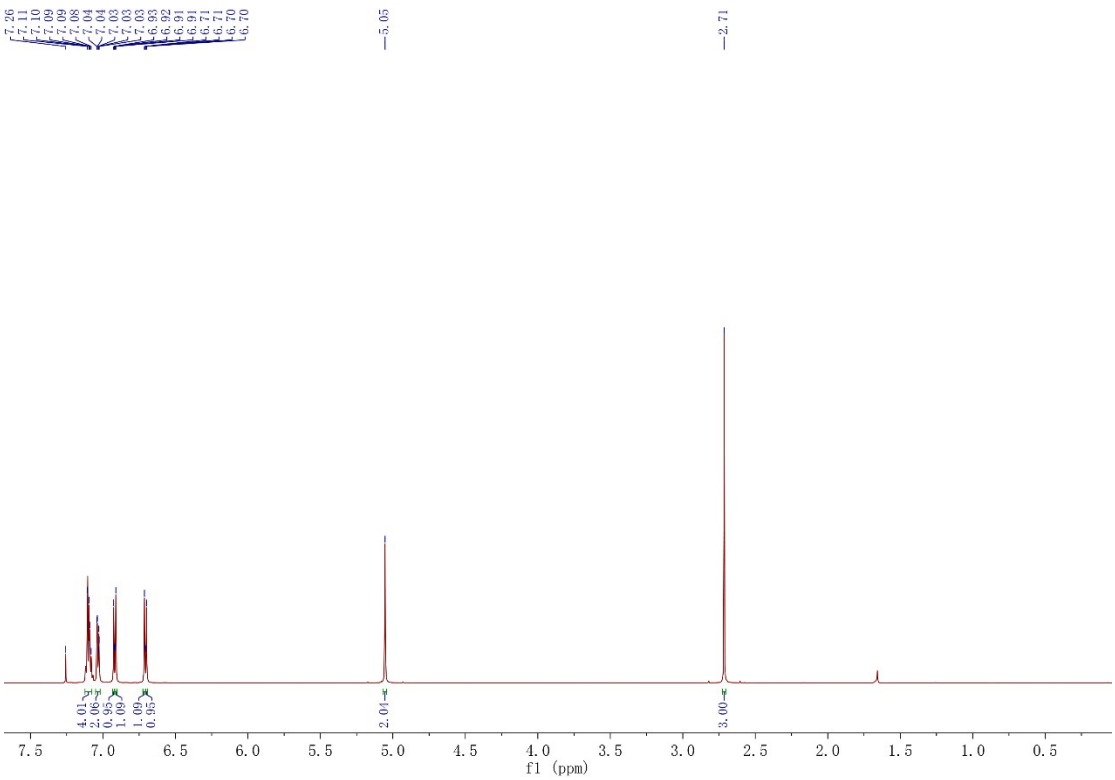

Fig. S25 ^{1}H NMR spectrum of compound TPE-2TZ-Z in $CDCl_3$.

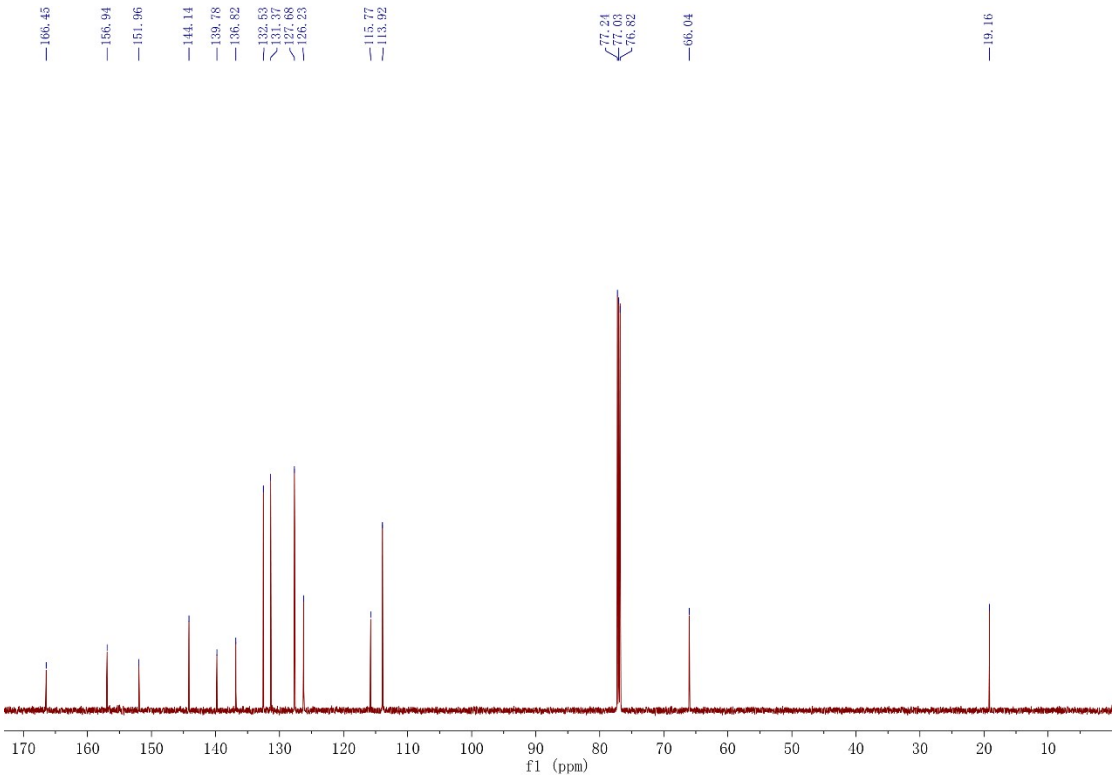

Fig. S26 ^{13}C NMR spectrum of compound TPE-2TZ-Z in $CDCl_3$.

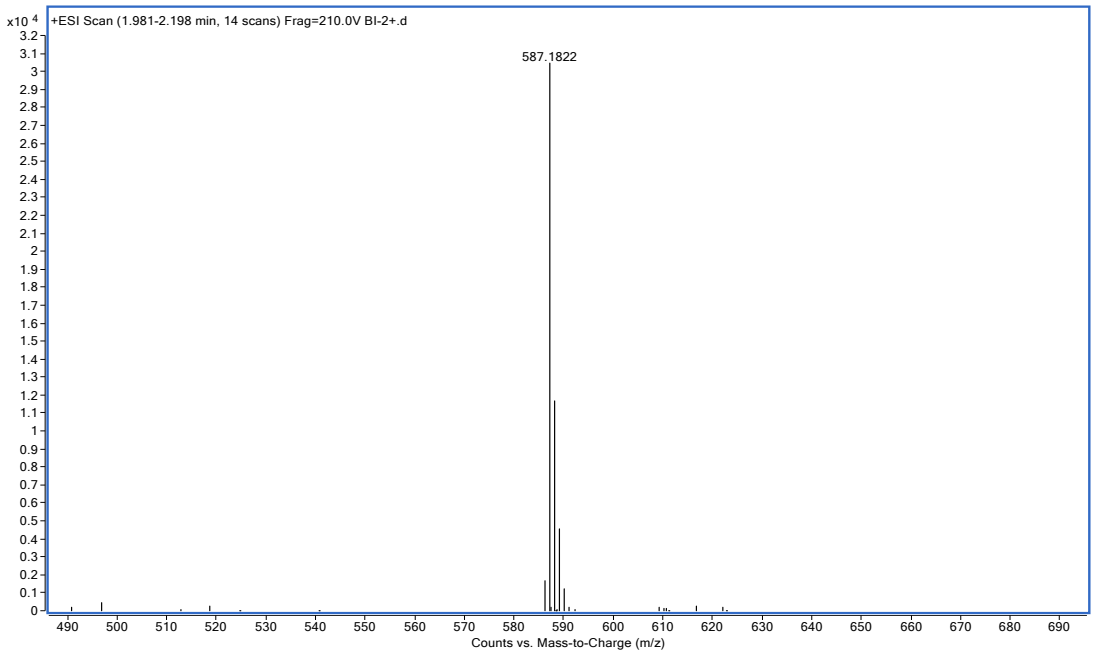

Fig. S27 High-resolution mass spectrum of compound TPE-2TZ-Z.

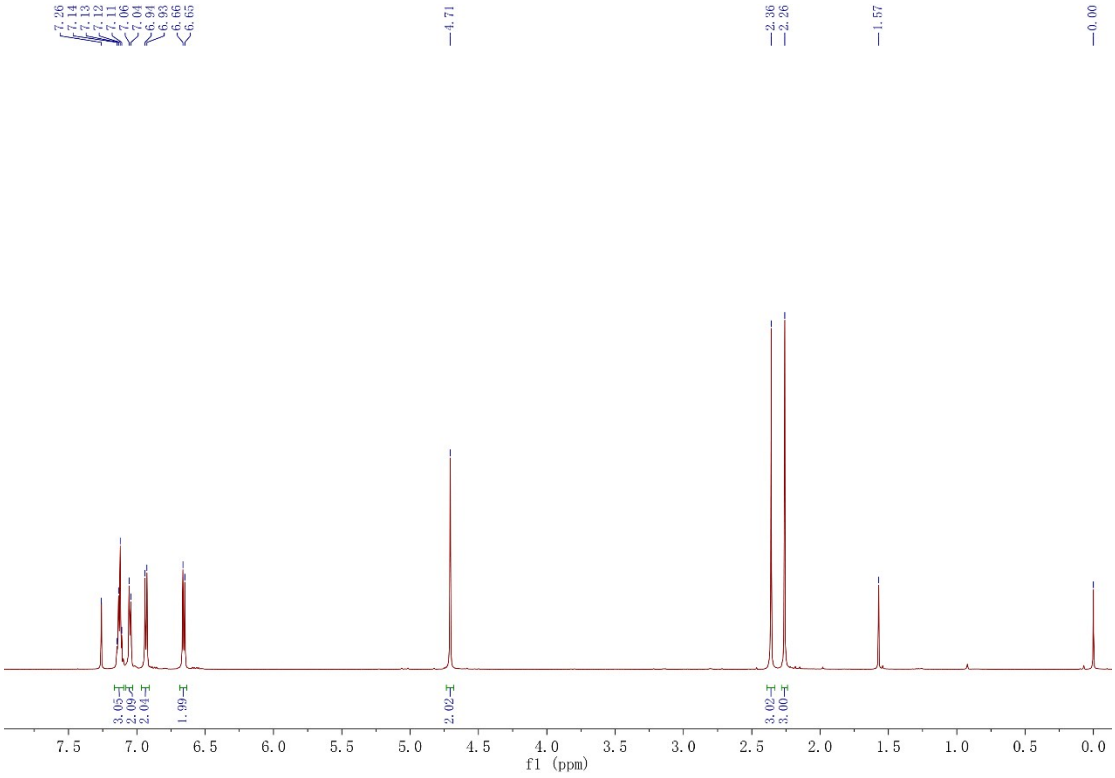

Fig. S28 ^{1}H NMR spectrum of compound TPE-2EZ-E in $CDCl_3$.

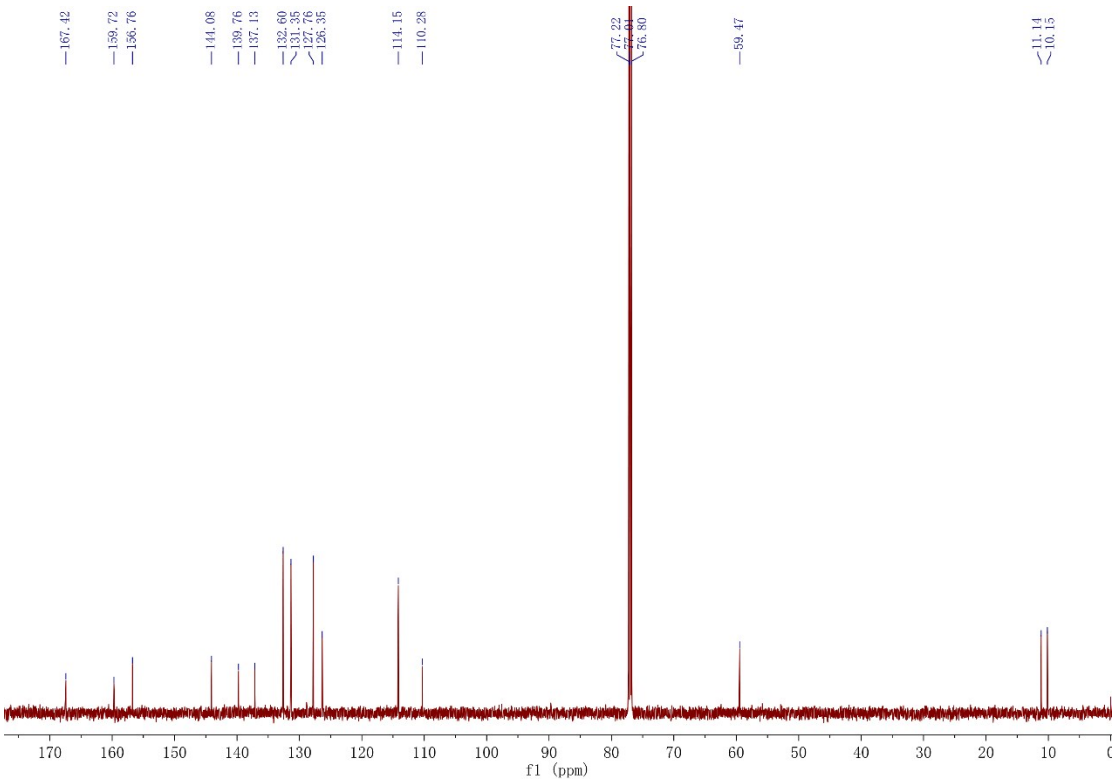

Fig. S29 ^{13}C NMR spectrum of compound TPE-2EZ-E in CDCl3.

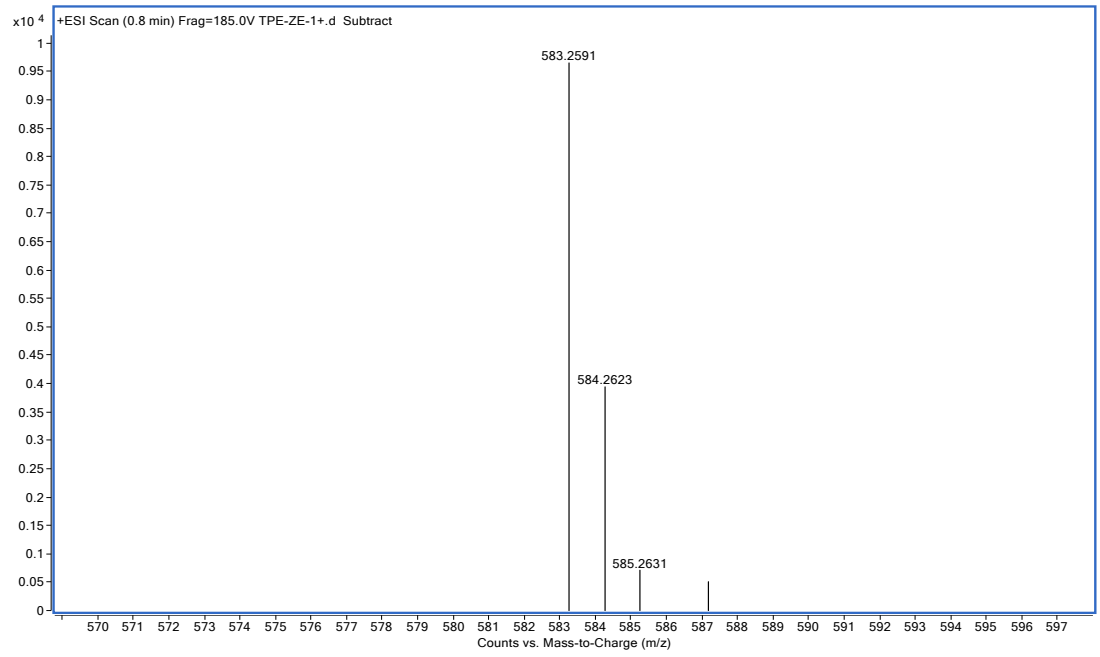

Fig. S30 High-resolution mass spectrum of compound TPE-2EZ-E.

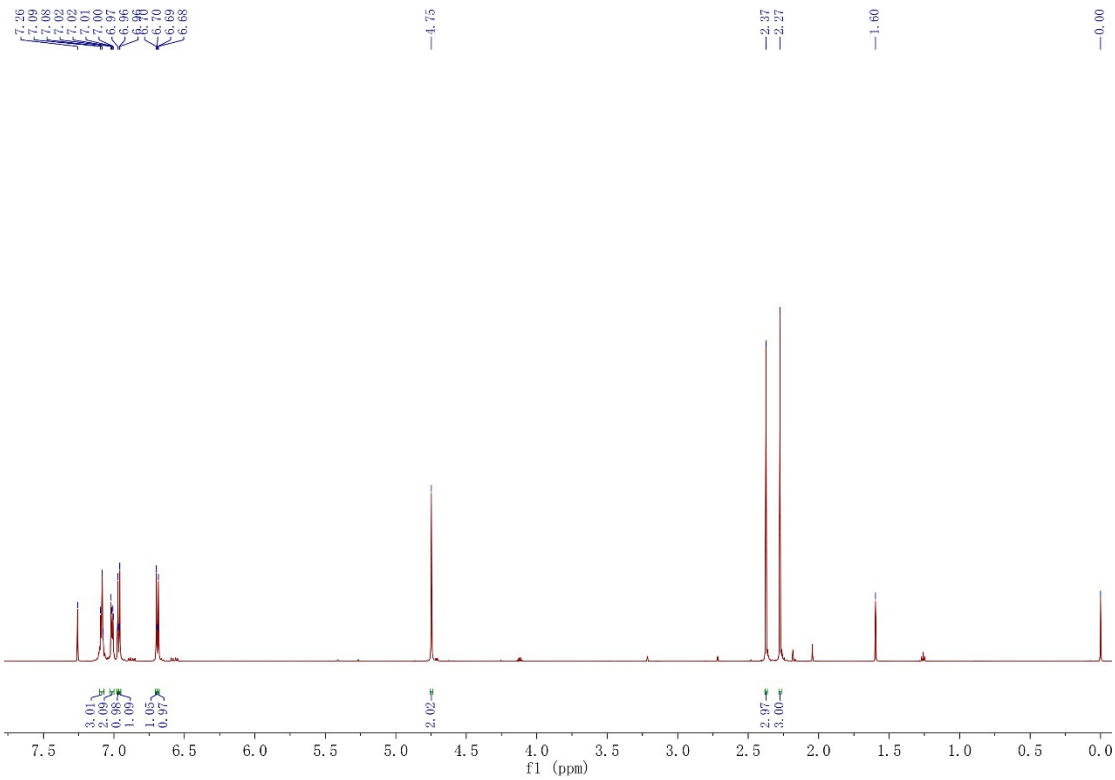

Fig. S31 ^{1}H NMR spectrum of compound TPE-2EZ-Z in $CDCl_3$.

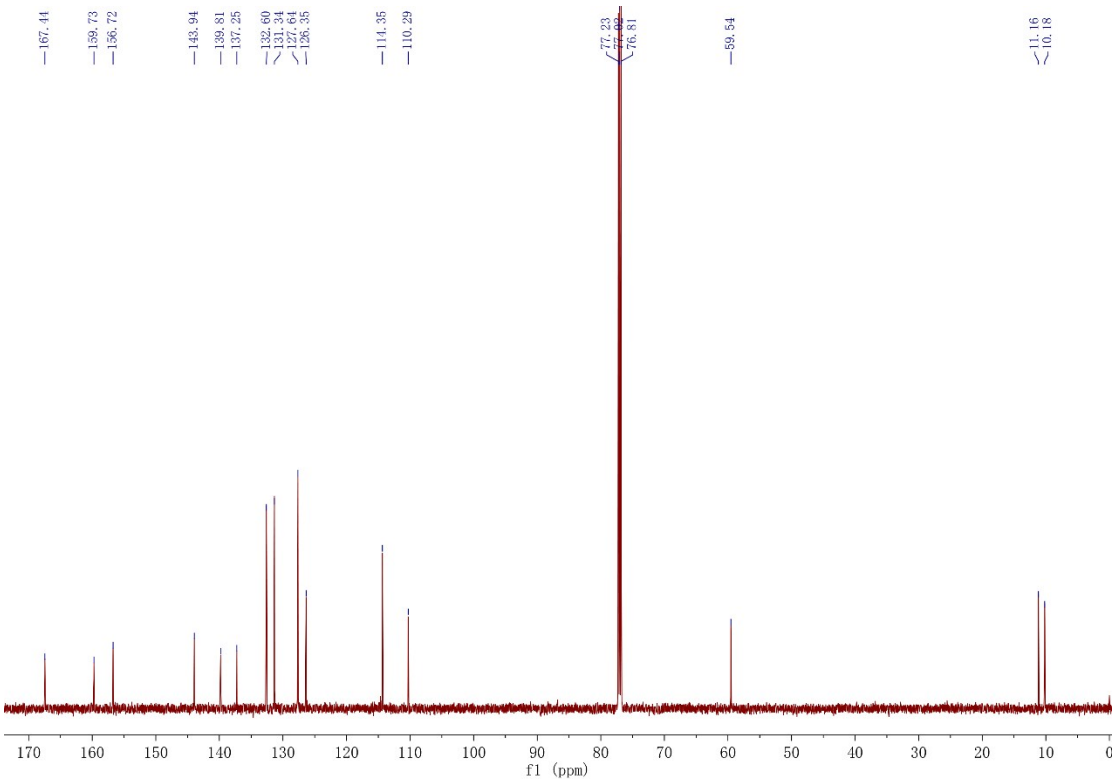

Fig. S32 ^{13}C NMR spectrum of compound TPE-2EZ-Z in $CDCl_3$.

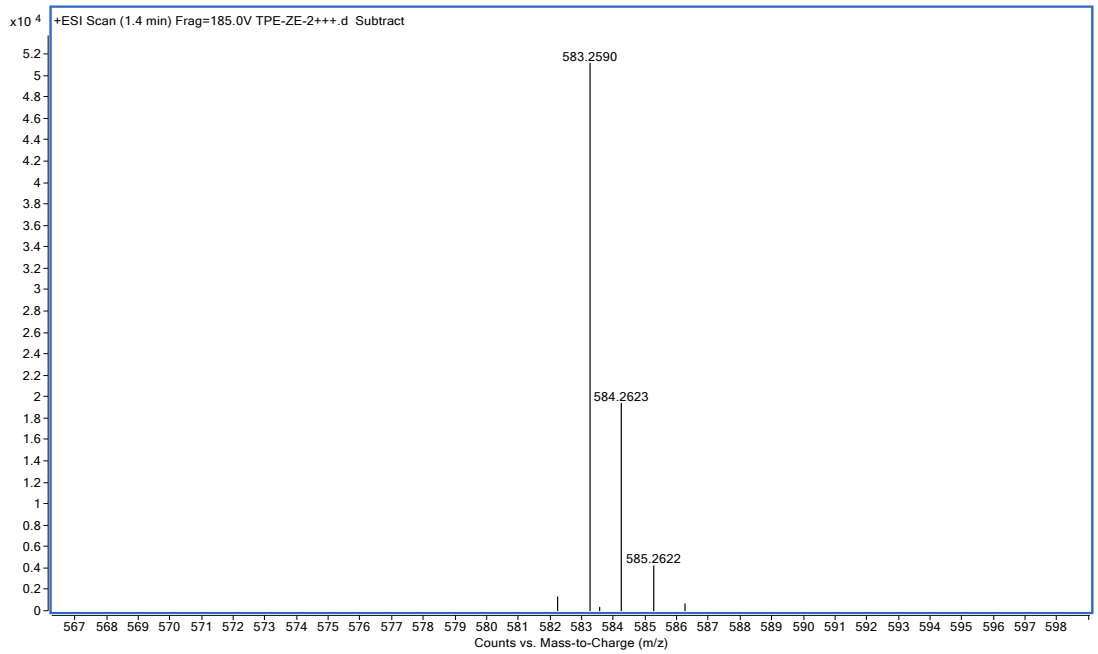

Fig. S33 High-resolution mass spectrum of compound TPE-2EZ-Z.

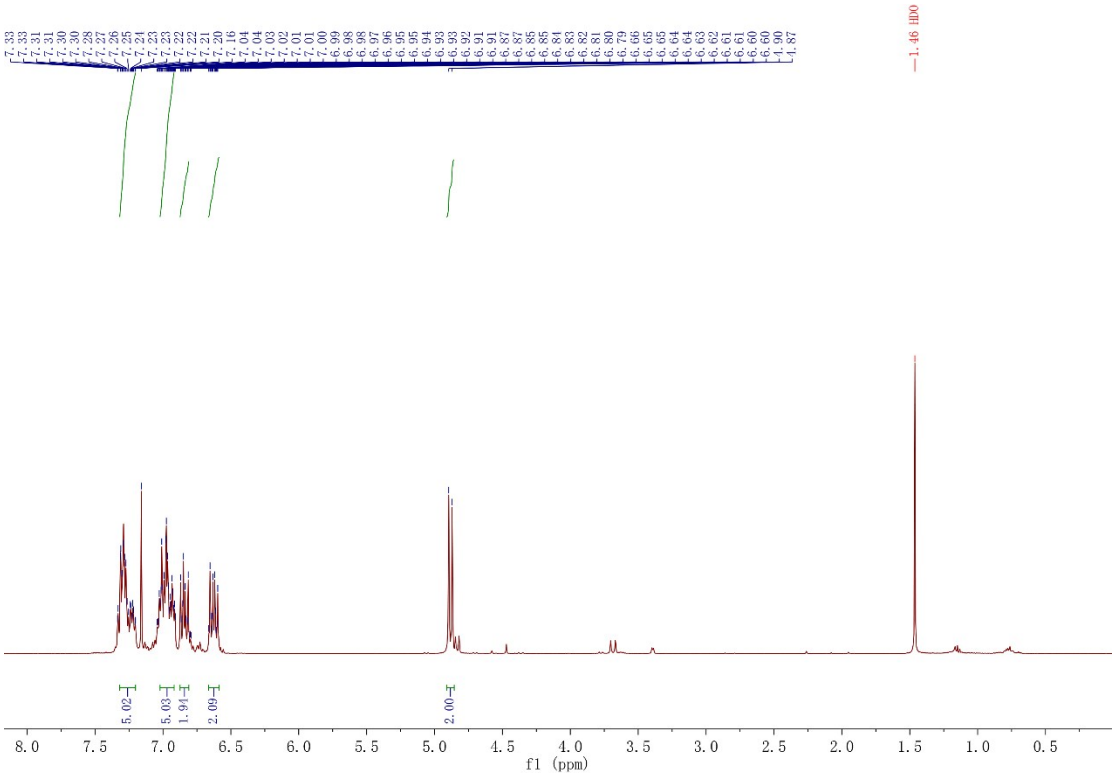

Fig. S34 ^{1}H NMR spectrum of compound TPE-2B in $CDCl_3$.

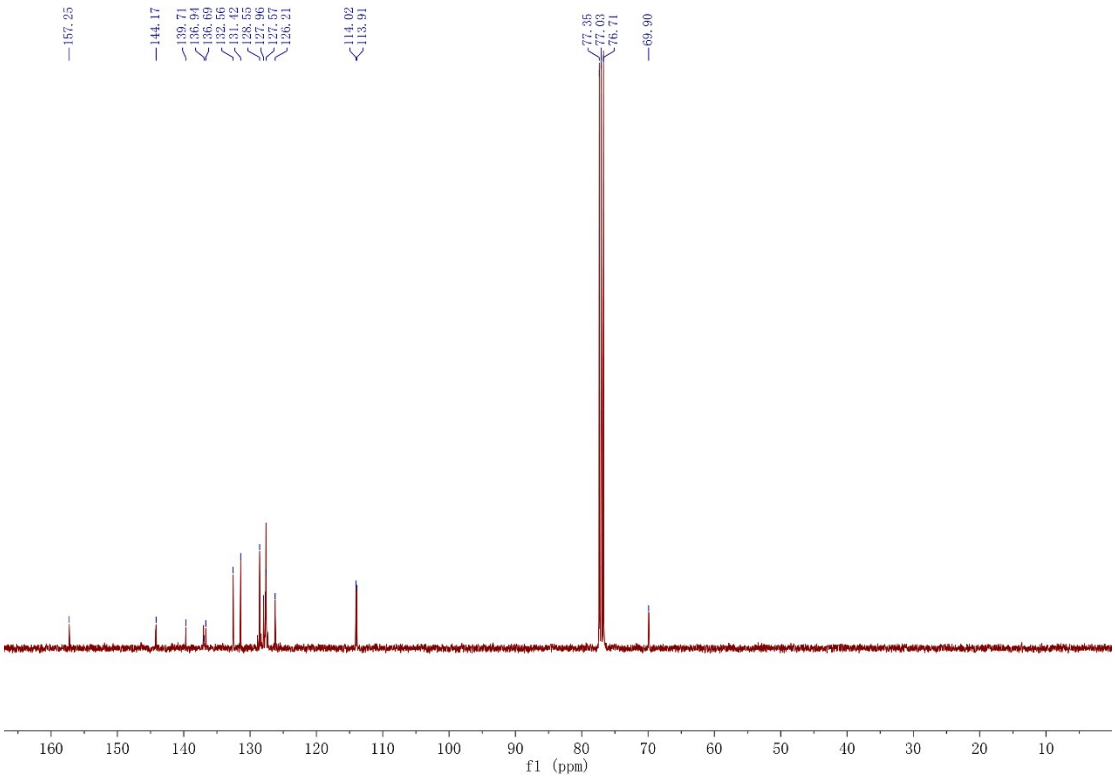

Fig. S35 ^{13}C NMR spectrum of compound TPE-2B in $CDCl_3$.

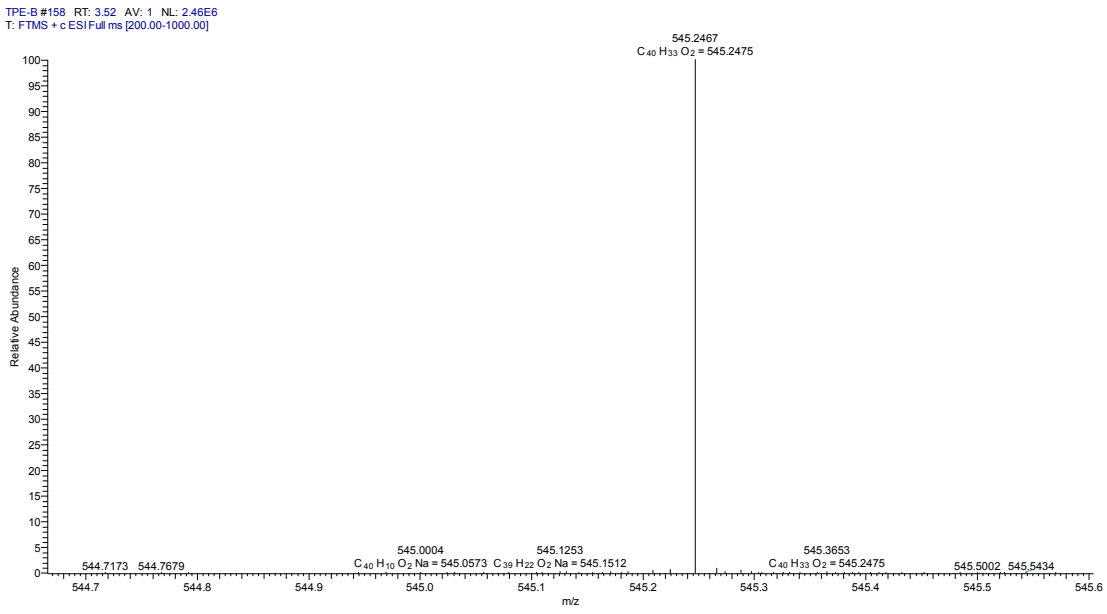

Fig. S36 High-resolution mass spectrum of compound TPE-2B.

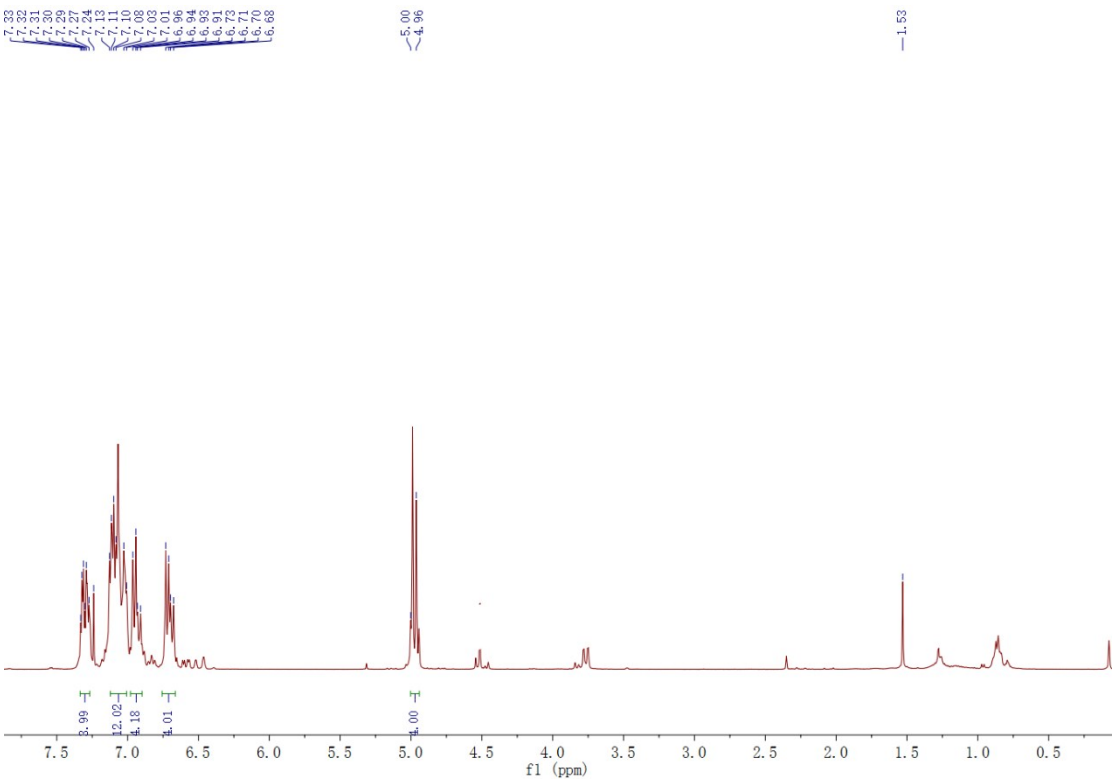

Fig. S37 ^{1}H NMR spectrum of compound TPE-2T in $CDCl_3$.

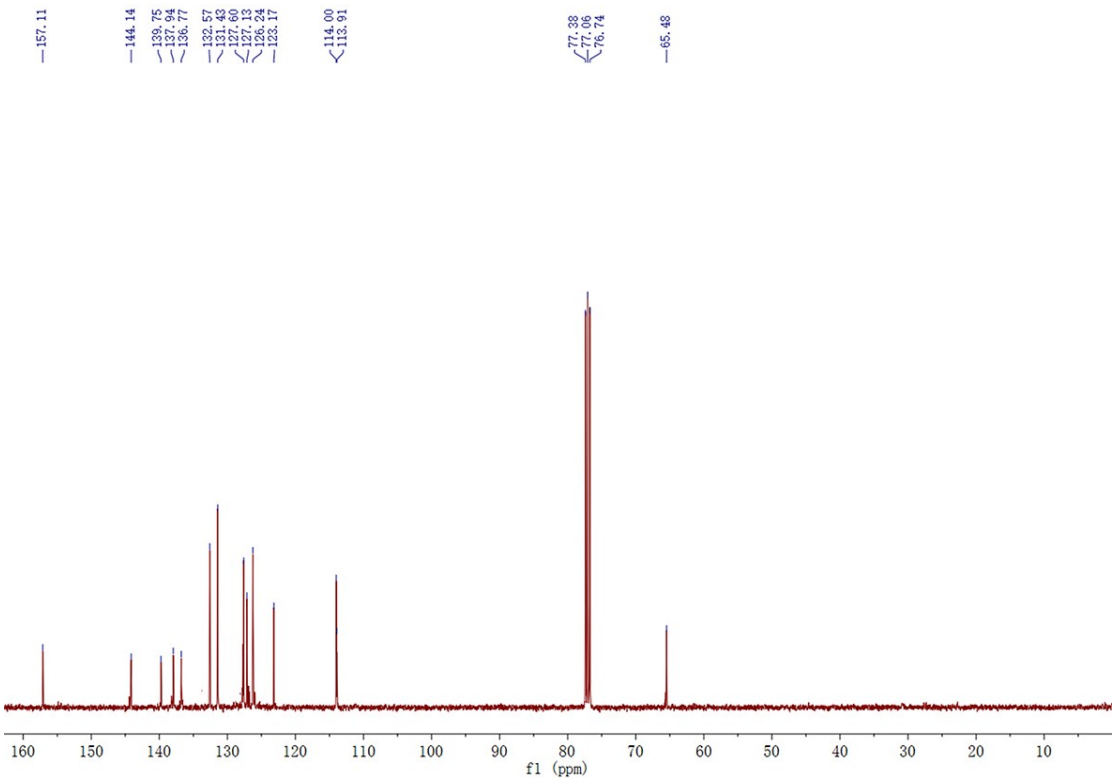

Fig. S38 ^{13}C NMR spectrum of compound TPE-2T in $CDCl_3$.

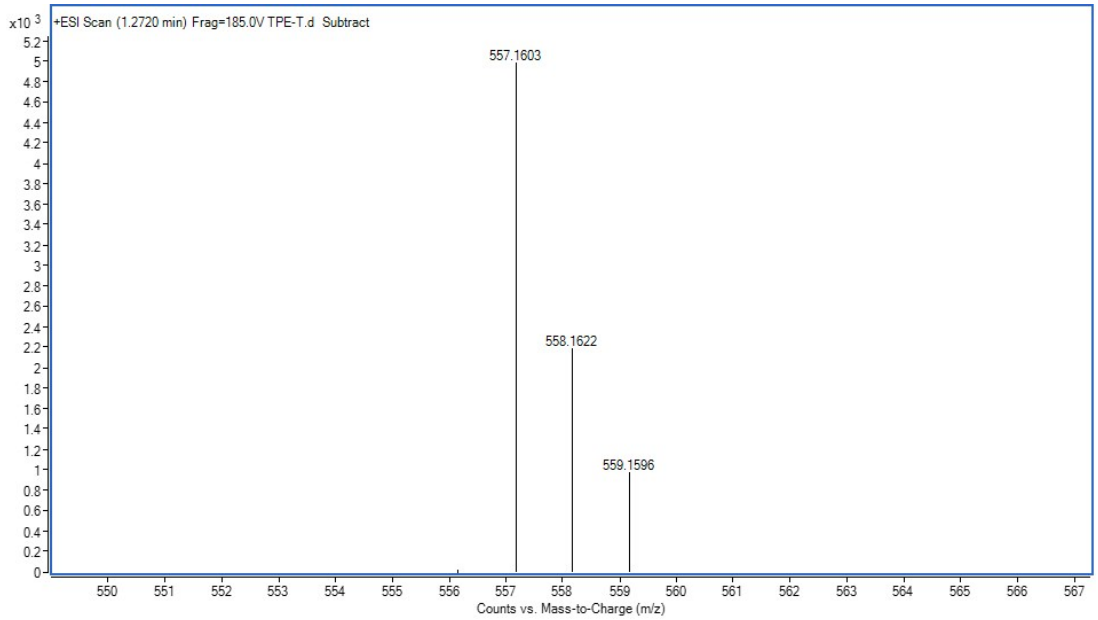

Fig. S39 High-resolution mass spectrum of compound TPE-2T.

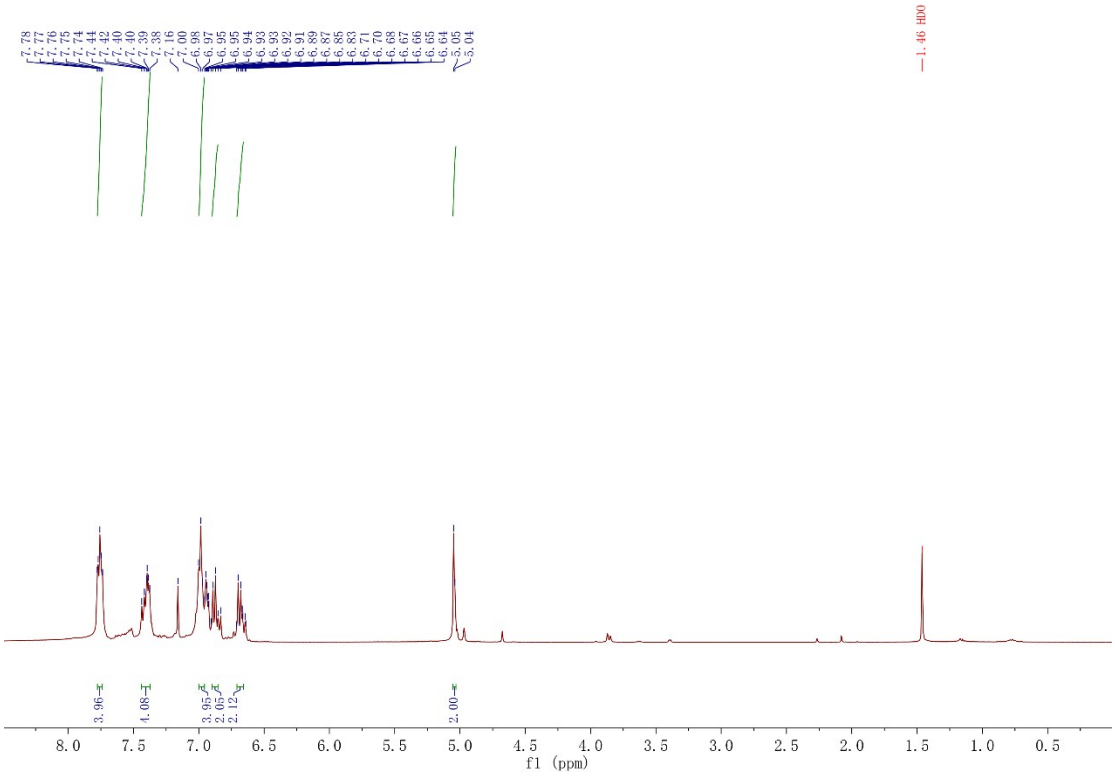

Fig. S40 ^{1}H NMR spectrum of compound TPE-2N in $CDCl_3$.

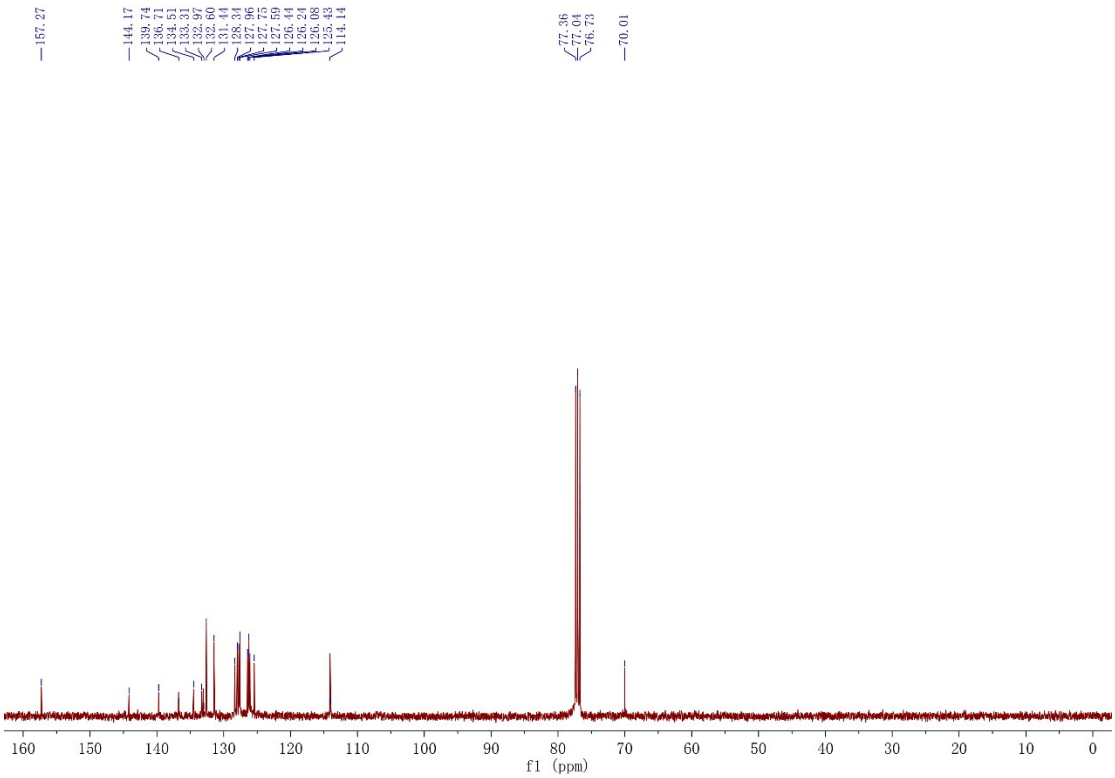

Fig. S41 ^{13}C NMR spectrum of compound TPE-2N in $CDCl_3$.

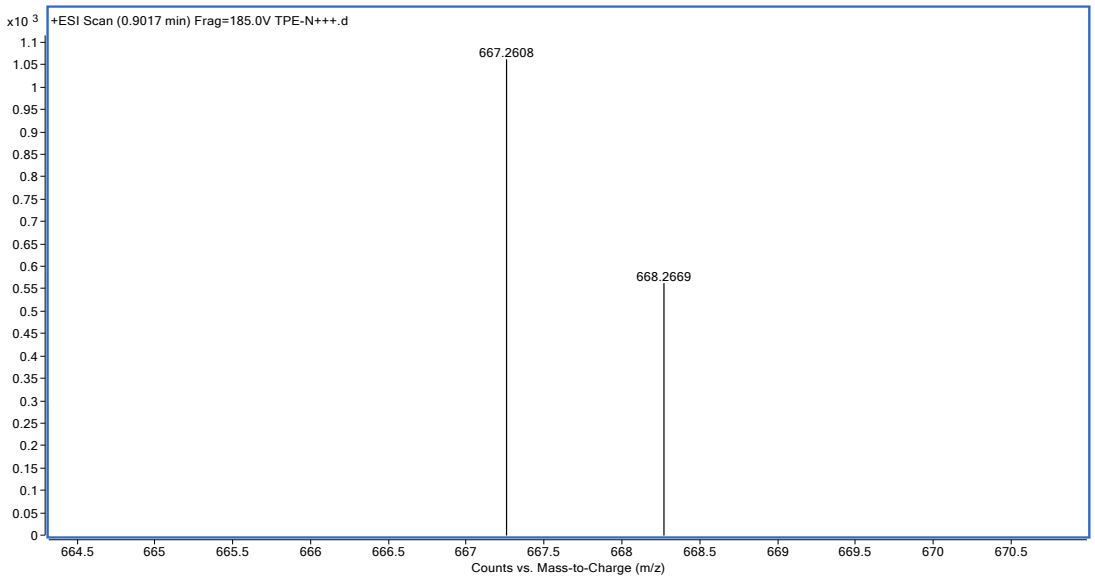

Fig. S42 High-resolution mass spectrum of compound TPE-2N.

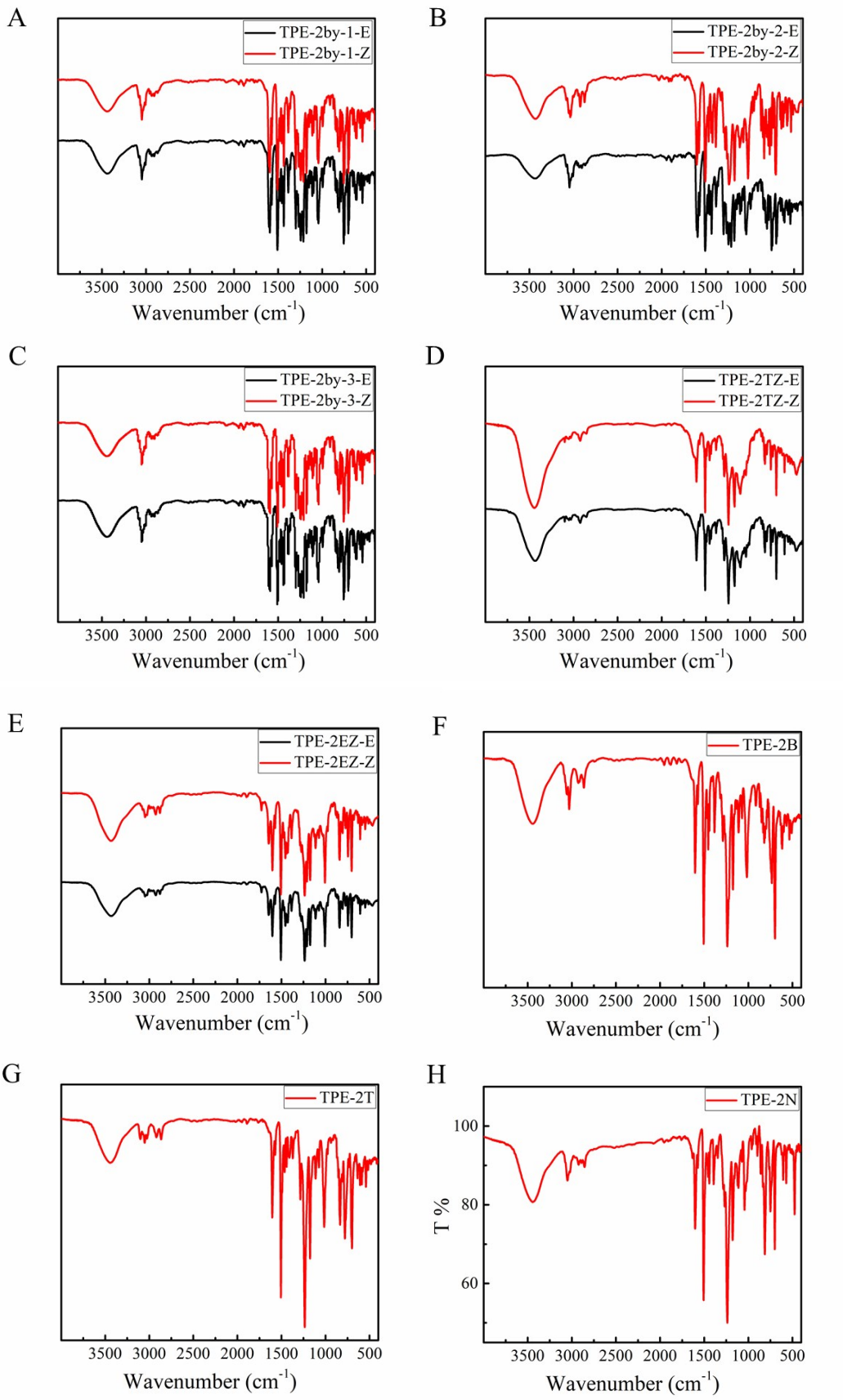

Fig. S43 FTIR spectra of TPE-2by-1(A),TPE-2by-2(B),TPE-2by-3(C),TPE-2TZ(D), TPE-2EZ(E), TPE-2B(F),TPE-2T(G) and TPE-2N(H).

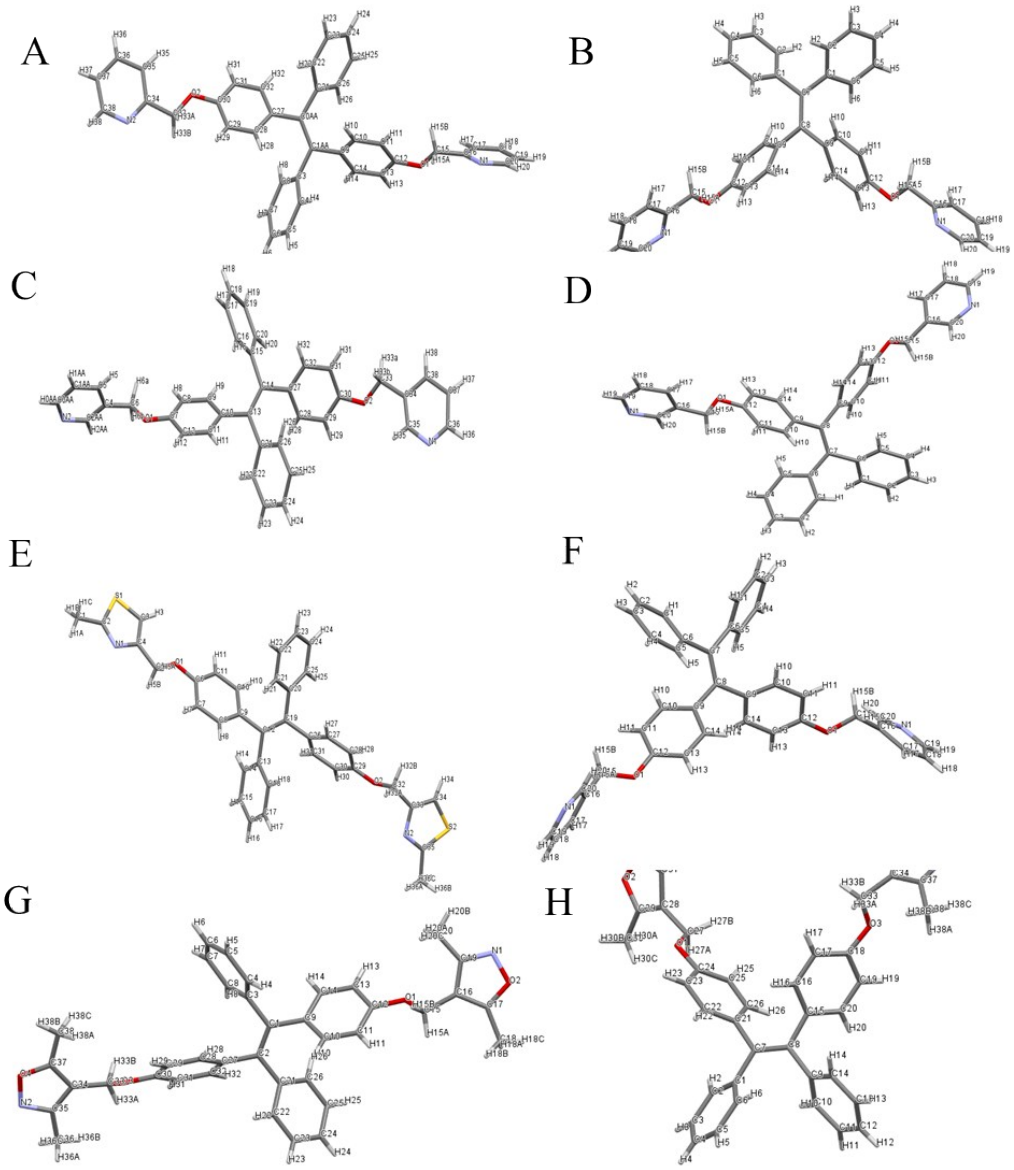

Fig. S44 Crystal structures of TPE-2by-1-E (A) ,TPE-2by-1-Z (B), TPE-2by-2-E (C) ,TPE-2by-2-Z (D), TPE-2TZ-E (E) ,TPE-2TZ-Z (F), TPE-2EZ-E (G) and TPE-2EZ-Z (H).

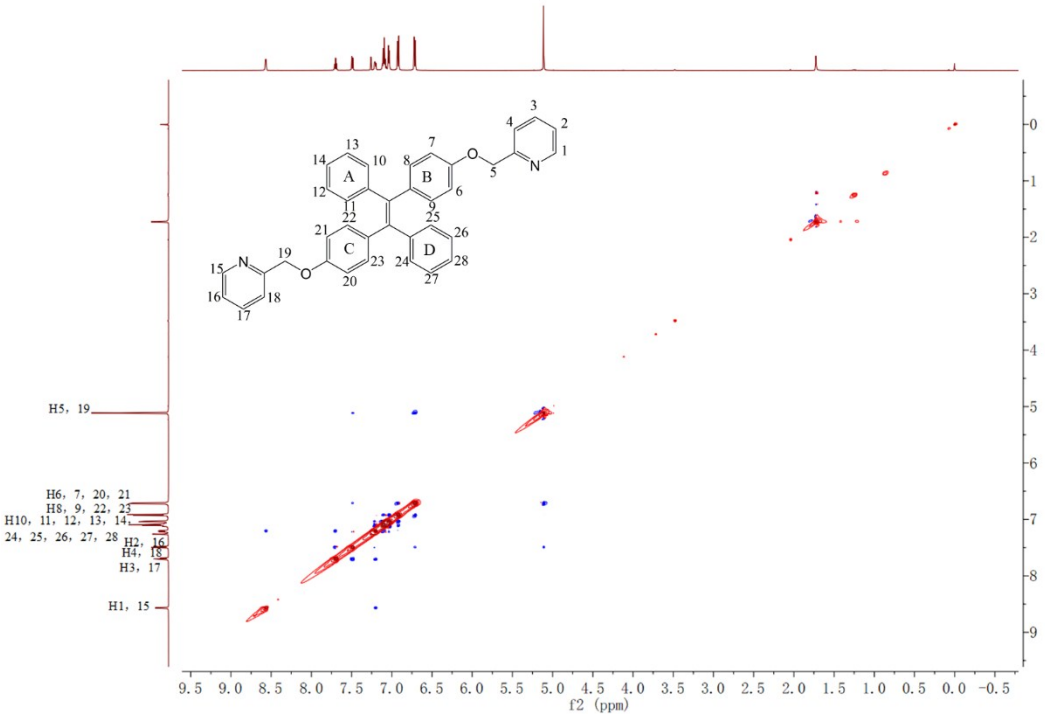

Fig. S45 NOESY-NMR of TPE-2by-1-E (full).

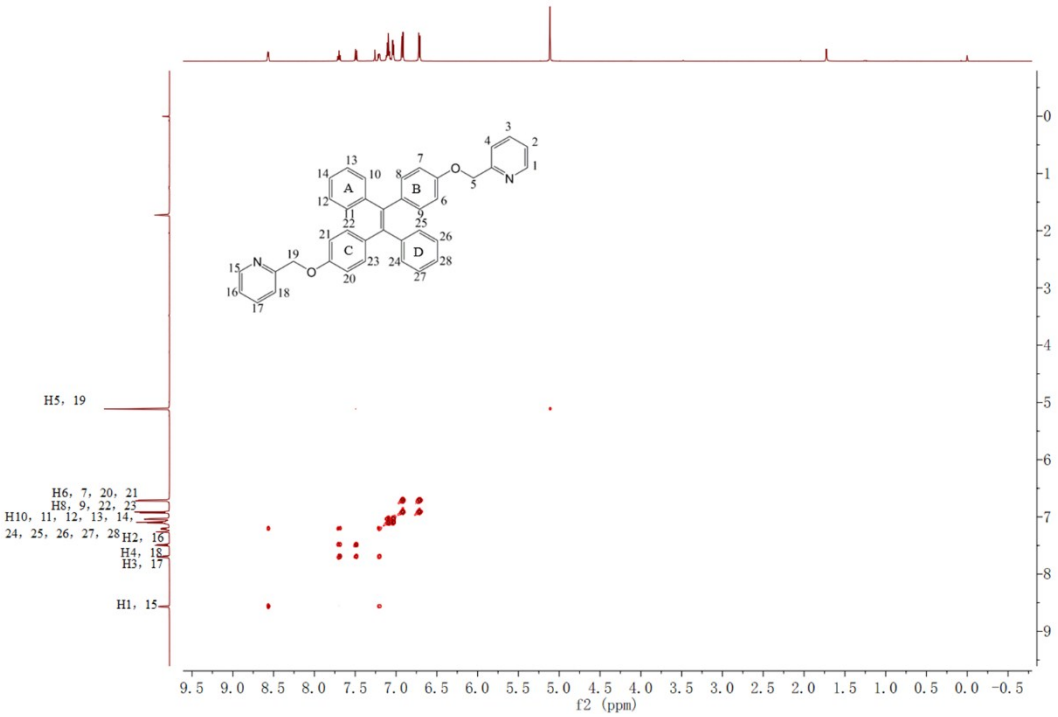

Fig. S46 COSY-NMR of TPE-2by-1-E (full).

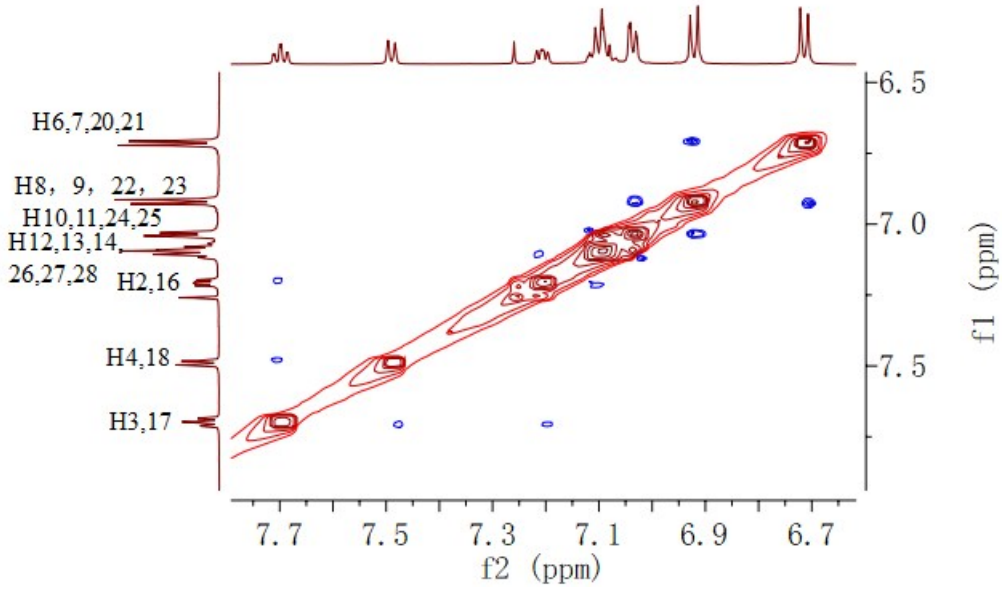

Fig. S47 NOESY-NMR of TPE-2by-1-E (enlarged).

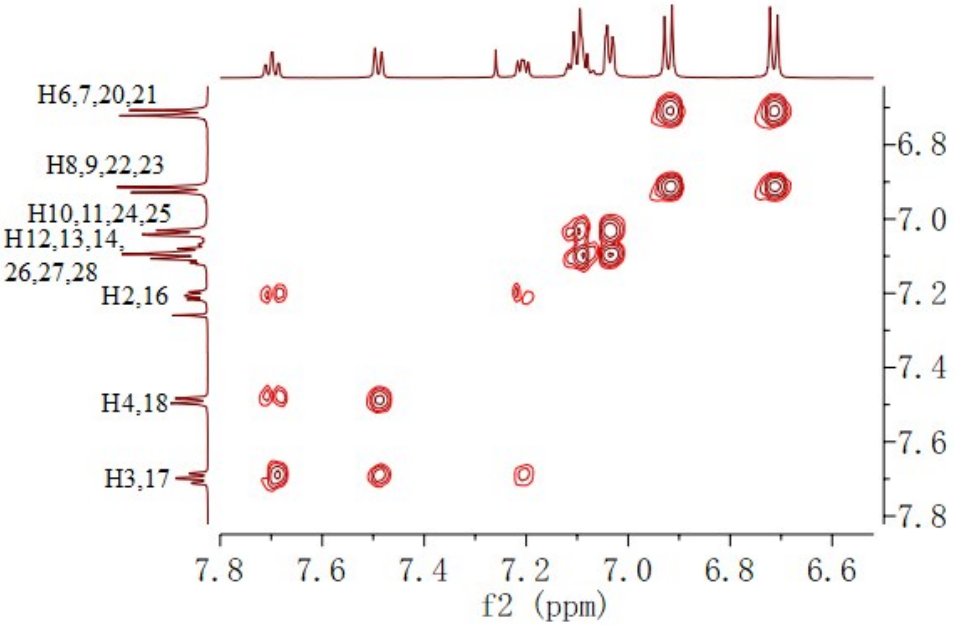

Fig. S48 COSY-NMR of TPE-2by-1-E (enlarged).

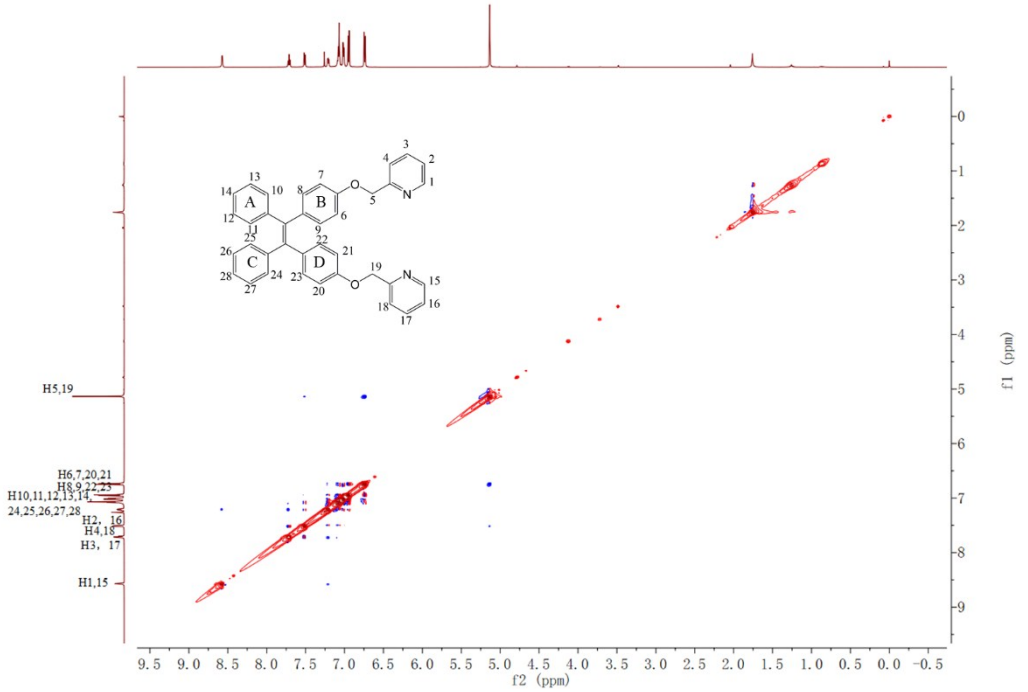

Fig. S49 NOESY-NMR of TPE-2by-1-Z (full).

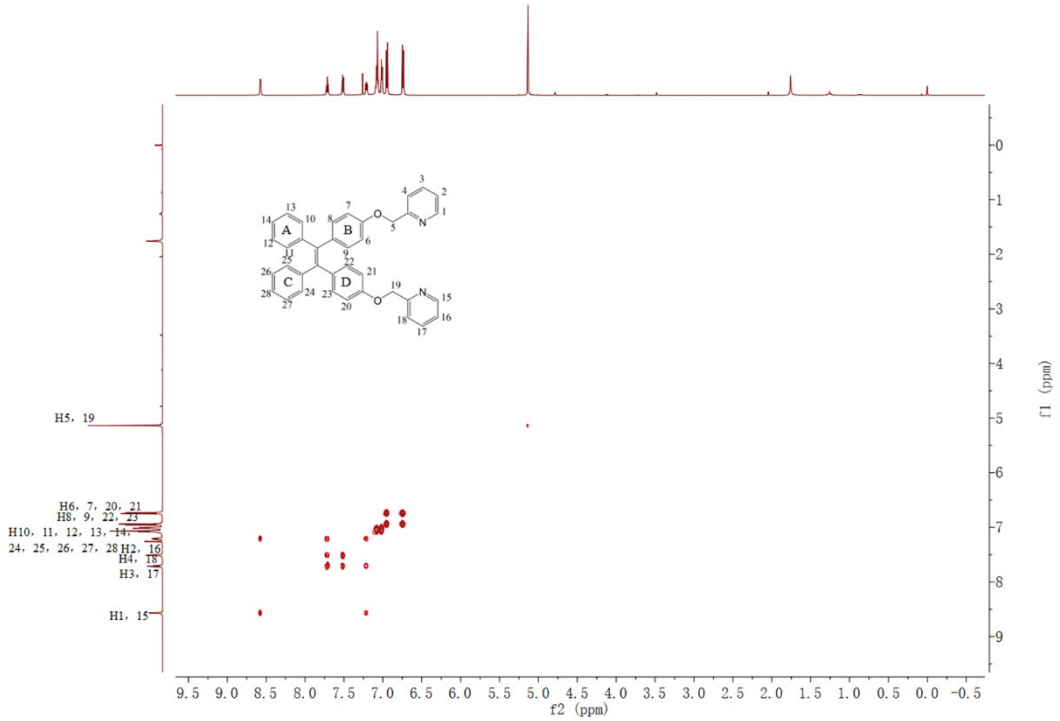

Fig. S50 COSY-NMR of TPE-2by-1-Z (full).

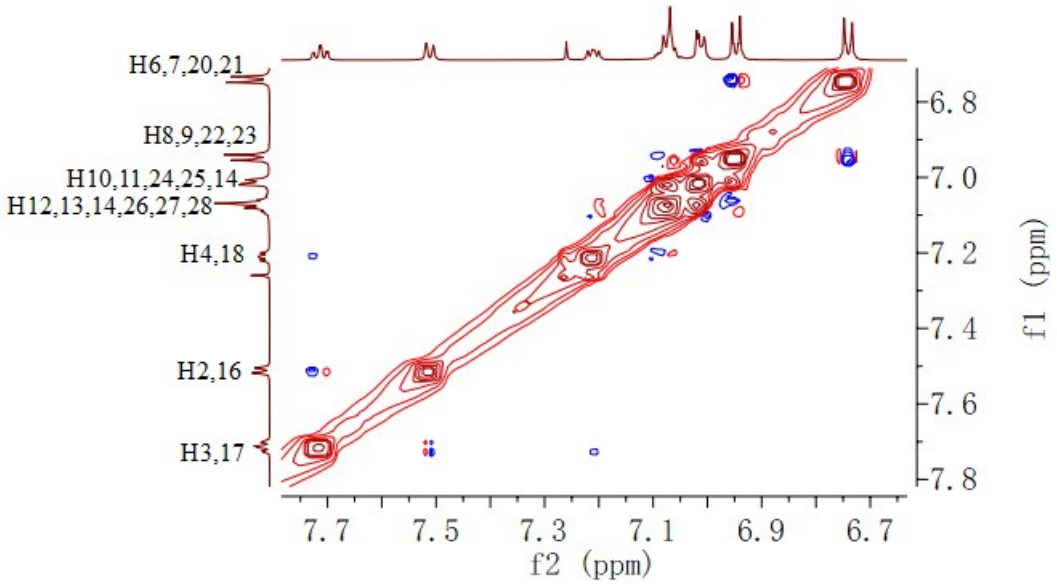

Fig. S51 NOESY-NMR of TPE-2by-1-Z (enlarged).

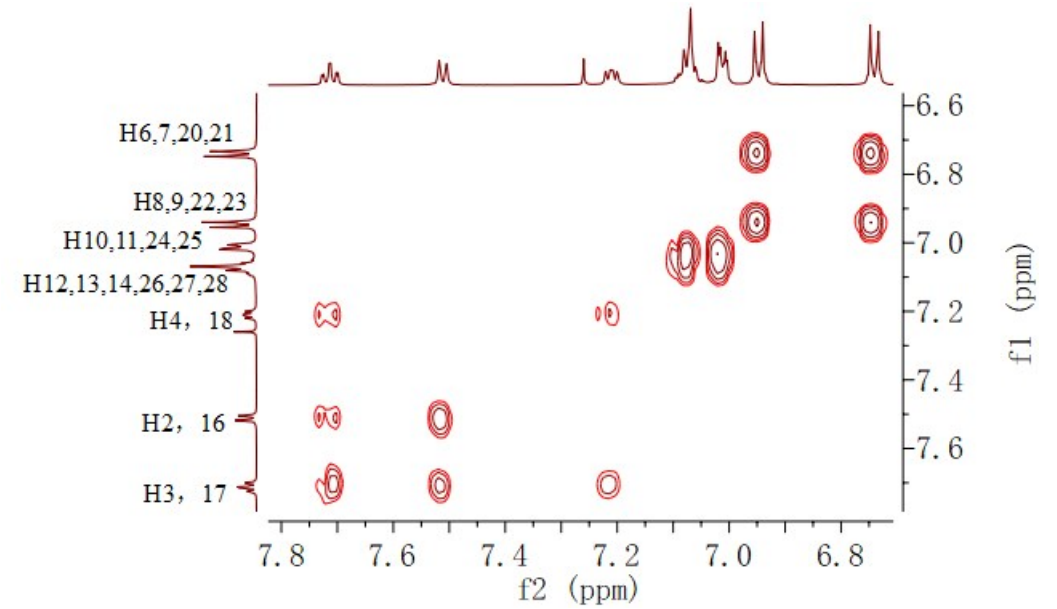

Fig. S52 COSY-NMR of TPE-2by-1-Z (enlarged).

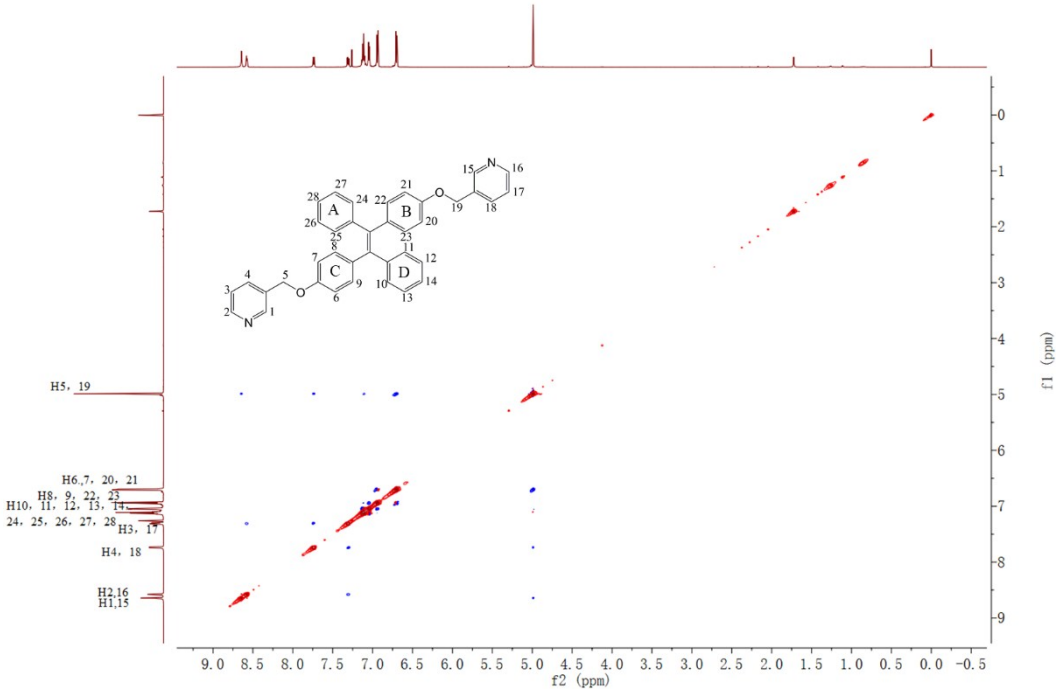

Fig. S53 NOESY-NMR of TPE-2by-2-E (full).

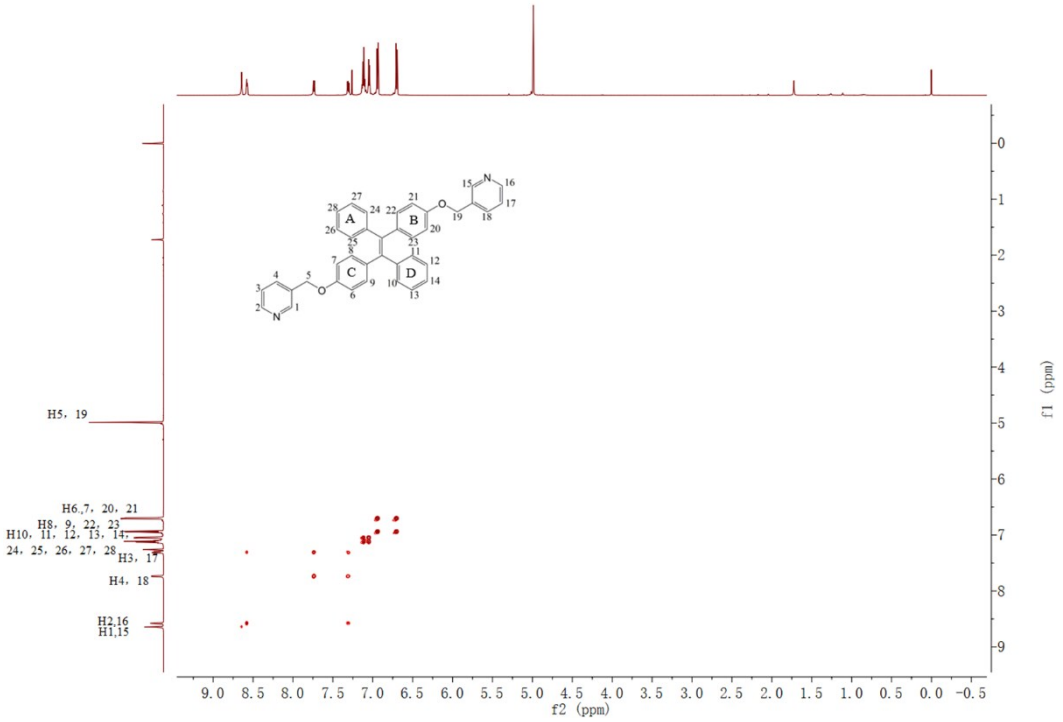

Fig. S54 COSY-NMR of TPE-2by-2-E (full).

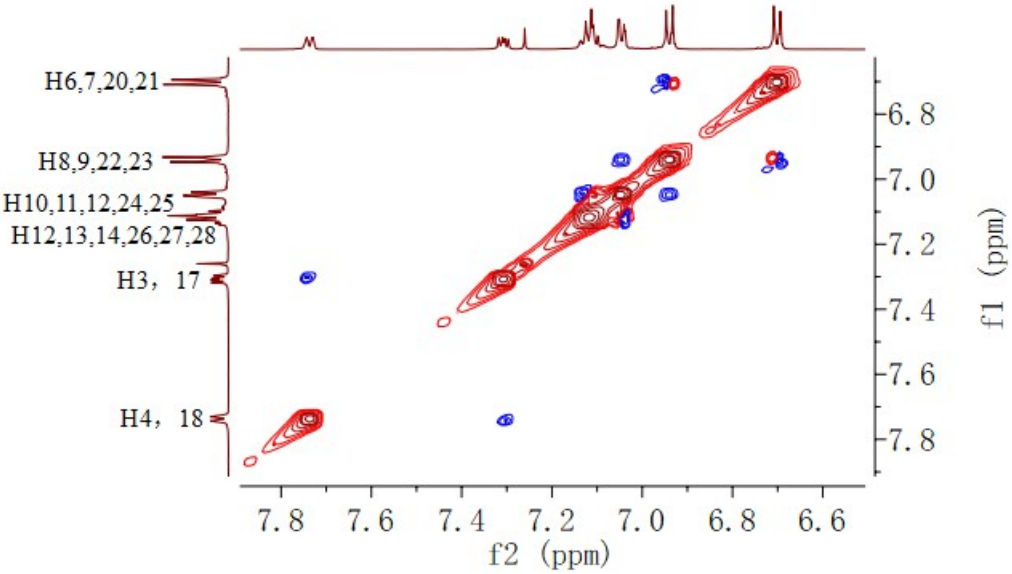

Fig. S55 NOESY-NMR of TPE-2by-2-E (enlarged).

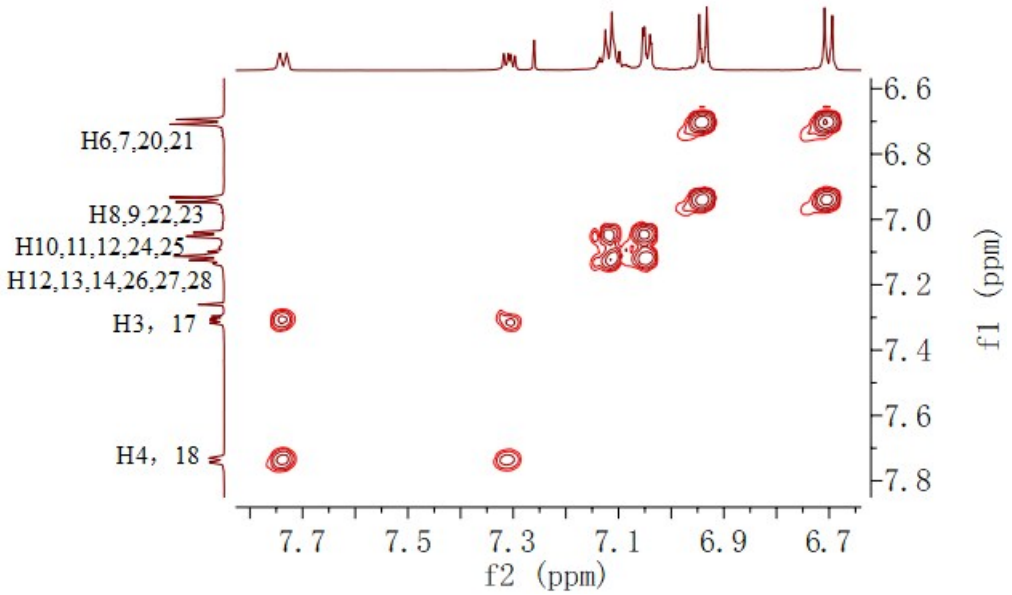

Fig. S56 COSY-NMR of TPE-2by-2-E (enlarged).

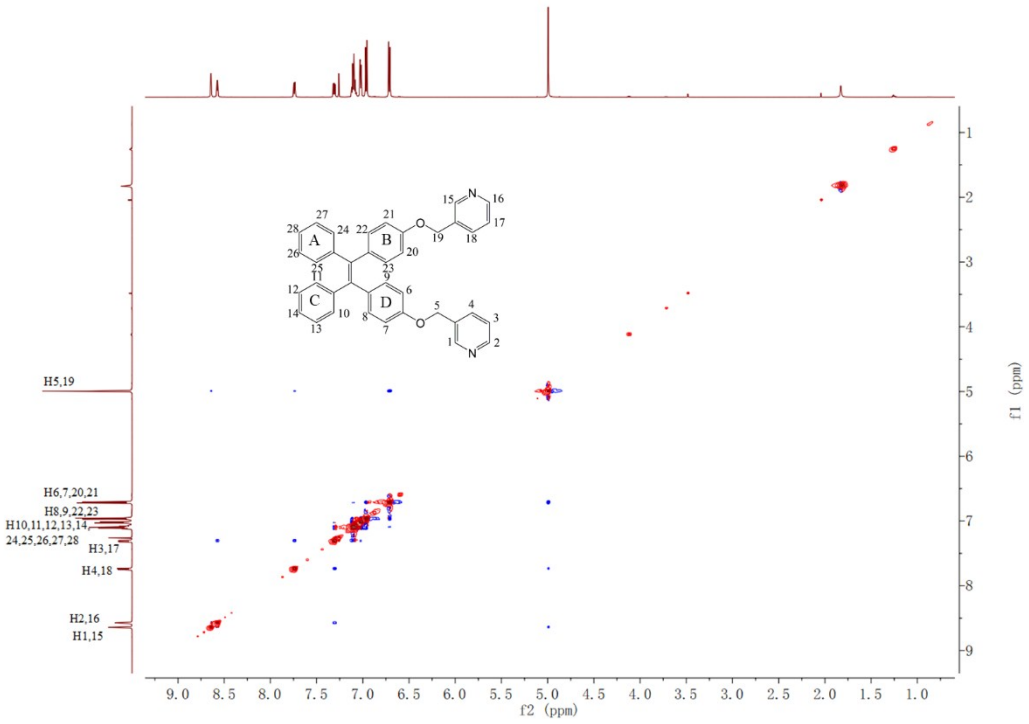

Fig. S57 NOESY-NMR of TPE-2by-2-Z (full).

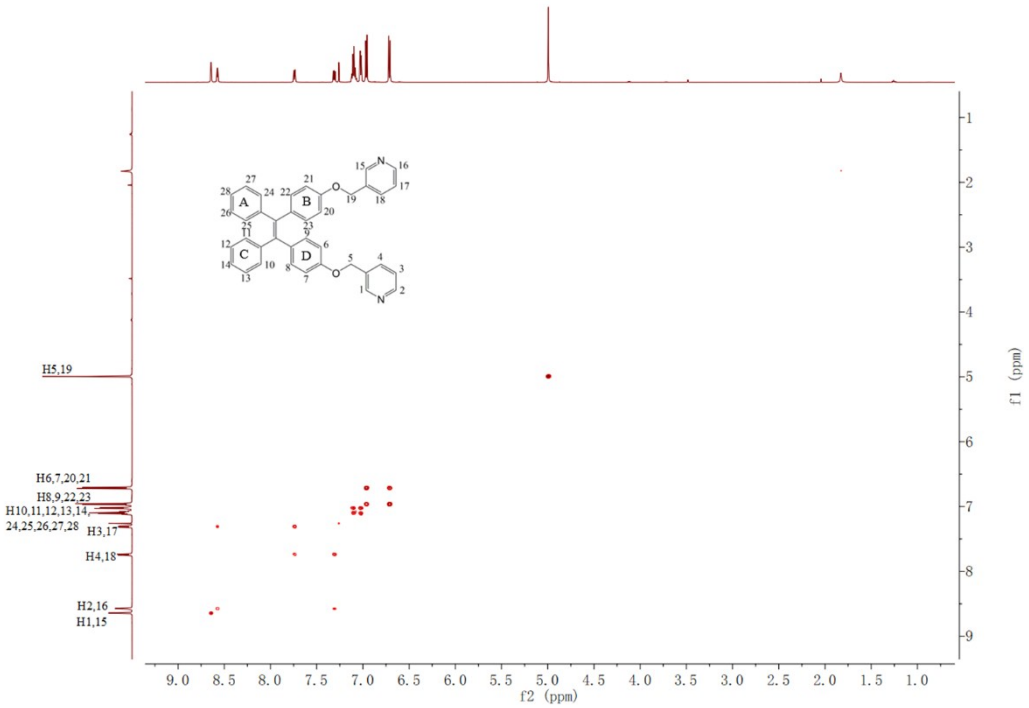

Fig. S58 COSY-NMR of TPE-2by-2-Z (full).

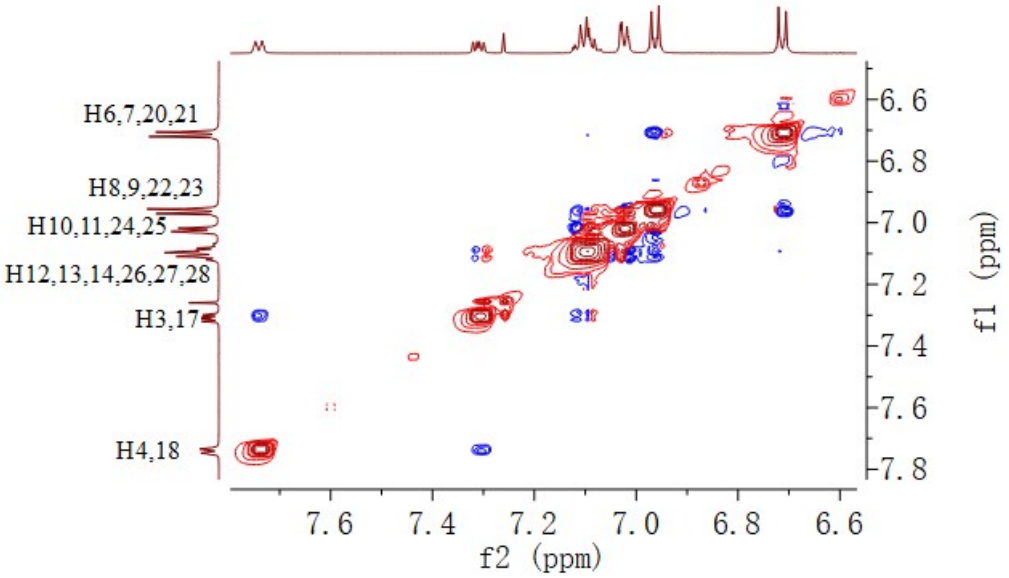

Fig. S59 NOESY-NMR of TPE-2by-2-Z (enlarged).

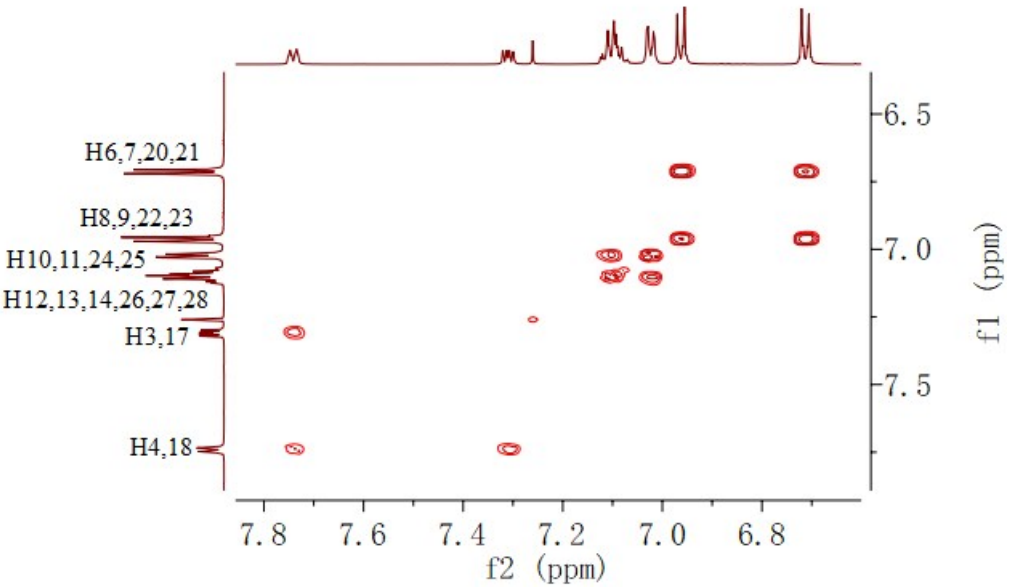

Fig. S60 COSY-NMR of TPE-2by-2-Z (enlarged).

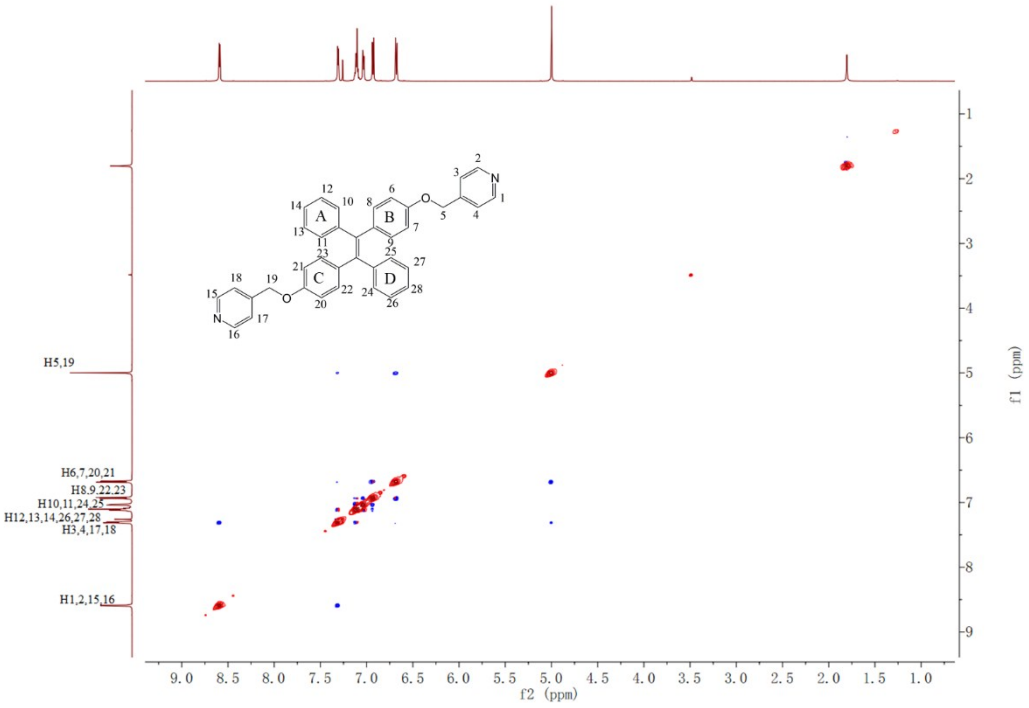

Fig. S61 NOESY-NMR of TPE-2by-3-E(full).

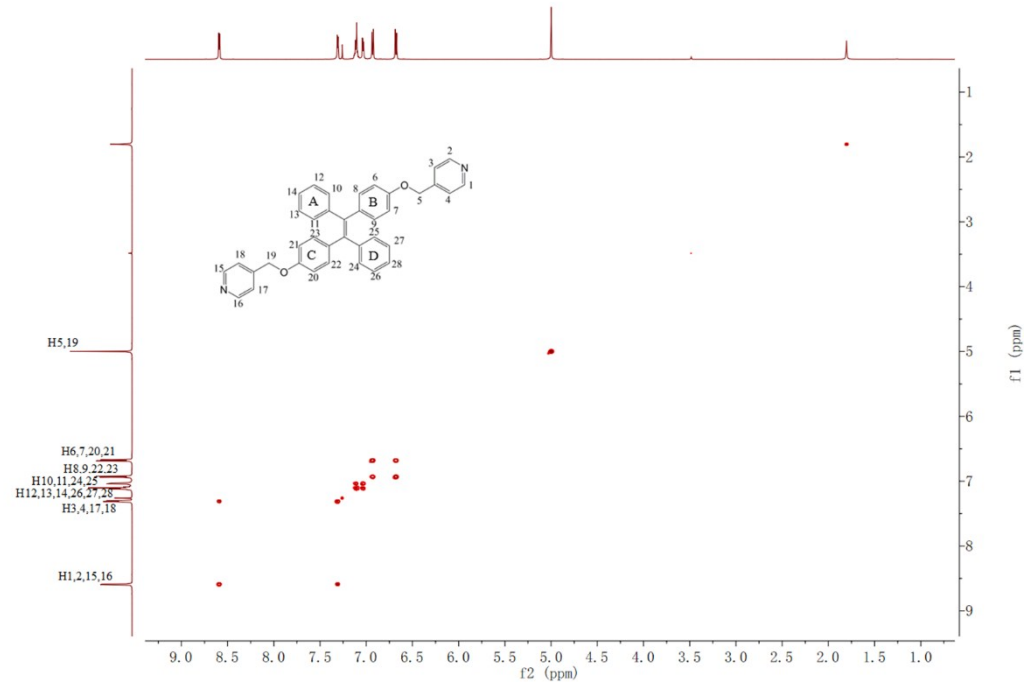

Fig. S62 COSY-NMR of TPE-2by-3-E(full).

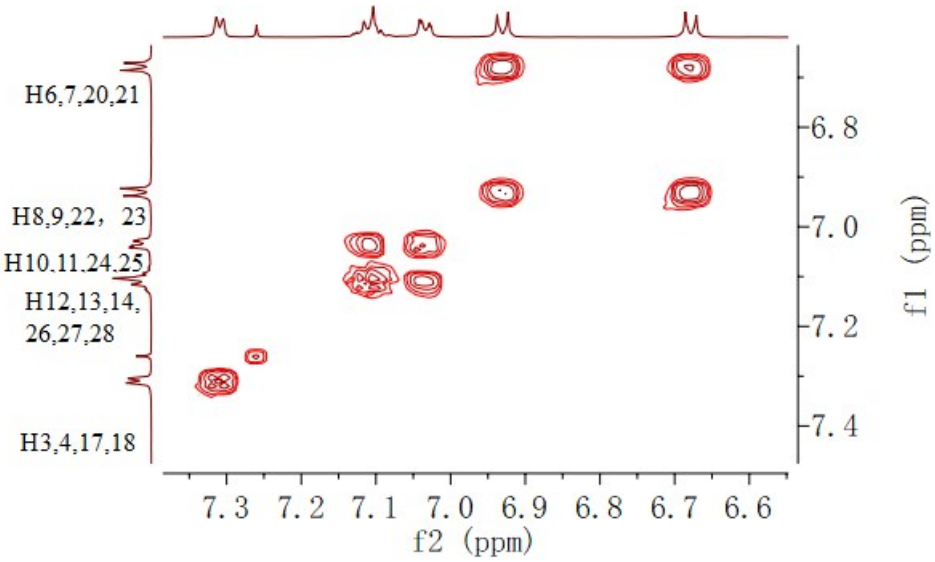

Fig. S63 COSY-NMR of TPE-2by-3-E(enlarged).

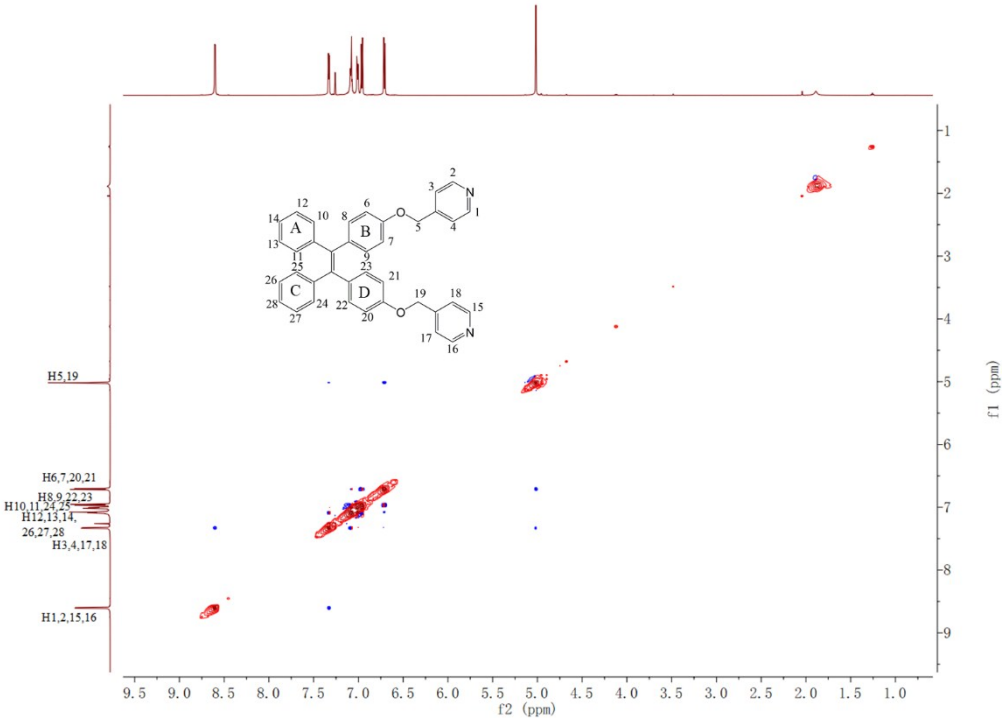

Fig. S64 NOESY-NMR of TPE-2by-3-Z(full).

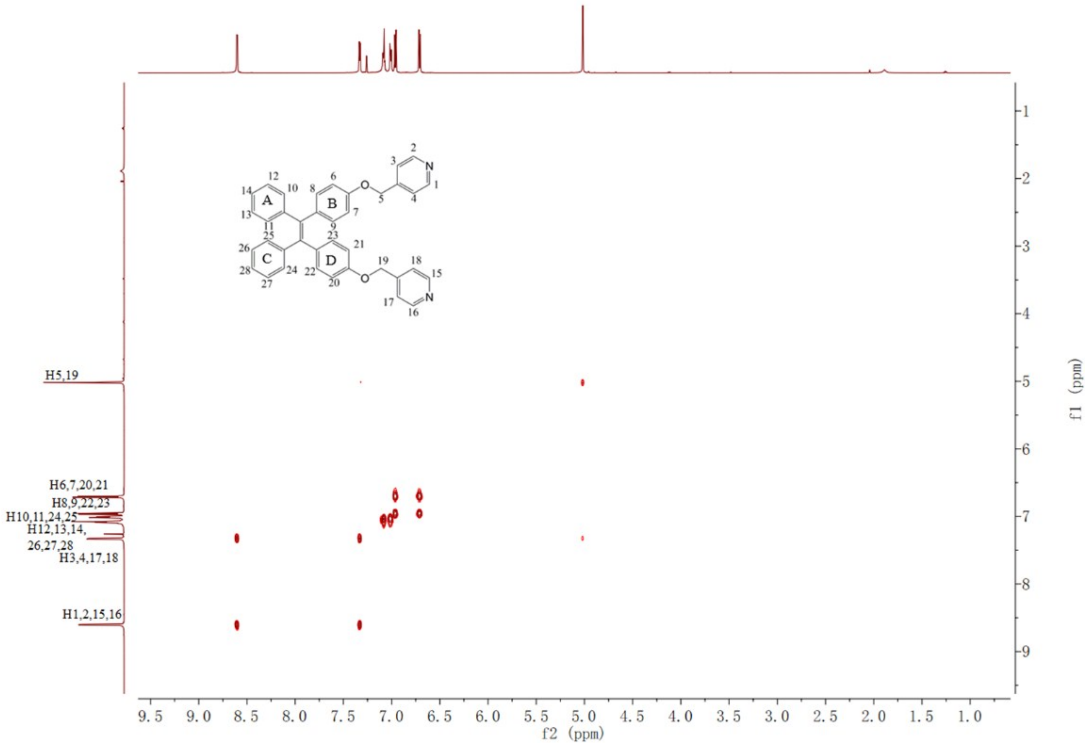

Fig. S65 COSY-NMR of TPE-2by-3-Z(full).

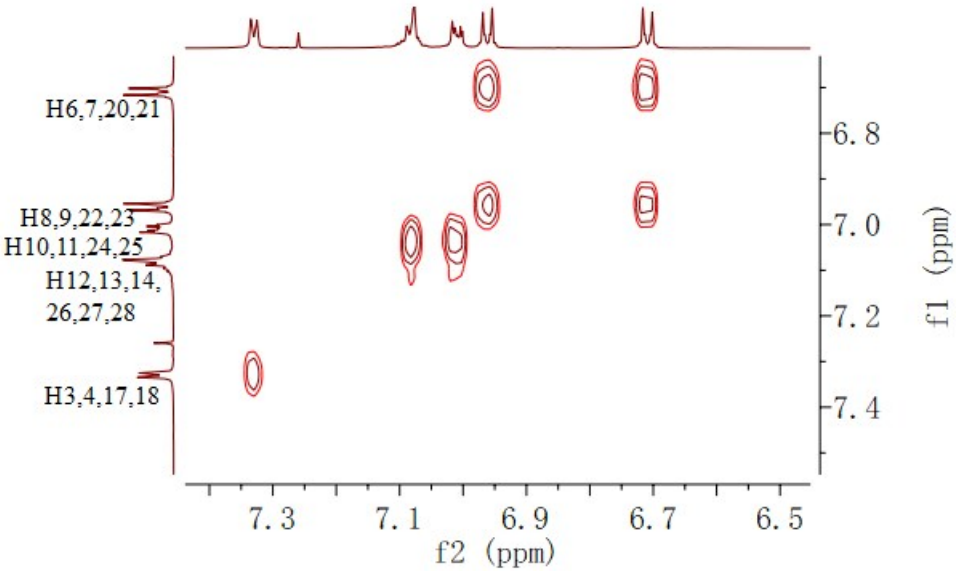

Fig. S66 COSY-NMR of TPE-2by-3-Z(enlarged).

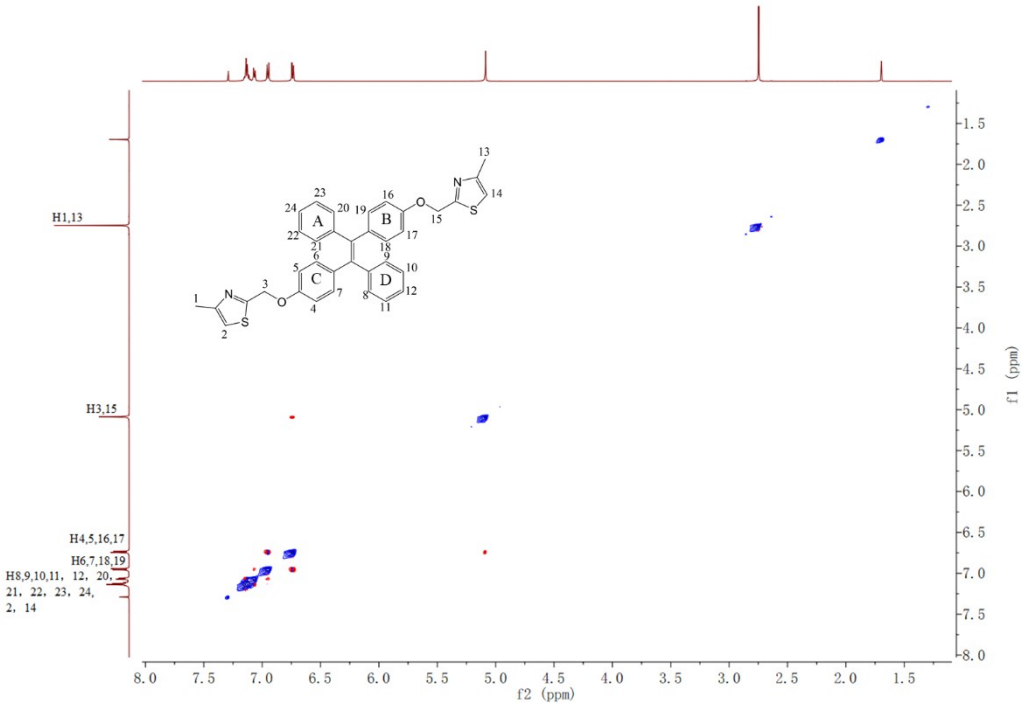

Fig. S67 NOESY-NMR of TPE-2TZ-E(full).

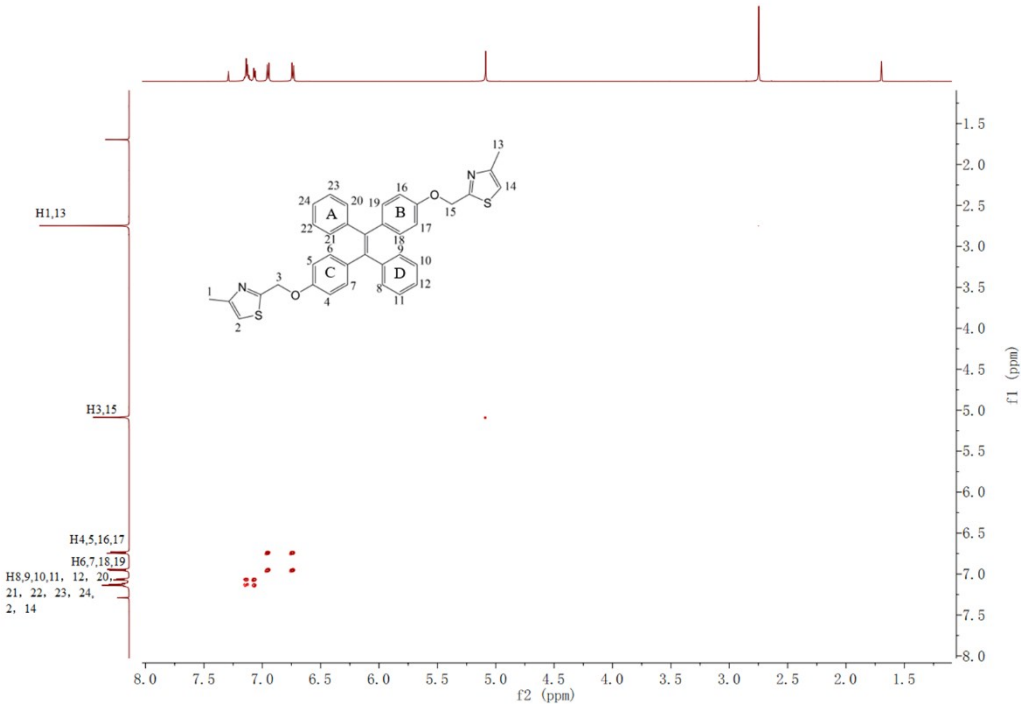

Fig. S68 COSY-NMR of TPE-2TZ-E(full).

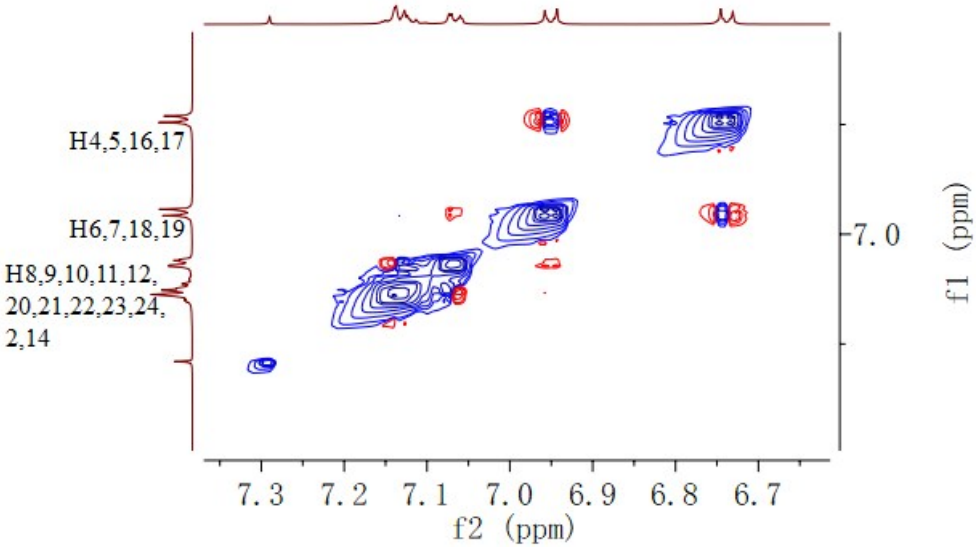

Fig. S69 NOESY-NMR of TPE-2TZ-E(enlarged).

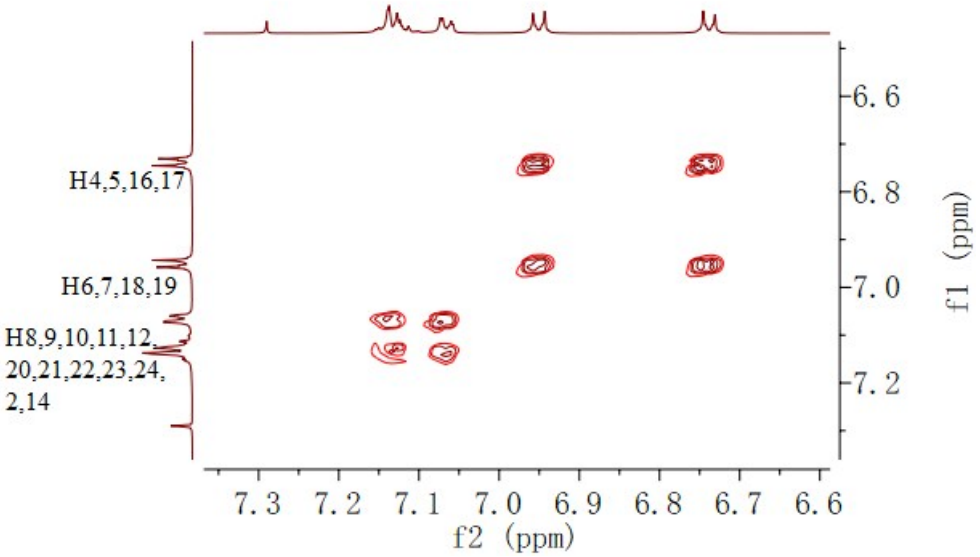

Fig. S70 COSY-NMR of TPE-2TZ-E(enlarged).

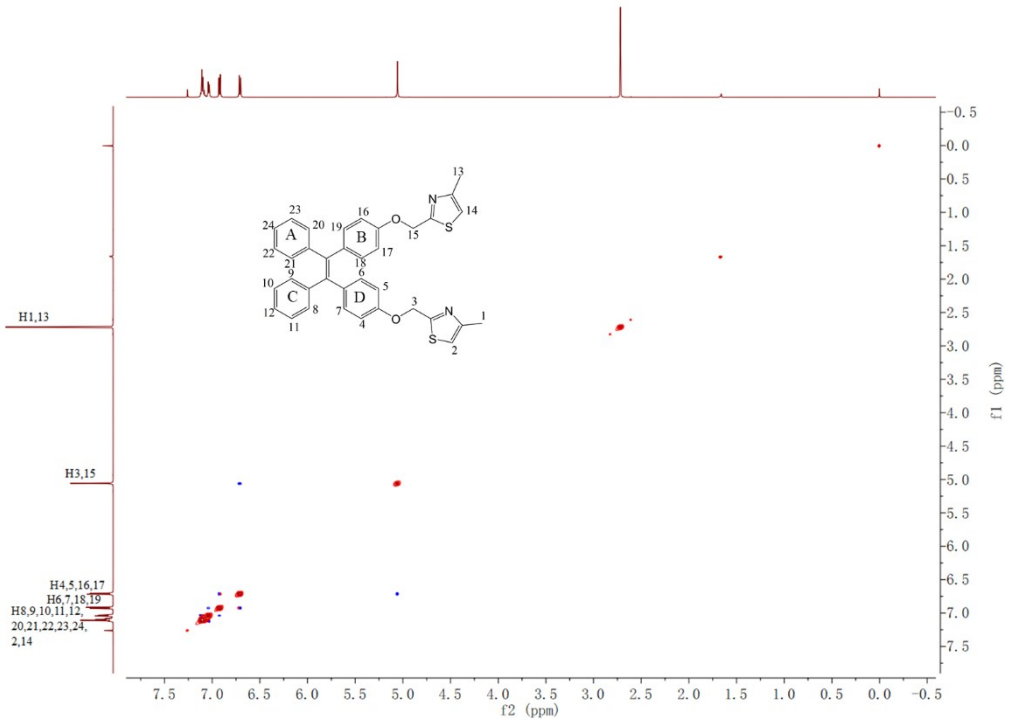

Fig. S71 NOESY-NMR of TPE-2TZ-Z(full).

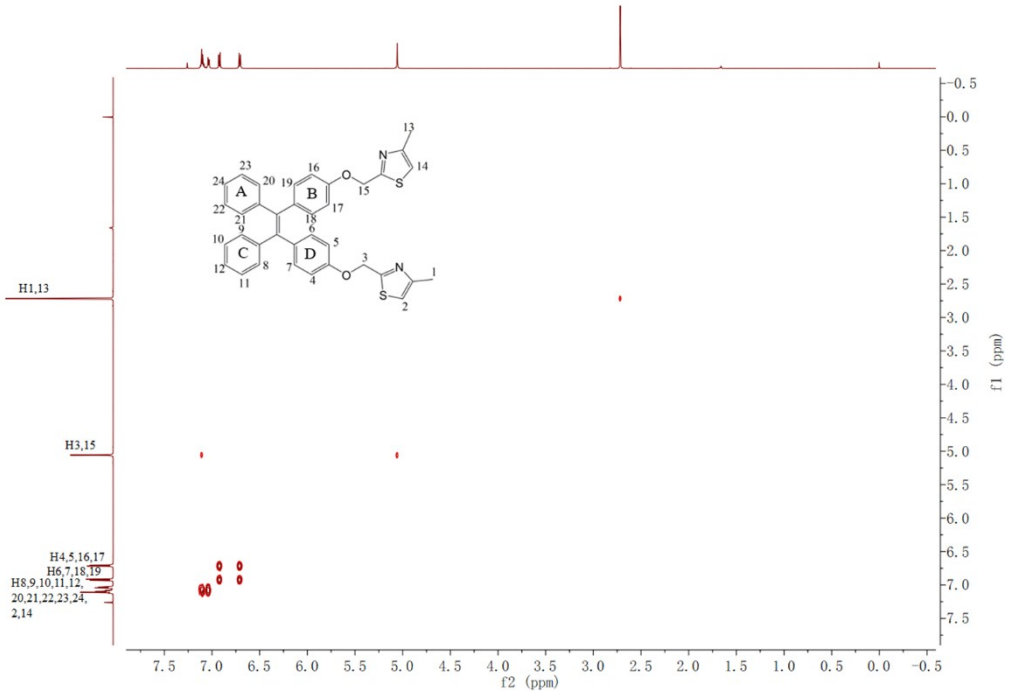

Fig. S72 COSY-NMR of TPE-2TZ-Z(full).

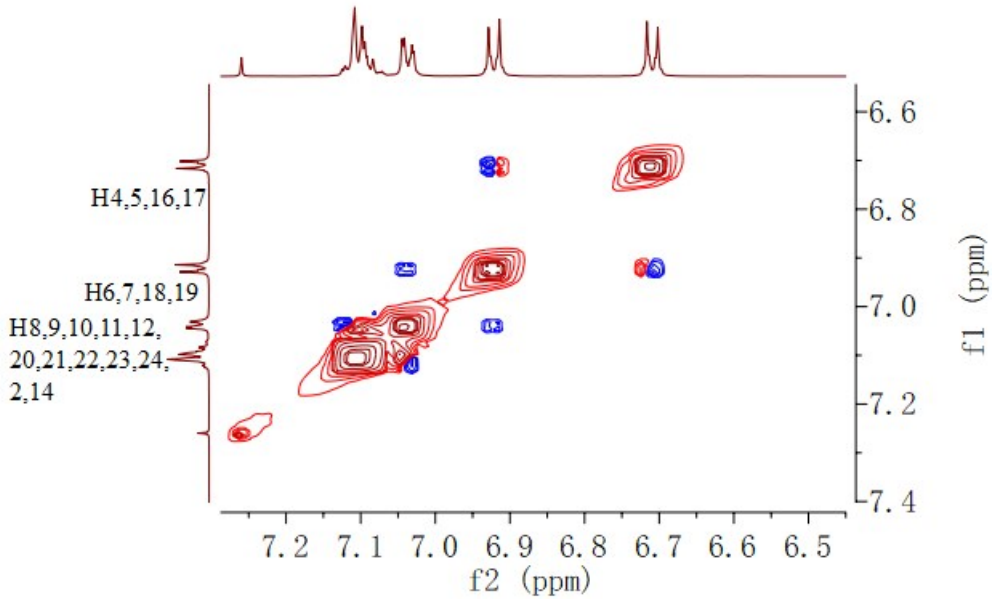

Fig. S73 NOESY-NMR of TPE-2TZ-Z(enlarged).

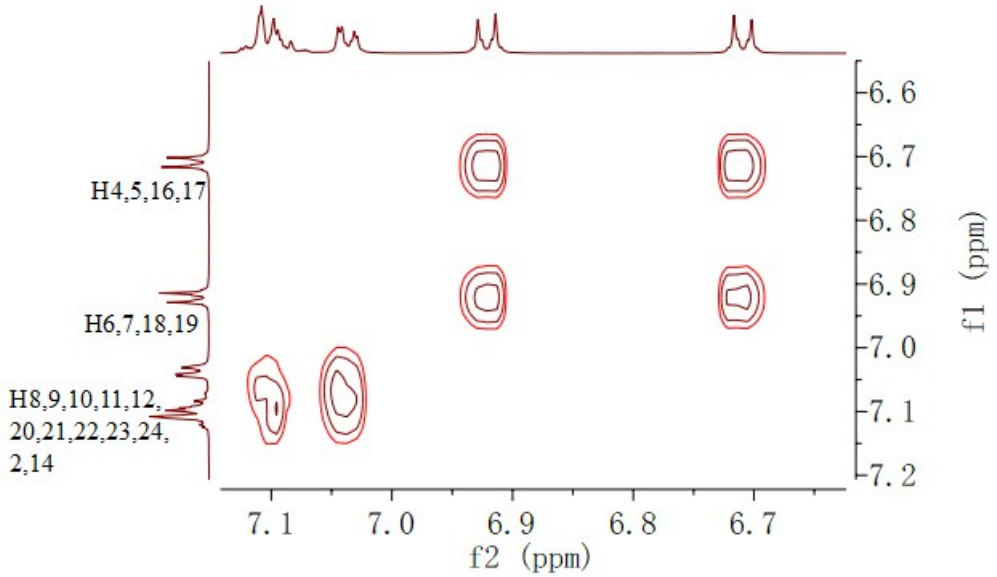

Fig. S74 COSY-NMR of TPE-2TZ-Z(enlarged).

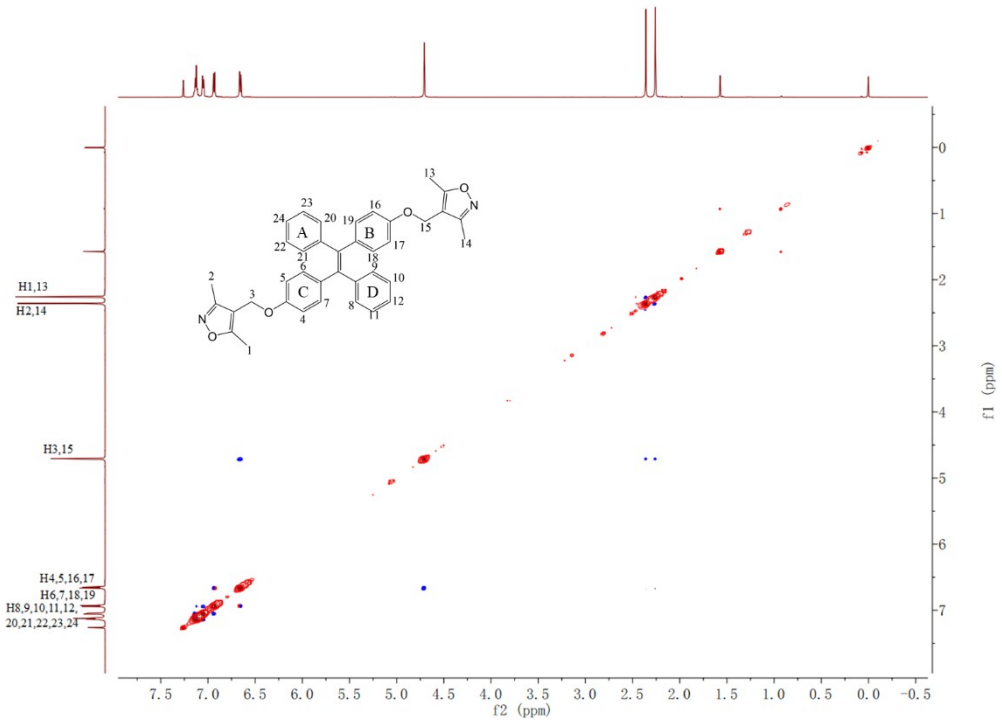

Fig. S75 NOESY-NMR of TPE-2EZ-E(full).

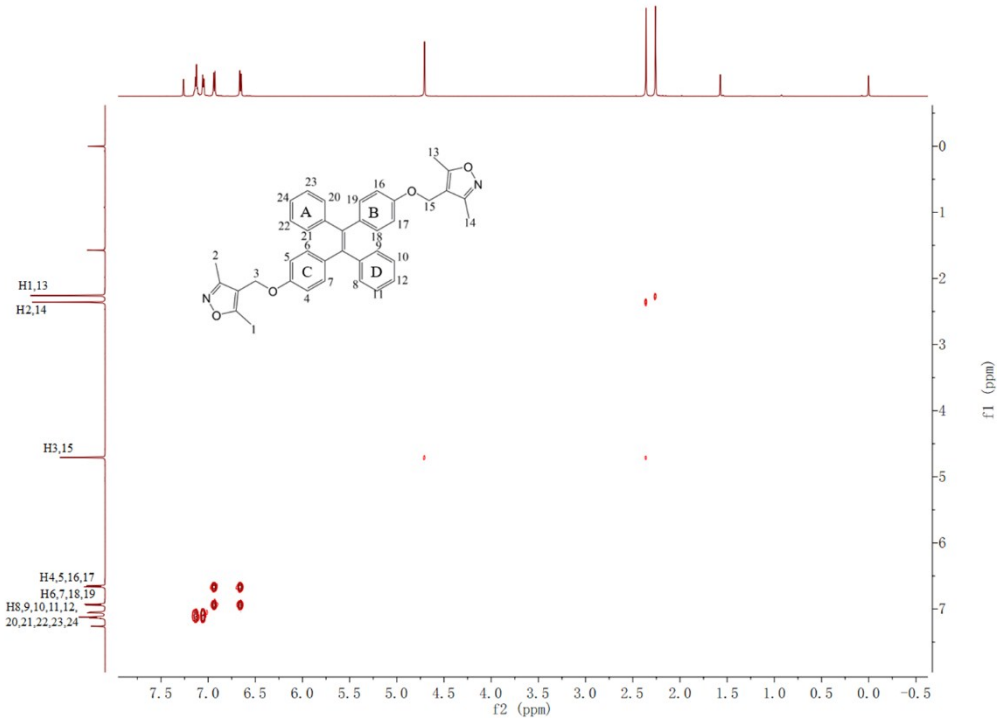

Fig. S76 COSY-NMR of TPE-2EZ-E(full).

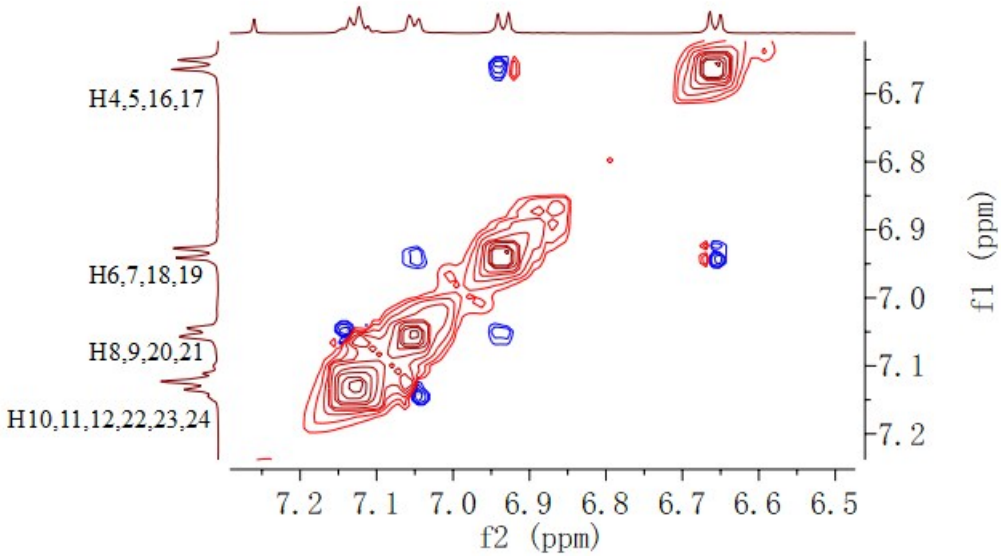

Fig. S77 NOESY-NMR of TPE-2EZ-E(enlarged).

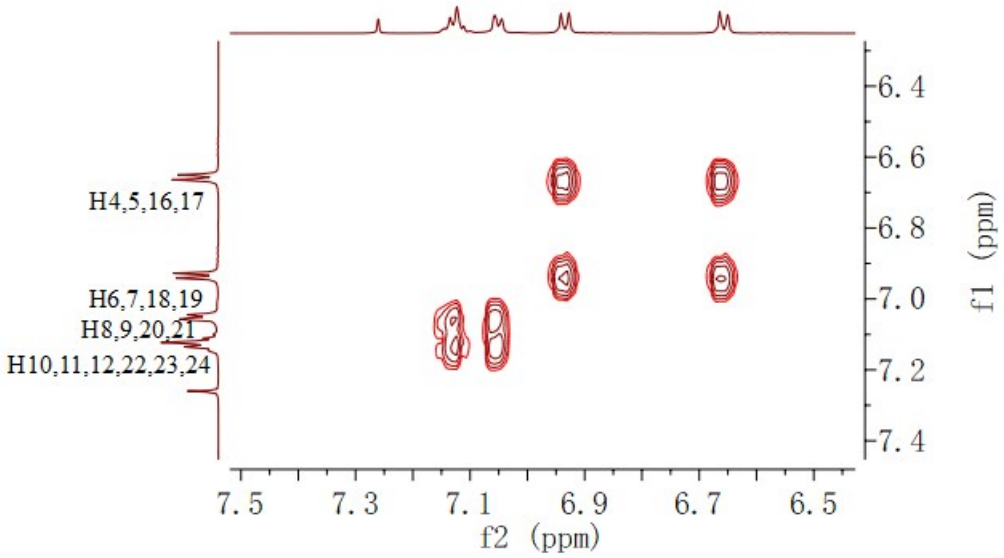

Fig. S78 COSY-NMR of TPE-2EZ-E(enlarged).

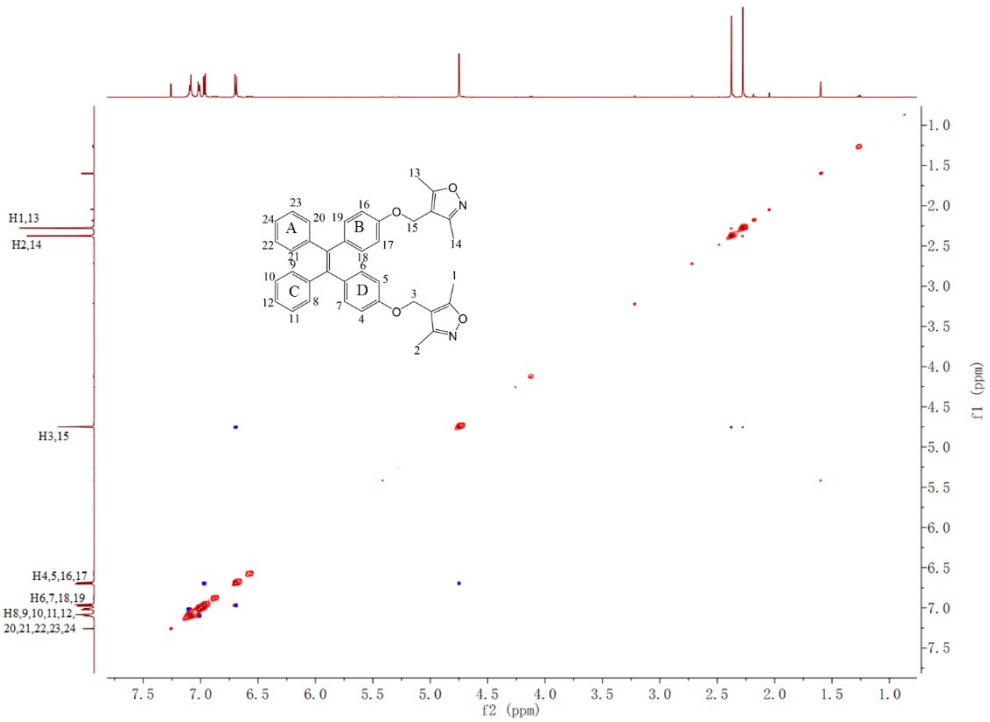

Fig. S79 NOESY-NMR of TPE-2EZ-Z(full).

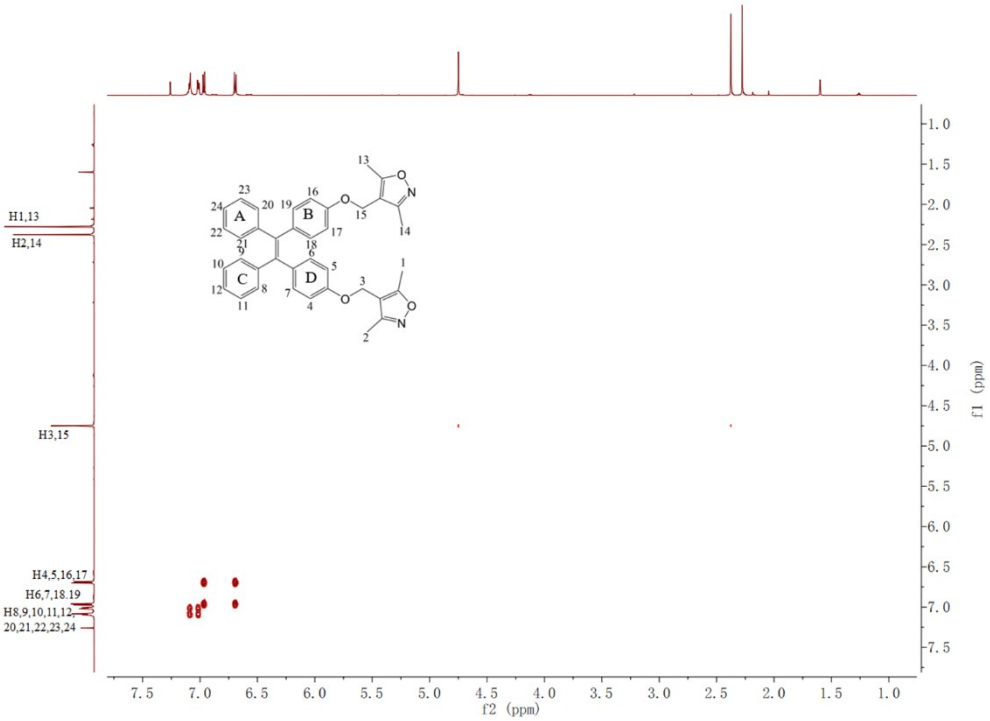

Fig. S80 COSY-NMR of TPE-2EZ-Z(full).

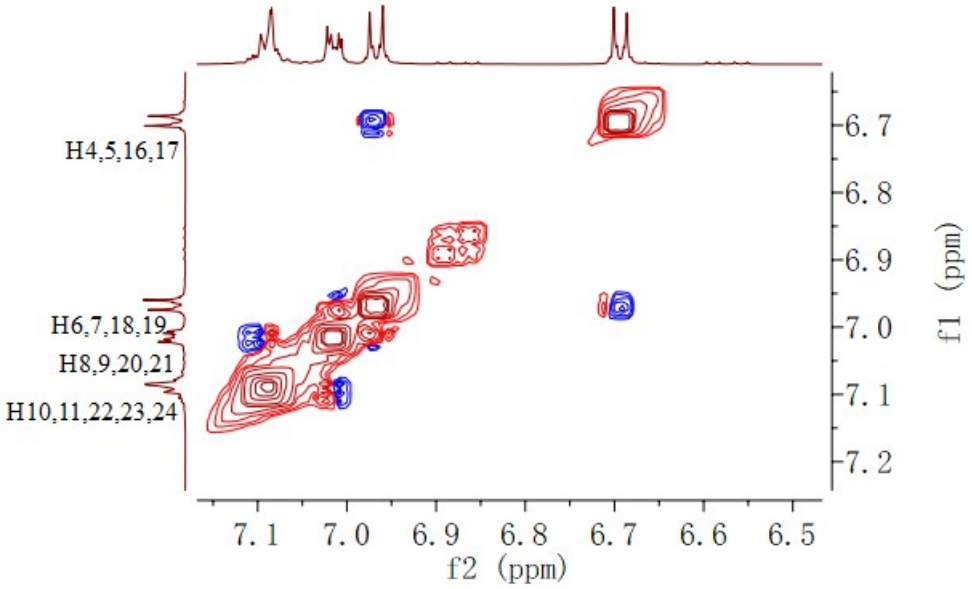

Fig. S81 NOESY-NMR of TPE-2EZ-Z(enlarged).

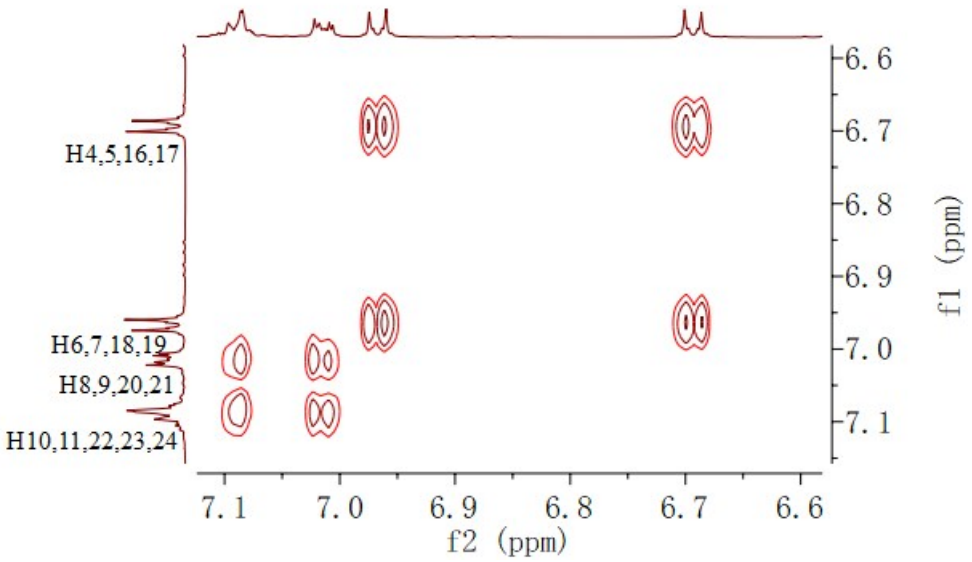

Fig. S82 COSY-NMR of TPE-2EZ-Z(enlarged).

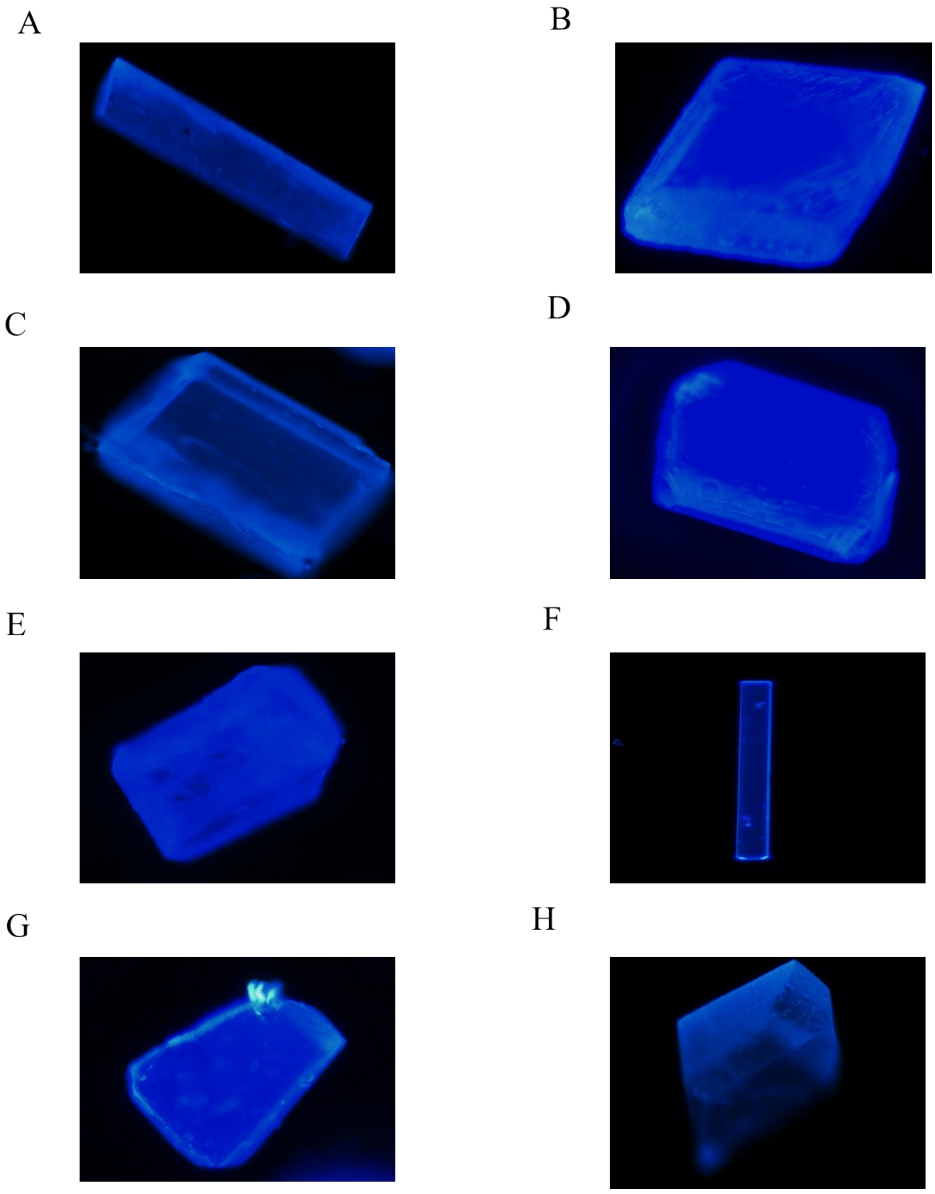

Fig. S83 Single crystal fluorescence pictures of TPE-2by-1-E (A) ,TPE-2by-1-Z (B), TPE-2by-2-E (C) ,TPE-2by-2-Z (D), TPE-2TZ-E (E) ,TPE-2TZ-Z (F), TPE-2EZ-E (G) , TPE-2EZ-Z (H) under the fluorescent inverted microscope.

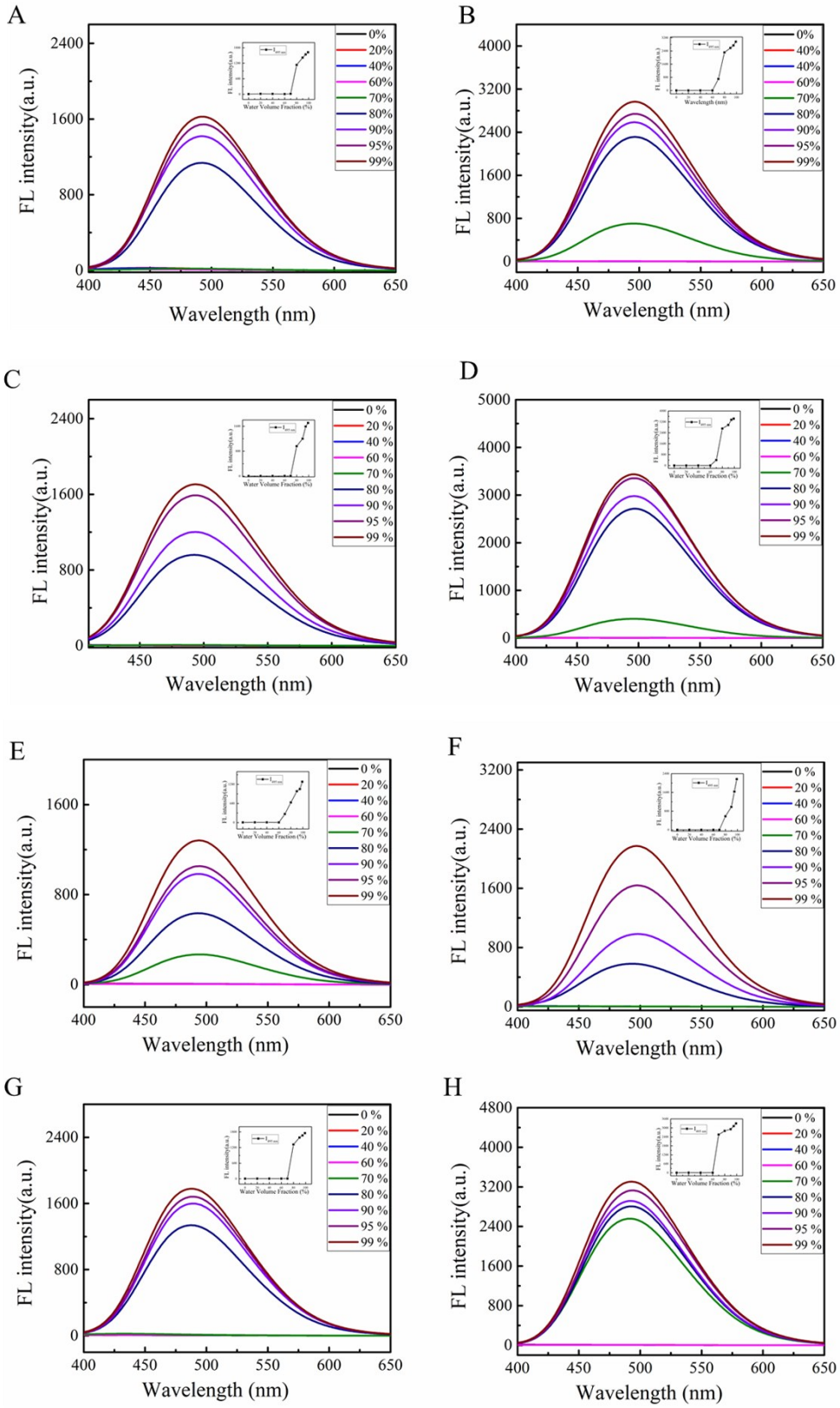
A
FL intensity(a.u.)
Wavelength (nm)
0%
20%
40%
60%
70%
80%
90%
95%
99%
B
FL intensity(a.u.)
Wavelength (nm)
0%
40%
40%
60%
70%
80%
90%
95%
99%
C
FL intensity(a.u.)
Wavelength (nm)
0 %
20 %
40 %
60 %
70 %
80 %
90 %
95 %
99 %
D
FL intensity(a.u.)
Wavelength (nm)
0 %
20 %
40 %
60 %
70 %
80 %
90 %
95 %
99 %
E
FL intensity(a.u.)
Wavelength (nm)
0 %
20 %
40 %
60 %
70 %
80 %
90 %
95 %
99 %
F
FL intensity(a.u.)
Wavelength (nm)
0 %
20 %
40 %
60 %
70 %
80 %
90 %
95 %
99 %
G
FL intensity(a.u.)
Wavelength (nm)
0 %
20 %
40 %
60 %
70 %
80 %
90 %
95 %
99 %
H
FL intensity(a.u.)
Wavelength (nm)
0 %
20 %
40 %
60 %
70 %
80 %
90 %
95 %
99 %

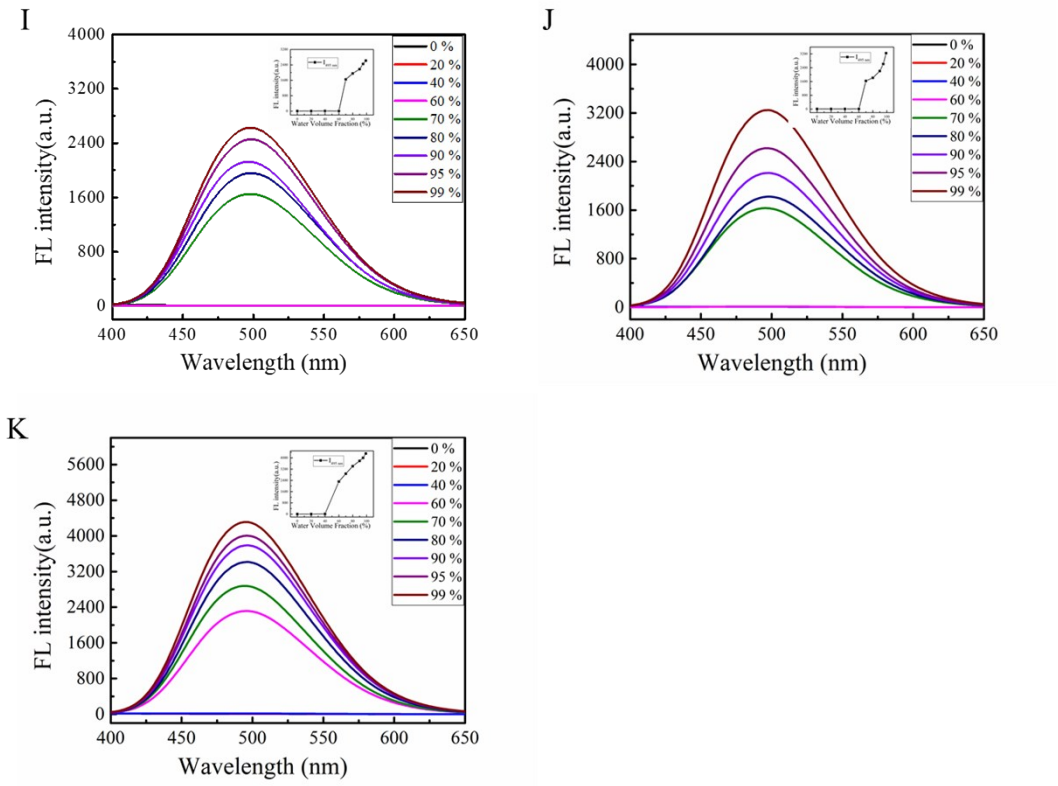

Fig. S84 Fluorescent spectra of TPE-2by-1-E (A) ,TPE-2by-1-Z (B), TPE-2by-2-E (C) ,TPE-2by-2-Z (D), TPE-2TZ-E (E) ,TPE-2TZ-Z (F), TPE-2EZ-E (G) , TPE-2EZ-Z (H), TPE-2B(I),TPE-2T(J) and TPE-2N(K). (1×10^{-5} M, λ_{ex} = 340 nm) in DMF and water mixtures with different water fractions (inset: and plots of fluorescence intensity versus water fractions).

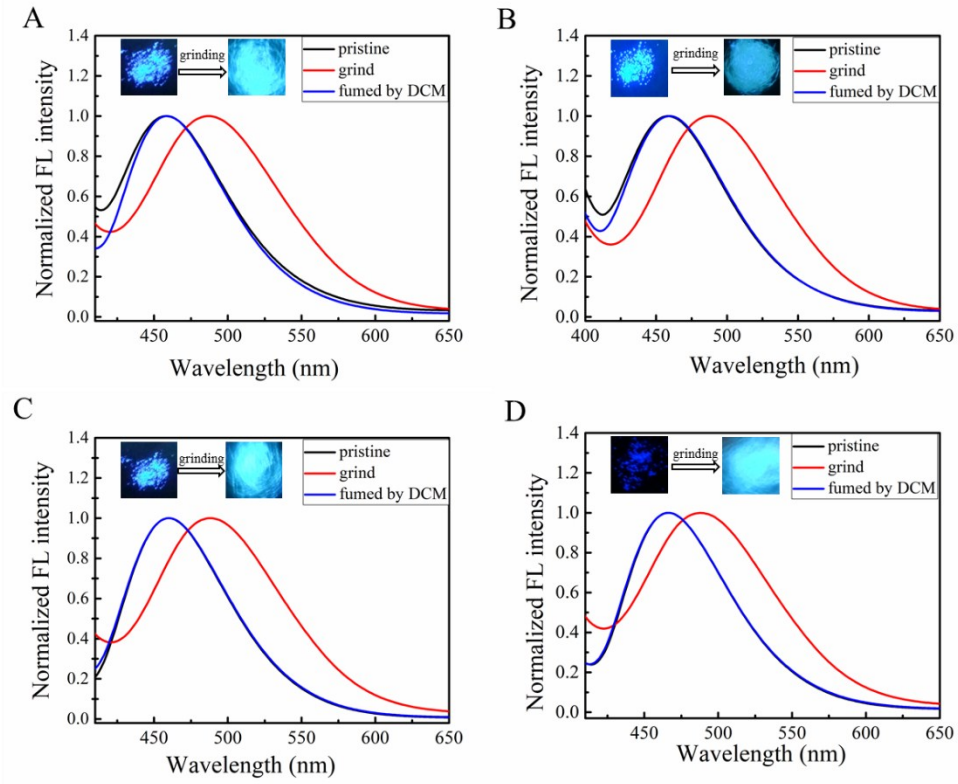
A
B
C
D
grinding
pristine
grind
fumed by DCM
Normalized FL intensity
Wavelength (nm)

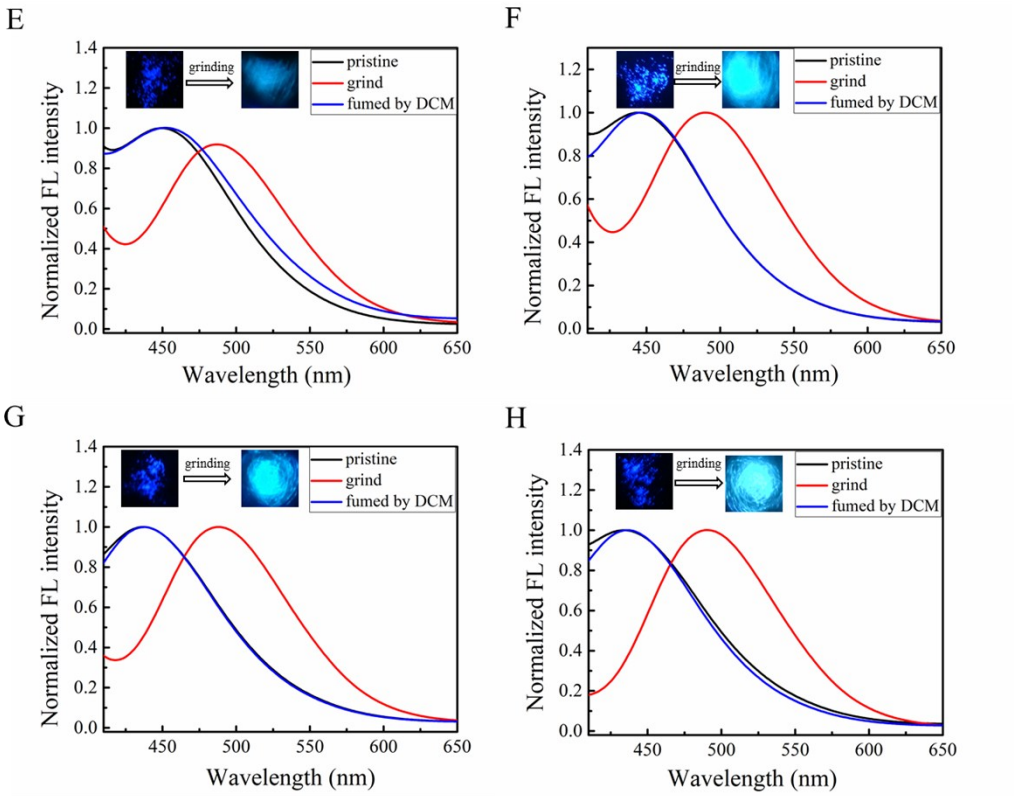
E
F
G
H
grinding
pristine
grind
fumed by DCM
Normalized FL intensity
Wavelength (nm)

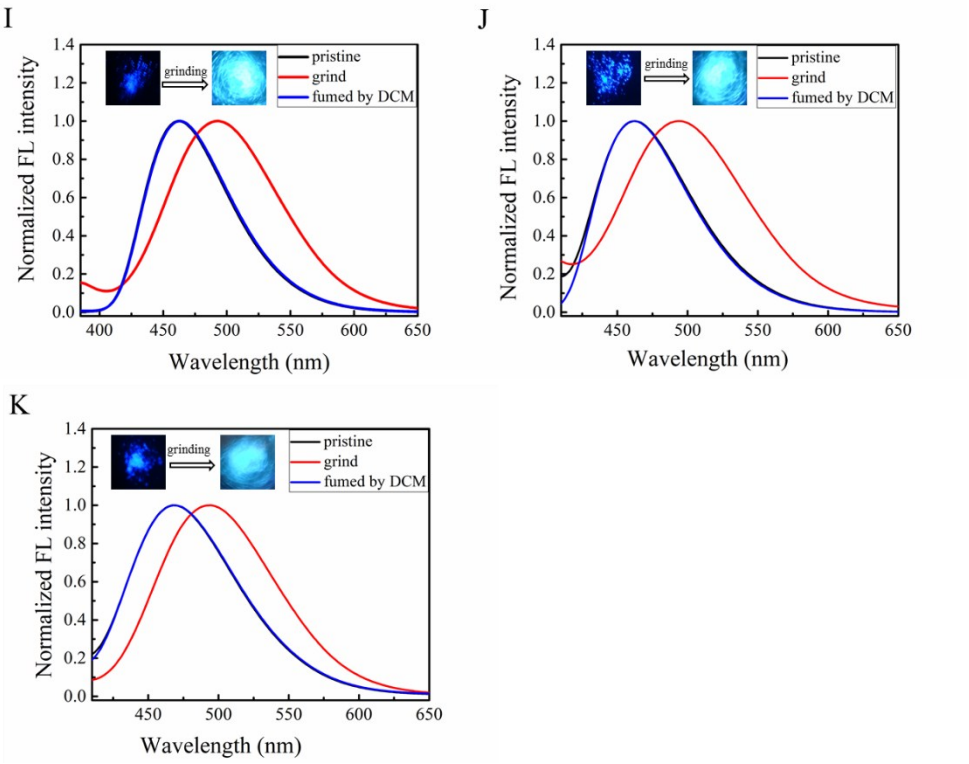

Fig. S85 Fluorescent spectra of TPE-2by-1-E (A) ,TPE-2by-1-Z (B), TPE-2by-2-E (C) ,TPE-2by-2-Z (D), TPE-2TZ-E (E) ,TPE-2TZ-Z (F), TPE-2EZ-E (G) , TPE-2EZ-Z (H), TPE-2B(I),TPE-2T(J) and TPE-2N(K) (inset: fluorescent images in pristine and grinding all).

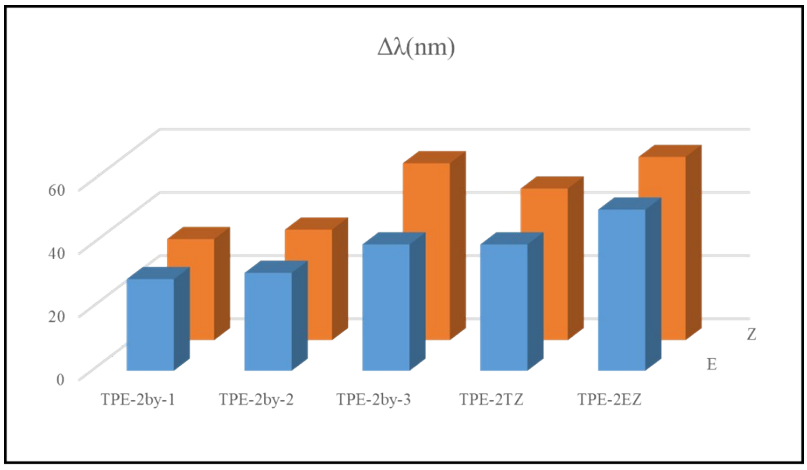

Fig. S86 The red-shifted wavelength histogram of all Z/E isomers.

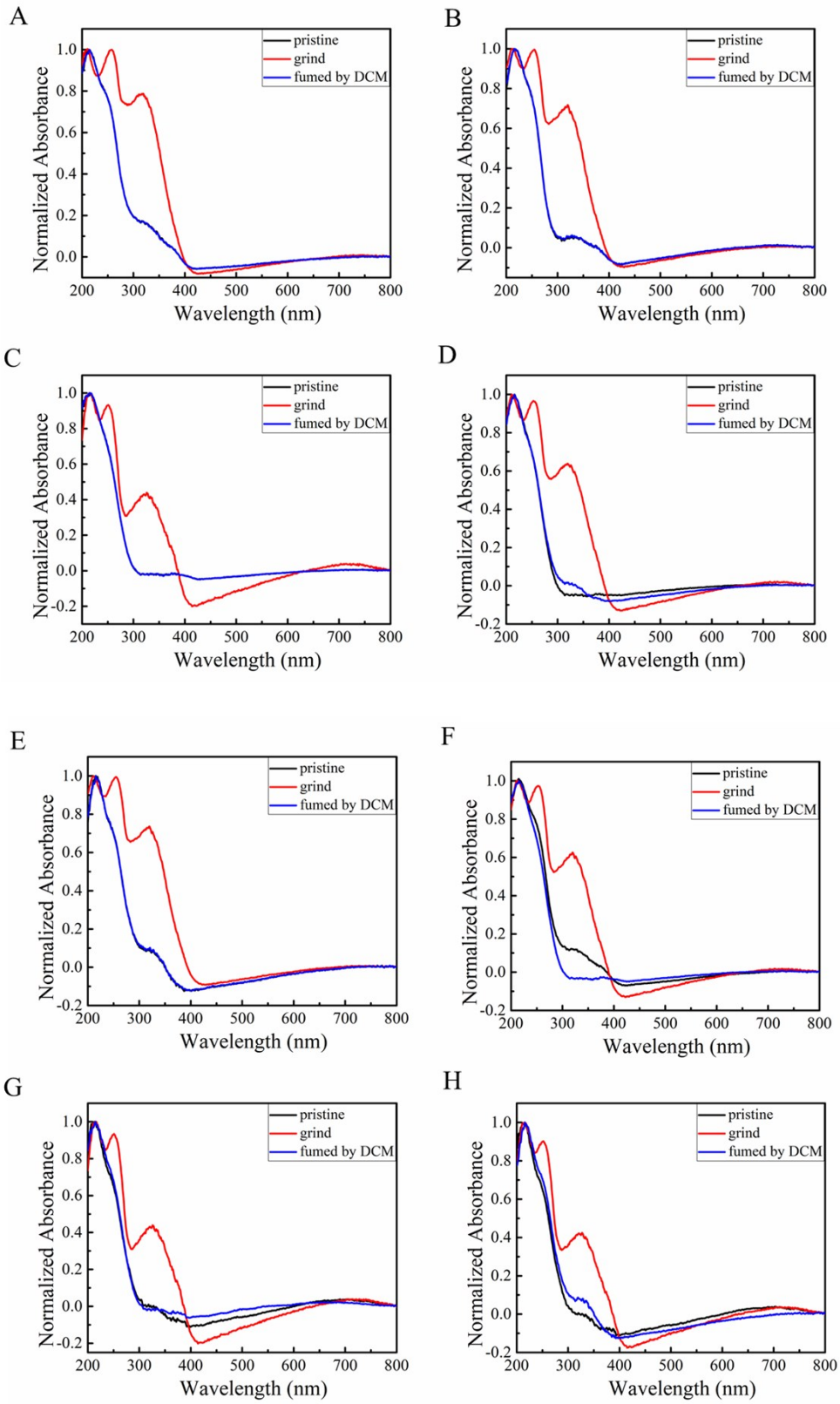
A
B
C
D
E
F
G
H
pristine
grind
fumed by DCM
Normalized Absorbance
Wavelength (nm)

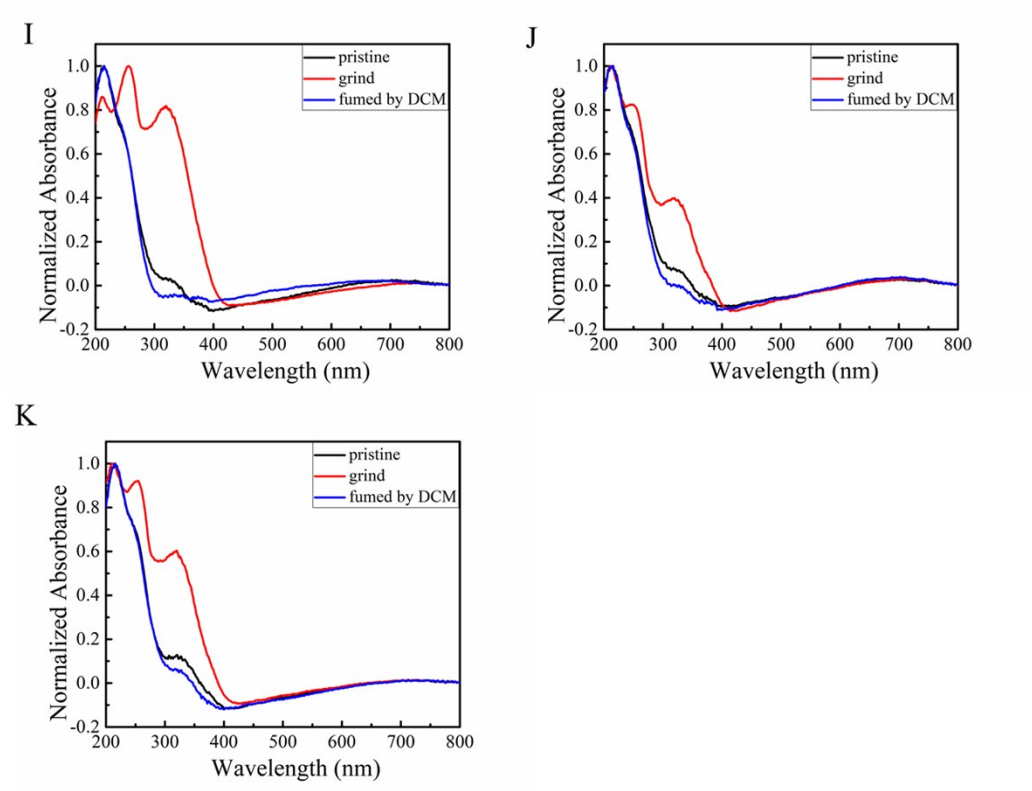

Fig. S87 Solid UV absorption of TPE-2by-1-E (A) ,TPE-2by-1-Z (B), TPE-2by-2-E (C) ,TPE-2by-2-Z (D), TPE-2TZ-E (E) ,TPE-2TZ-Z (F), TPE-2EZ-E (G) , TPE-2EZ-Z (H), TPE-2B(I),TPE-2T(J) and TPE-2N(K) in di□erent treatments.

Name	treatment	E_m (nm)	Δλ (nm)	Φ_f (%)	τ (ns)	$k_r/10^8(s^{-1})$	$k_{nr}/10^8(s^{-1})$	ΔE（*KJ*/mol）
TPE-2by-1-E	pristine	458	29	10	2.89	0.35	3.11	379.79
	grind	487		33.2	4.00	0.83	1.67	
	fumed by DCM	459		9.8	2.89	0.34	3.12	
TPE-2by-1-Z	pristine	458	30	14.1	3.10	0.46	2.78	380.09
	grind	488		34	4.02	0.85	1.64	
	fumed by DCM	459		13.9	3.09	0.45	2.78	

Table S1. Spectroscopic data for TPE-2by-1-E TPE-2by-1-Z.

Name	treatment	E_m (nm)	Δλ (nm)	Φ_f (%)	τ (ns)	$k_r/10^8(s^{-1})$	$k_{nr}/10^8(s^{-1})$	ΔE（*K*J/mol）
TPE-2by-2-E	pristine	466	22	19.5	2.98	0.47	2.88	379.91
	grind	488		37.4	4.13	0.90	1.51	
	fumed by DCM	466		19	2.98	0.48	2.98	
TPE-2by-2-Z	pristine	460	29	22.1	3.12	0.71	2.50	381.19
	grind	489		37.7	4.23	0.89	1.47	
	fumed by DCM	460		21.7	3.12	0.70	2.51	

Table S2. Spectroscopic data for TPE-2by-2-E TPE-2by-2-Z.

Name	treatment	E_m (nm)	Δλ(nm)	Φ_f (%)	τ (ns)	$k_r/10^8(s^{-1})$	$k_{nr}/10^8(s^{-1})$	ΔE（*K*J/mol）
TPE-2TZ-E	pristine	448	40	7.5	1.29	0.58	7.18	394.58
	grind	488		22.1	3.82	0.58	2.05	
	fumed by DCM	451		7.46	1.28	0.59	7.17	
TPE-2TZ-E	pristine	443	48	13.5	1.55	0.87	5.59	395.248
	grind	491		34.6	4.40	0.79	1.49	
	fumed by DCM	445		13	1.53	0.85	5.60	

Table S3. Spectroscopic data for TPE-2TZ-E TPE-2 TZ -Z.

Name	treatment	E_m (nm)	Δλ (nm)	Φ_f (%)	τ (ns)	$k_r/10^8(s^{-1})$	$k_{nr}/10^8(s^{-1})$	ΔE（*K*J/mol）
TPE-2EZ-E	pristine	437	51	14.2	1.82	0.78	4.71	410.39
	grind	488		32.9	3.88	0.85	1.73	
	fumed by DCM	438		14.1	1.78	0.78	4.72	
TPE-2EZ-Z	pristine	443	58	25.1	3.20	0.79	2.34	411.25
	grind	491		38.4	4.40	0.87	1.40	
	fumed by DCM	445		24.9	3.19	0.78	2.35	

Table S4. Spectroscopic data for TPE-2EZ-E TPE-2 EZ -Z.

Name	treatment	E_m (nm)	Δλ (nm)	Φ_f (%)	τ (ns)	$k_r/10^8(s^{-1})$	$k_{nr}/10^8(s^{-1})$
TPE-2B	pristine	462	31	21.2	3.71	0.579	2.129
	grind	493		36.3	4.401	0.829	1.45
	fumed by DCM	463		20.4	3.69	0.559	2.16

Table S5. Spectroscopic data for TPE-2B.

Name	treatment	E_m (nm)	Δλ (nm)	Φ_f (%)	τ (ns)	$k_r/10^8(s^{-1})$	$k_{nr}/10^8(s^{-1})$
TPE-2T	pristine	462	33	20.7	1.77	1.17	4.49
	grind	495		27.3	4.017	0.68	1.81
	fumed by DCM	462		20.1	1.76	1.14	4.53

Table S6. Spectroscopic data for TPE-2T.

Name	treatment	E_m (nm)	Δλ (nm)	Φ_f (%)	τ (ns)	$k_r/10^8(s^{-1})$	$k_{nr}/10^8(s^{-1})$
TPE-2N	pristine	467	28	9.8	3.23	0.30	2.79
	grind	495		30.7	4.24	0.72	1.63
	fumed by DCM	468		9.6	3.23	0.30	2.80

Table S7. Spectroscopic data for TPE-2N.

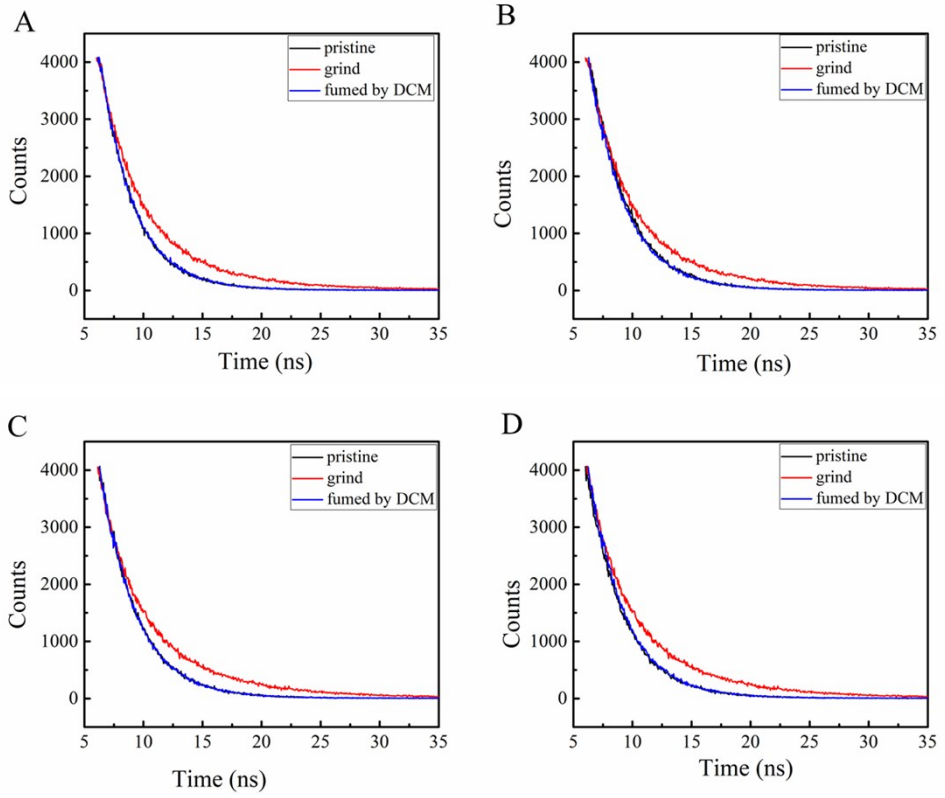

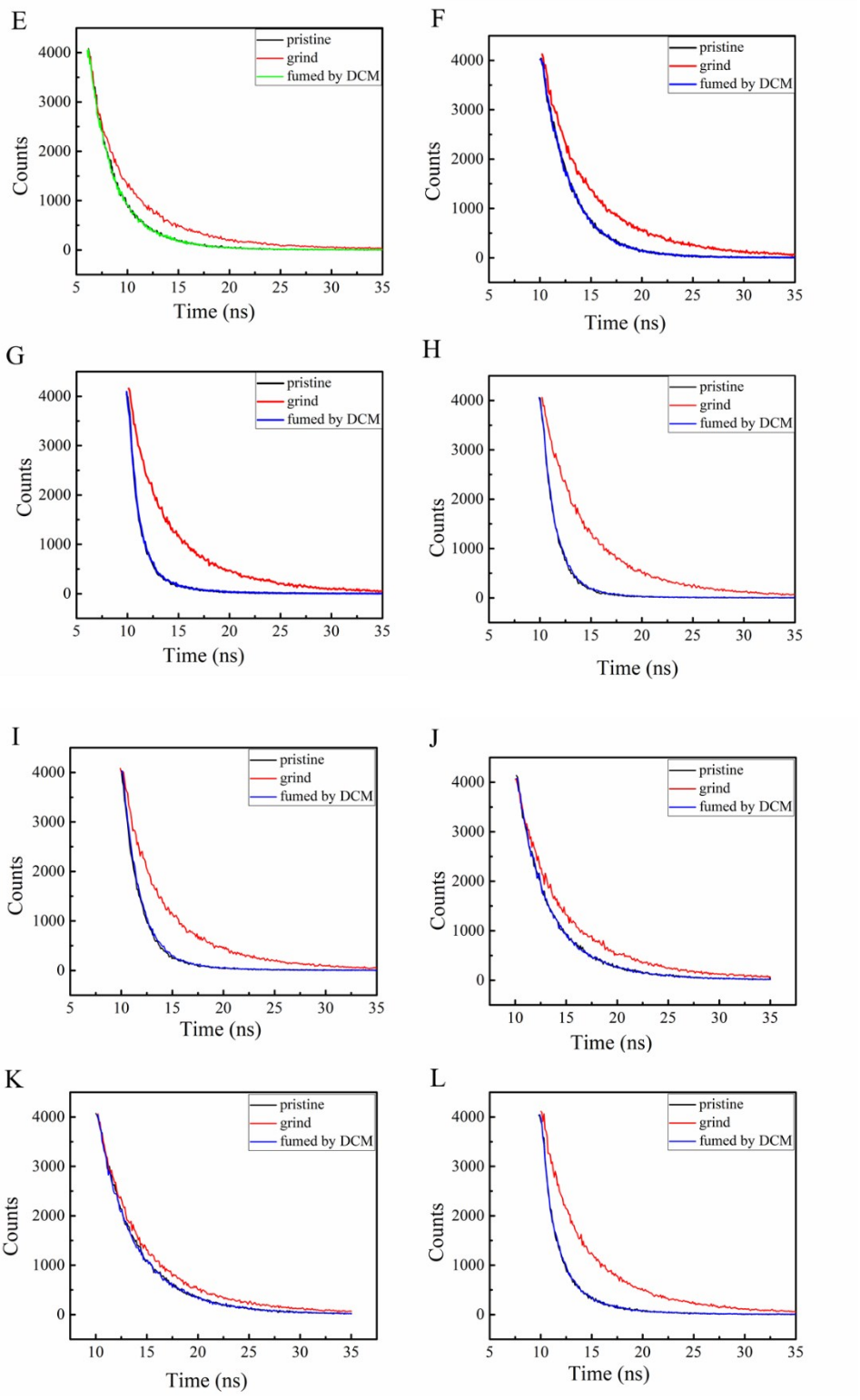
E
F
G
H
I
J
K
L
pristine
grind
fumed by DCM
Counts
Time (ns)

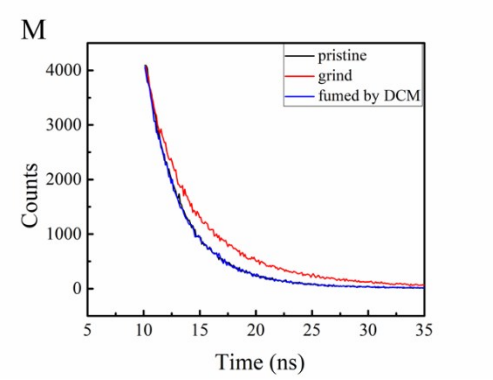

Fig. S88 Fluorescence lifetime of TPE-2by-1-E (A) ,TPE-2by-1-Z (B), TPE-2by-2-E (C) ,TPE-2by-2-Z (D), TPE-2by-3-E (E) ,TPE-2by-3-Z (F),TPE-2TZ-E (G) ,TPE-2TZ-Z (H), TPE-2EZ-E (I) , TPE-2EZ-Z (J), TPE-2B(K),TPE-2T(L) and TPE-2N(M) in di□erent treatments.

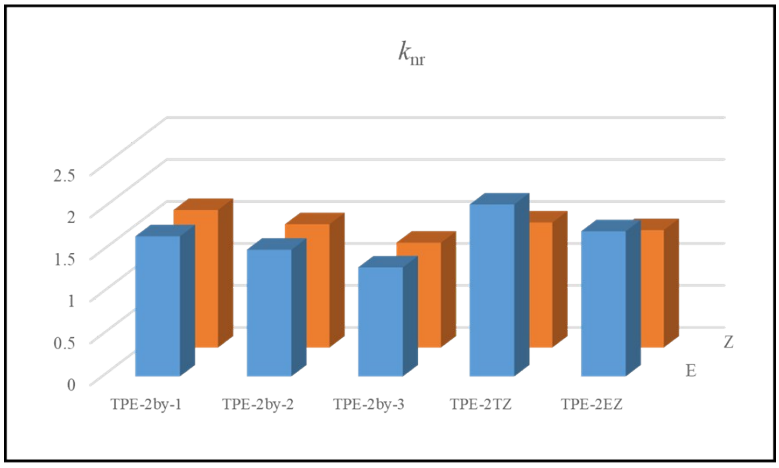

Fig. S89 The non-radiative rate constant (k_{nr}) histogram of all Z/E isomers.

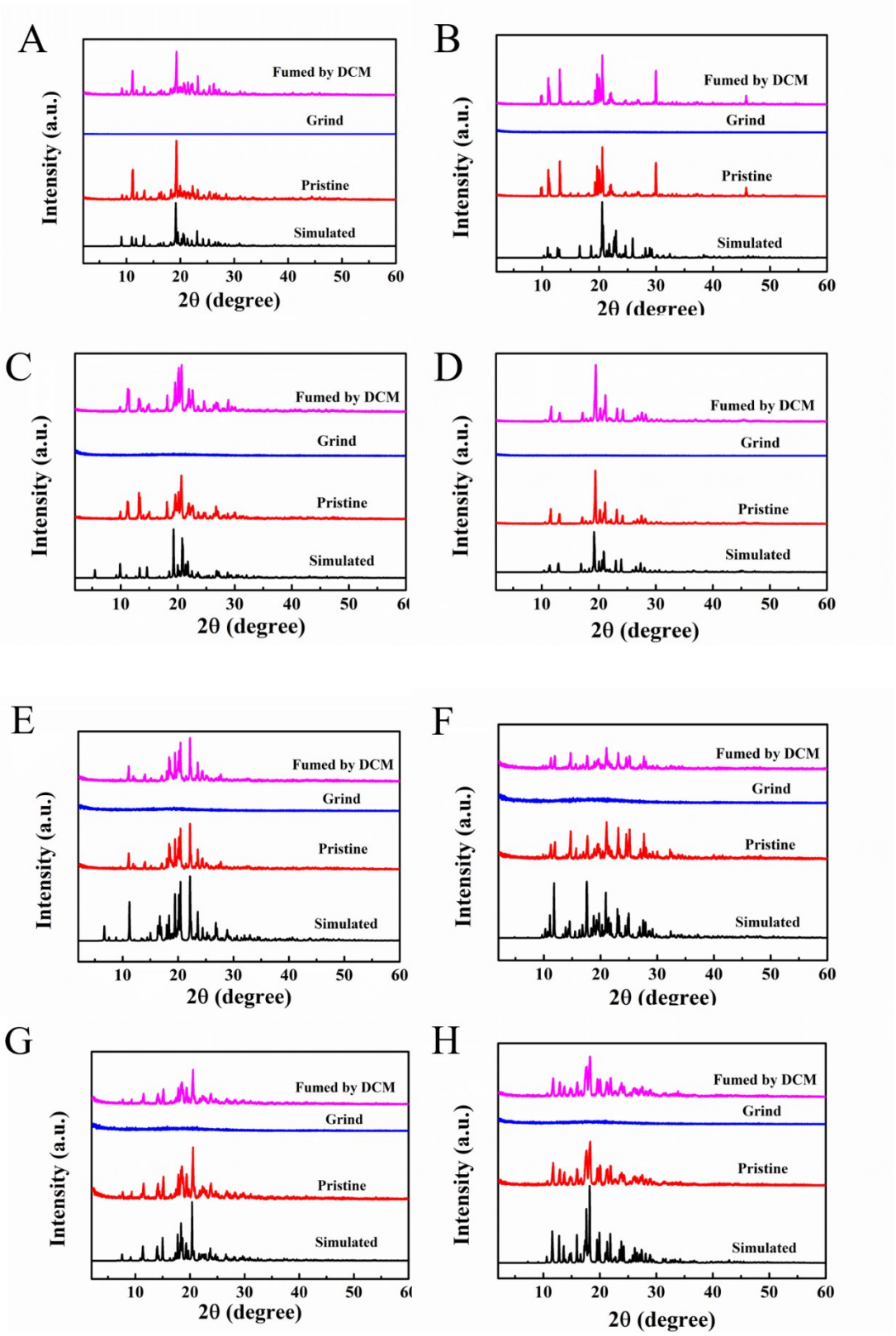
A
B
C
D
E
F
G
H
Fumed by DCM
Grind
Pristine
Simulated
Intensity (a.u.)
2θ (degree)
10
20
30
40
50
60

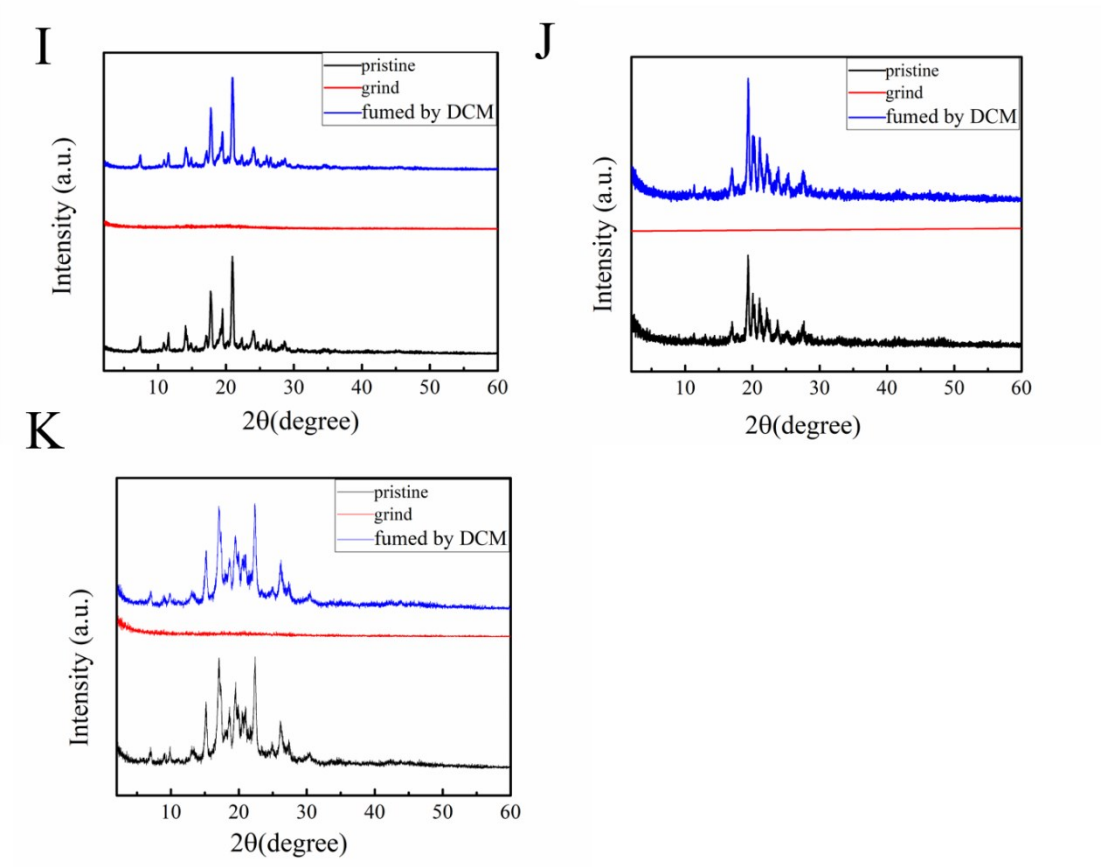

Fig. S90 XRD patterns of TPE-2by-1-E (A) ,TPE-2by-1-Z (B), TPE-2by-2-E (C) ,TPE-2by-2-Z (D), TPE-2TZ-E (E) ,TPE-2TZ-Z (F), TPE-2EZ-E (G) , TPE-2EZ-Z (H), TPE-2B (I),TPE-2T (J) and TPE-2N (K) in di□erent treatments.

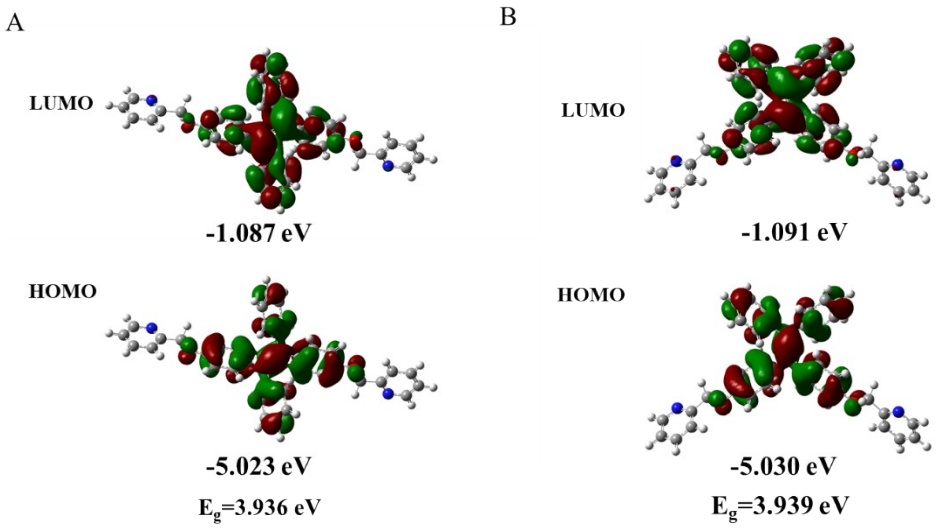

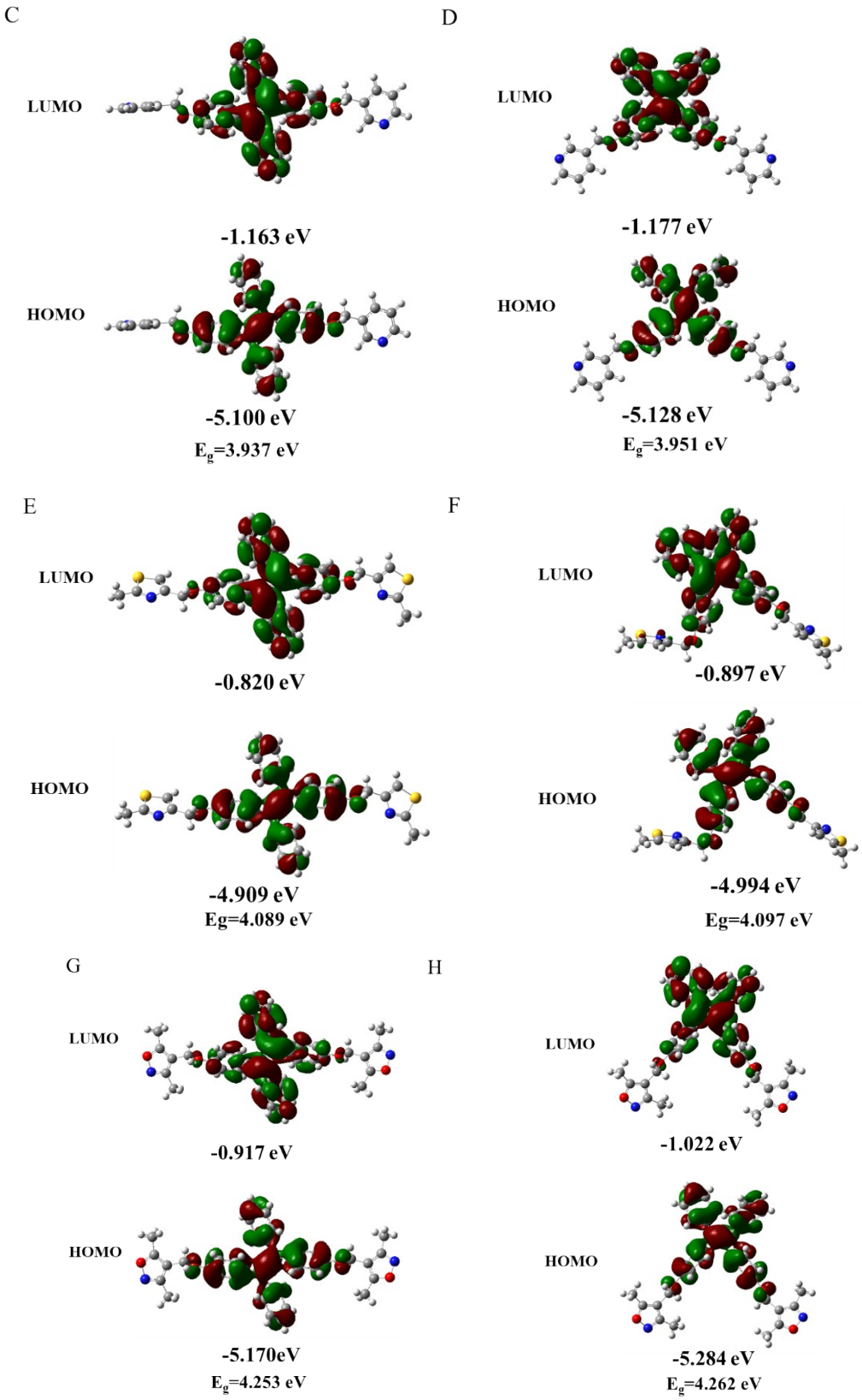

Fig. S91 Energy levels of LUMO and HOMO, energy gaps, and electron cloud distributions of TPE-2by-1-E (A) ,TPE-2by-1-Z (B), TPE-2by-2-E (C) ,TPE-2by-2-Z (D), TPE-2TZ-E (E) ,TPE-2TZ-Z (F), TPE-2EZ-E (G) , TPE-2EZ-Z (H).

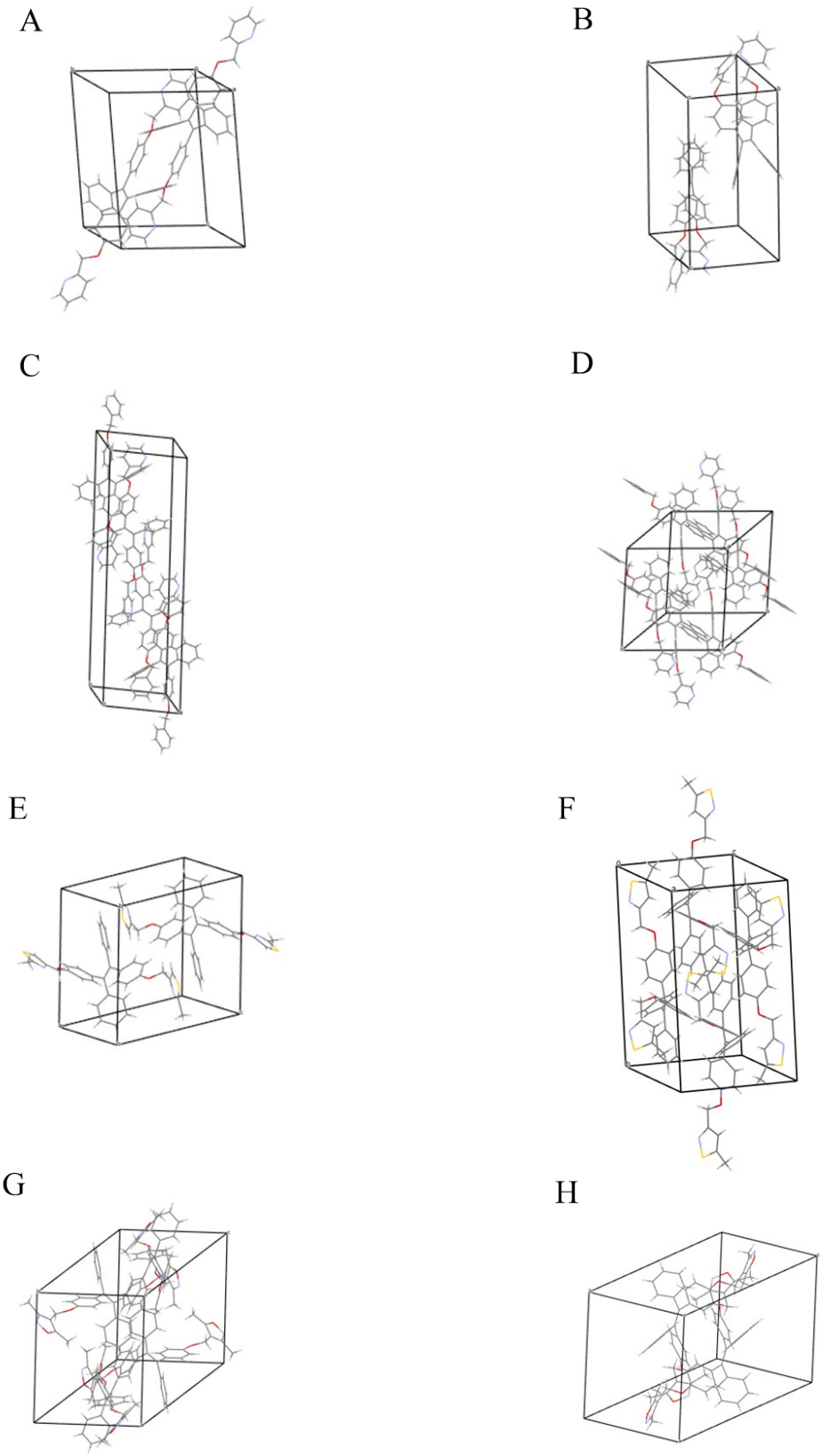

Fig. S92 Packing structures of single crystal about TPE-2by-1-E (A) ,TPE-2by-1-Z (B), TPE-2by-2-E (C) ,TPE-2by-2-Z (D), TPE-2TZ-E (E) ,TPE-2TZ-Z (F), TPE-2EZ-E (G) and TPE-2EZ-Z (H).

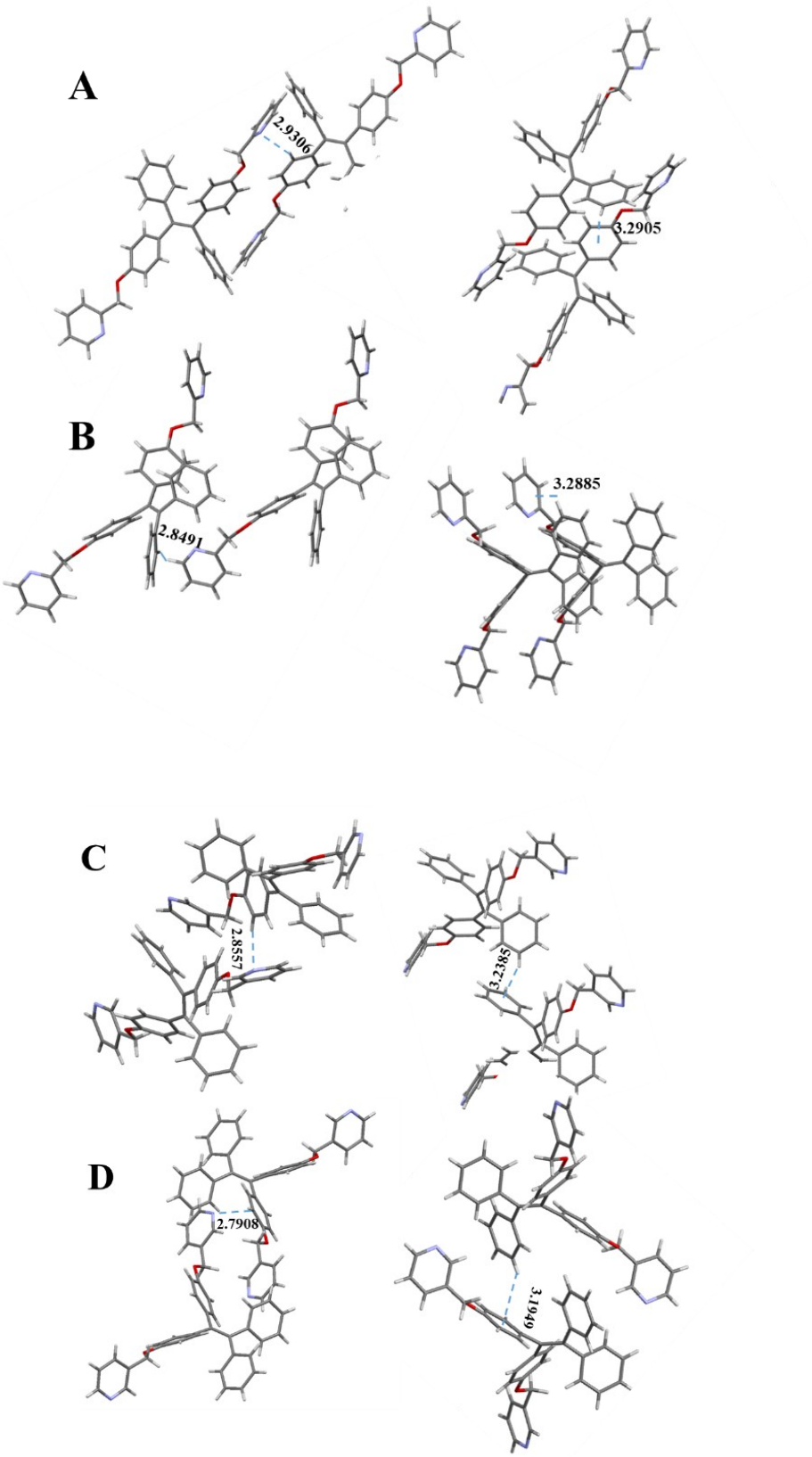
A
2.9306
3.2905
B
3.2885
2.8491
C
2.8557
3.2385
D
2.7908
3.1949

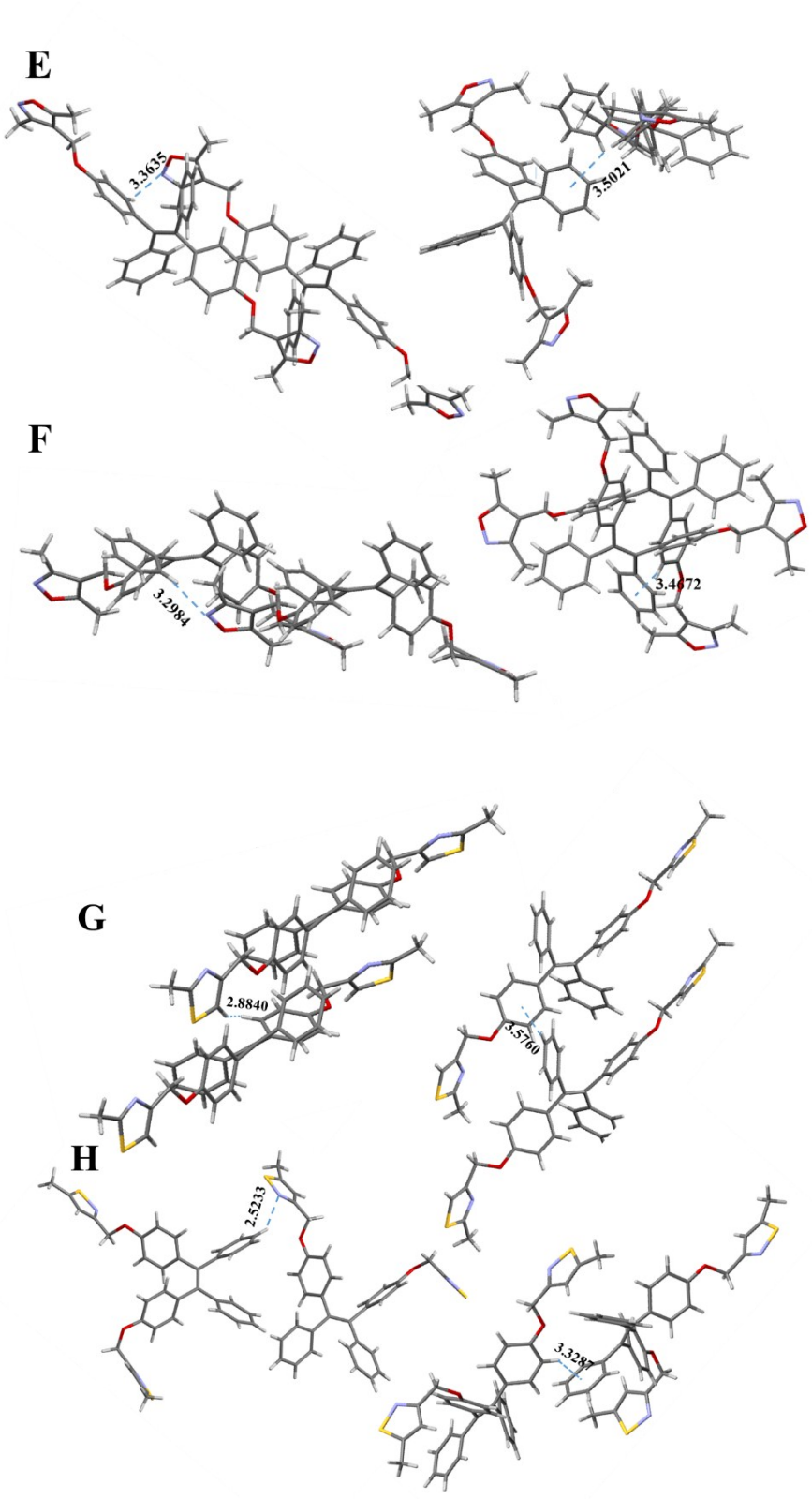

Fig. S93 Intermolecular interactions of TPE-2by-1-E (A) ,TPE-2by-1-Z (B), TPE-2by-2-E (C) ,TPE-2by-2-Z (D), TPE-2TZ-E (E) ,TPE-2TZ-Z (F), TPE-2EZ-E (G) and TPE-2EZ-Z (H).